BASIC REQUIREMENTS FOR MANUSCRIPTS

Original papers and discussions of papers and papers should be submitted to the Manager of Technical Publications, ASCE, 33 [illegible] indicate the technical division to which the paper is referred. The final date on which discussion should reach the Society is given as a footnote with each paper. Those who are planning to submit material will expedite the review and publication procedures by complying with the following basic requirements:

1. Titles must have a length not exceeding 50 characters and spaces.

2. A summary of approximately 50 words must accompany the paper; a 100-word synopsis must precede it; and a set of conclusions must end it.

3. The manuscript (the original ribbon copy and two duplicate copies) should be double-spaced on one side of 8½-inch by 11-inch paper. Three copies of all illustrations, tables, etc., must be included.

4. The author's full name, Society membership grade, and footnote reference stating present employment must appear on the first page of the paper.

5. Mathematics are superimposed from the copy that is submitted. Because of this, it is necessary that letters be drawn correctly, and that unusual symbols be properly identified. The latter symbols used should be defined where they first appear, in the illustrations or in the text, and arranged alphabetically in an Appendix.

6. Tables should be typed (on original ribbon copy and two duplicate copies) on one side of 8½-inch by 11-inch paper. Specific illustrations and explanations must be made in the text for each table.

7. Illustrations must be drawn in black ink on one side of 8½-inch by 11-inch paper. Normal illustrations will be reproduced with a width of between 3-inches and 4½-inches; the lettering must be large enough to be legible at this width. Photographs should be submitted as glossy prints. Explanations and descriptions must be made within the text for each illustration.

8. The desirable average length of a paper is about 12,000 words and the absolute maximum of 18,000 words. As an approximation, each full page of typed text, table, or illustration is the equivalent of 300 words.

9. Technical papers intended for publication must be written in the third person.

10. The author should distinguish between a list of "Reading References" and a "Bibliography," which would encompass the subject of his paper.

Reprints from this Journal may be made on condition that the full title, name of author, name of publication, page reference, and date of publication by the Society are given. The Society is not responsible for any statement made or opinion expressed in its publications.

This Journal is published [illegible] by the American Society of Civil Engineers. Publication office is at 2500 South State Street, Ann Arbor, Michigan. Editorial and General Offices are at 33 West 39 Street, New York 18, New York. $4.00 of a member's dues are applied as a subscription to this Journal. Second class postage paid at Ann Arbor, Michigan.

The index for 1959 was published as ASCE Publication [illegible] (free to members, $2.00); indexes for previous years are also available.

Vol. 87 No. EM 4

DIVISION ACTIVITIES

ENGINEERING MECHANICS DIVISION

Proceedings of the American Society of Civil Engineers

ENGINEERING MECHANICS DIVISION
EXECUTIVE COMMITTEE
Egor P. Popov, Chairman; Bruce G. Johnston, Vice Chairman;
John W. Clark; Merit P. White; Edward Wenk, Jr., Secretary
Elmer K. Timby, Board Contact Member

COMMITTEE ON PUBLICATIONS
Bruce G. Johnston, Chairman; Hans H. Bleich; Jack E. Cermak;
Donald L. Dean; John E. Goldberg; William J. Hall; John D. Haltiwanger;
Herbert S. Suer; Joseph F. Throop

CONTENTS

August, 1961

Papers

Page

Hydrodynamics of Flow into Curb-Opening Inlets
by Richard J. Wasley 1

Stability of Frames in the Presence of Primary Bending Moments
by E. F. Masur, I. C. Chang, and L. H. Donnell 19

Analysis of Frames Loaded into the Plastic Range
by Morris Ojalvo and Le-Wu Lu 35

Analysis of Noncoplanar Elastic Rings
by D. H. Pletta, W. C. Liessner, and Yen-Ming Yeh 49

Uniformly Moving Load on a Layered Half Plane
by J. L. Sackman 75

Conjugate Beam Simulated by Electric Circuits
by S. Freiberg 91

(over)

Copyright 1961 by the American Society of Civil Engineers.

Note.—Part 2 of this Journal is the 1961-31 Newsletter of the Engineering Mechanics Division.

The three preceding issues of this Journal are dated February 1961, April 1961, and June 1961.

Page

Method of Internal Constraints and Its Application
by Enrico Volterra 103

DISCUSSION

Comparative Study of a Segmental Arch Ring, by O. C. Zienkiewicz. (January, 1960. Prior discussion: July, 1960. Discussion closed.)
by O. C. Zienkiewicz (closure) 131

Vibrations and Stability of Plates Under Initial Stress, by George Herrmann and Anthony Armenakas. (June, 1960. Prior discussion: December, 1960. Discussion closed.)
by George Herrmann and Anthony Armenakas (closure) 133

Ultimate Strength of Over-Reinforced Beams, by Ladislav B. Kriz and Seng-Lip Lee. (June, 1960. Prior discussion: December, 1960. Discussion closed.)
by Ladislav B. Kriz and Seng-Lip Lee (closure). 135

Restrained Columns, by Morris Ojalvo. (October, 1960. Prior discussion: February, 1961. Discussion closed.)
by Morris Ojalvo (closure). 137

Wind Stresses in Domes, by P. Gondikas and Mario G. Salvadori. (October, 1960. Prior discussion: March, 1961. Discussion closed.)
by P. Gondikas and Mario G. Salvadori (closure) 139

Elasto-Plastic Analysis by Numerical Procedures, by Annabel L. Tong. (December, 1960. Prior discussion: April, 1961. Discussion closed.)
by G. C. Reynolds. 141

Vibration of Shear Building by Flexibility Method, by M. L. Pei. (February, 1961. Prior discussion: None. Discussion closed.)
by Shan S. Kuo 143

Dynamic Elastic-Plastic Analysis of Structures, by Melvin L. Baron, Hans H. Bleich, and Paul Weidlinger. (February, 1961. Prior discussion: None. Discussion closed.)
by A. A. Eremin. 145

Moire Fringes as a Means of Analyzing Strains, by C. A. Sciammarella and A. J. Durelli. (February, 1961. Prior discussion: None. Discussion closed.)
by Stanley Morse 147

Continuous Beam-Columns on Elastic Foundation, by S. L. Lee, T. M. Wang, and J. S. Kao. (April, 1961. Prior discussion: None. Discussion closes August 1, 1961.)
by Le-Wu Lu 149

Journal of the
ENGINEERING MECHANICS DIVISION
Proceedings of the American Society of Civil Engineers

HYDRODYNAMICS OF FLOW INTO CURB-OPENING INLETS

By Richard J. Wasley,[1] A. M. ASCE

SYNOPSIS

A theoretical analysis of the hydrodynamic problem associated with the curb-opening inlet is presented. The investigation is divided into two phases: (1) the instantaneous failure of a dam retaining a triangular reservoir superposed on (2) a certain incoming velocity distribution. Experimental verification is given

INTRODUCTION

At present, several methods are available for conveying water from road surfaces into storm drainage systems. The scope of this paper is confined to curb-opening inlets without depression in the gutter line.[2]

The analysis concerns an open channel (Fig. 1) placed on a continuous grade; it is of triangular cross-section, one side of which is nearly vertical (the two sides of the section are mutually perpendicular). At a distance from the upper end of the channel sufficient to establish steady, uniform flow conditions (see "Comparison of Theory and Experiment"), the vertical side ends abruptly. The termination of this wall marks the beginning of the curb inlet

Note.—Discussion open until January 1, 1962. Separate discussions should be submitted for the individual papers in this symposium. To extend the closing date one month, a written request must be filed with the Executive Secretary, ASCE. This paper is part of the copyrighted Journal of the Engineering Mechanics Division, Proceedings of the American Society of Civil Engineers, Vol. 87, No. EM 4, August, 1961.

[1] Research Asst., Dept. of Civ. Engrg., Stanford Univ., Stanford, Calif.

[2] "Hydrodynamics of Flow into Curb-Opening Inlets," by R. J. Wasley, Ph. D. Dissertation, Stanford Univ., Stanford, Calif., Nov., 1960 (available as Tech. Report No. 6, Dept. of Civ. Engrg., Stanford Univ., Stanford, Calif.

section under study. The length of opening is sufficient to allow all the flow to pass over the edge of the inlet lip. Rainfall and lateral inflow are not considered.

Slopes greater than the critical are considered; this is easier to analyze theoretically than the subcritical case. In the latter situation, the complication arises that the flow passes through critical depth at some position as it flows toward the opening, since the transverse slope is almost always supercritical. In addition, a certain amount of drawdown will occur before the control section is reached.

The analytical problem is to obtain a mathematical model of the flow as it moves into the study section, makes the transition in direction, and passes over the edge of the inlet lip. The one-dimensional component velocities (defined by averaging the point velocities in the vertical direction) and the depths, as functions of position, are the parameters of interest and are documented theoretically; the results are verified experimentally.

THEORETICAL DEVELOPMENT

Notation.—The letter symbols adopted for use in this paper are defined where they first appear and are arranged alphabetically, for convenience of reference, in the Appendix.

General Problem.—The water passes down the channel in a uniform state as given by the flow rate, Q, and the pertinent one-dimensional velocity component, $\bar{u}$. (Fig. 1) shows the essential nature of the problem and the relevant parameters. Upon reaching the section $\overline{ODA}$ the water begins the transition in direction in order to pass over the inlet lip, $\overline{OC}$. The general movement of the fluid down the channel suggests considering the total flow as a main flow in the x-direction combined with a cross flow in the y-direction. Such an approach resolves the actual flow into two simpler components, each of which may be treated theoretically. Hence the investigation is divided into two phases: (1) the main flow, i.e., a steady open-channel flow with a certain incoming velocity distribution (either experimental or theoretical), upon which is superposed (2) the cross flow, which corresponds approximately to the instantaneous failure of a dam, behind which there is a triangular reservoir.

By this procedure (i.e., by initially considering the inlet problem as actually two problems, solving them separately, and later combining the results), a difficult steady flow situation is transformed into a relatively simpler problem involving an analysis of an unsteady flow coupled with a steady flow. There is a similarity in approach here to the slender-body method utilized frequently in aerodynamics in which two vector fields are superposed. The present problem, however, is more difficult because of the rotationality of the main flow in the transverse direction.

From Fig. 2, it may be seen that because of the assumption of supercritical flow in the downstream direction, there is no $\bar{v}$ component at time $t = 0$ ($x = 0$), and hence the dam failure is directly applicable without considering some initial unknown or uncertain velocity.

Some interaction between the two phases involved in this superposition is unaccounted for, but not so much as might be originally expected (as seen by the agreement of theoretical and experimental results).

Incoming Velocity Distribution.—By use of a form of Darcy's equation, the velocity distribution can be described analytically without any experimental

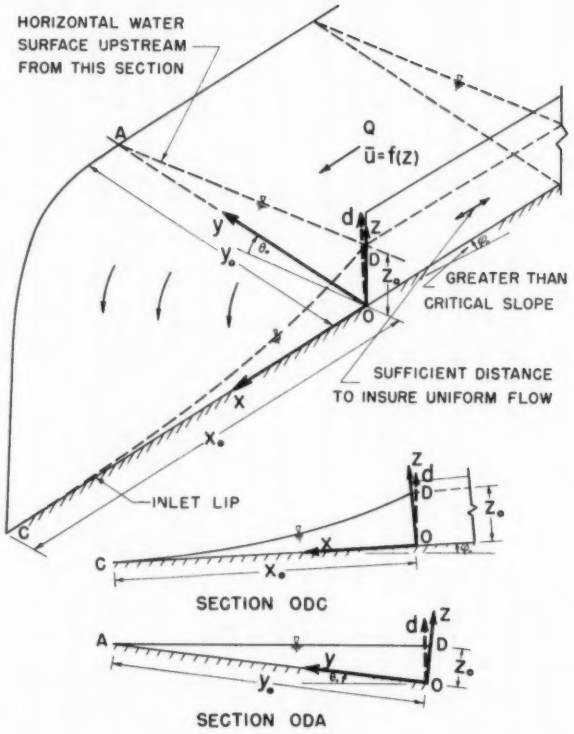

FIG. 1.—SCHEMATIC DRAWING AND SECTIONS OF PROBLEM

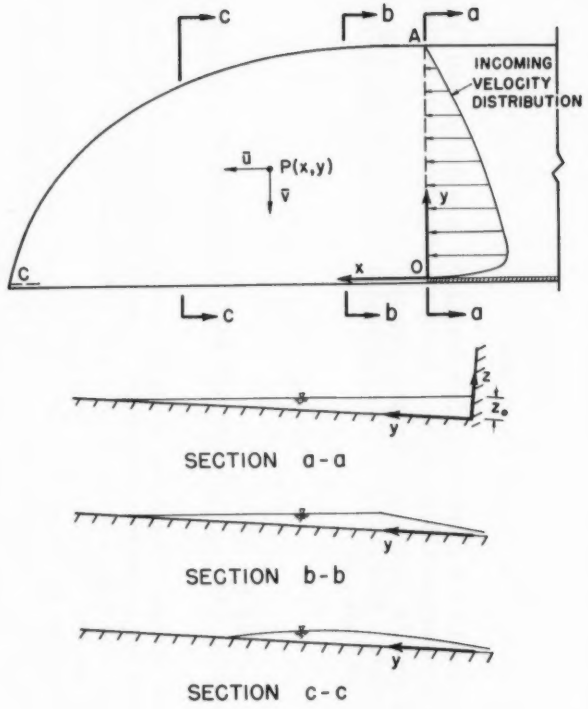

FIG. 2.—SCHEMATIC FLOW PLAN AND SECTIONAL VIEWS

coefficients except the friction factor, f. From experimental information (or handbooks) an average friction factor across the channel can be given by[3]

$$f = \frac{8\,g\,R\,\phi_o}{\bar{u}^2} \qquad \ldots\ldots\ldots\ldots\ldots (1)$$

assuming that d = 4 R is the "equivalent diameter." R is the hydraulic radius, and u is the average velocity of the channel; these quantities can be readily computed from the known upstream parameters.

Considering a certain point on this transverse section, and rewriting Darcy's equation, one finds that

$$\bar{u} = C_o\, z^{1/2} \qquad \ldots\ldots\ldots\ldots\ldots (2)$$

in which $C_o = \left(\frac{8\,g\,\phi_o}{f}\right)^{1/2}$ with the depth being substituted for the hydraulic radius.

Because of such a simple representation of the distribution as Eq. 2, it could be expected that complete agreement with experiment would be more coincidence than consequence of the theory. It is seen, however, from Fig. 12 that in general the distribution is quite well defined.

It is noted that Eq. 2 does not account for the curb shear which would cause the velocity there to approach zero. If the equation could be modified to account for this, only a small correction would result.

Some arguments could be raised that an "average" friction factor, defined by Eq. 1, might be questioned because of the complicated variation of f across the channel. Also, the use of the "equivalent diameter" (d = 4 R) for such a shallow channel might cause some concern.

Instantaneous Failure of Dam.—It is readily possible to derive the differential equations governing the motion of fluid down a channel after instantaneous failure of a dam. J. J. Stoker[4] has presented a two-dimensional linearized solution for small time, based upon work done by F. V. Pohle, but attention here will be focused upon a one-dimensional approach.

Considering this phase of the total problem alone, a sketch (Fig. 3) can be drawn indicating the parameters necessary to describe the dam break problem. (A variable with an asterisk superscript refers to distance measured to the sudden "break" in slope.)

For ease of experimental measurement, the y- and z- coordinates are defined as in Fig. 2 and shown dotted in Fig. 3. However, owing to the small slope, θ_o, the axes may be rotated slightly counter-clockwise as shown, to aid in the mathematical treatment. The slope, of course, is still considered in the analytical solution. The error introduced when comparing the solution with experimental results using the nonrotated coordinate system is negligible. (Actually however, the vertical depths, given by the distance, d (see Fig. 1), were the measurements taken.) Note that the channel bottom is assumed to continue in the negative y-direction.

---

3 "Elementary Fluid Mechanics," by J. K. Vennard, John Wiley and Sons, Inc., New York, N. Y., 1954.

4 "Water Waves," by J. J. Stoker, Interscience Publishers, Inc., New York, N. Y., 1957.

Using Fig. 4 and employing Newton's Second Law (making the ordinary small angle approximations, i.e., sin $\theta_o \approx \theta_o$ and sin $\theta_f \approx \theta_f$) leads to the equation of motion

$$\frac{\gamma}{2} z^2 - \gamma x\, \theta_o\, dy + \gamma z\, \theta_f\, dy - \frac{\gamma}{2}\left(z + \frac{\partial z}{\partial y} dy\right)^2 = \rho x\, dy \frac{d\bar{v}}{dt} .$$

Here θ_f is the friction slope $\left(\text{defined by } \frac{f\bar{u}^2}{8 g R}\right)$; this term is included in the derivation of the governing equations but omitted in the solution. By neglecting those terms in which differential quantities of second order appear, this reduces to

$$\bar{v} \frac{\partial \bar{v}}{\partial y} + \frac{\partial \bar{v}}{\partial t} + g \frac{\partial z}{\partial y} = g\ (\theta_f - \theta_o) \quad \ldots\ldots\ldots\ldots (3)$$

which is the appropriate form of the dynamic equation for the problem considered.

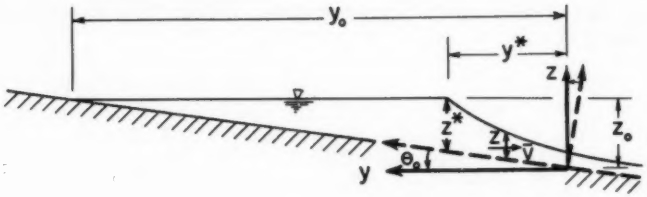

FIG. 3.—FAILURE OF DAM WITH TRIANGULAR RESERVOIR

From the principle of mass conservation, the expression is obtained

$$\left(z + \frac{\partial z}{\partial y} dy\right)\left(\bar{v} + \frac{\partial \bar{v}}{\partial y} dy\right) dt + \frac{\partial z}{\partial t} dt\, dy = z \bar{v}\, dt.$$

Neglecting the second order differential terms as before leads to

$$\bar{v} \frac{\partial z}{\partial y} + z \frac{\partial \bar{v}}{\partial y} + \frac{\partial z}{\partial t} = 0 \quad \ldots\ldots\ldots\ldots\ldots (4)$$

which is the desired form of the continuity equation for the present problem.

The exact solution to Eq. 3 (excluding θ_f) and Eq. 4 is rather complicated, but by a technique proposed by R. F. Dressler,[5] this can be achieved. Dressler states that in general the exact solution to every non-degenerate unsteady water-wave problem (governed by the above equations) in a straight channel at an arbitrary slope can be obtained in terms of the complete elliptic integral of the second kind. By means of a non-Newtonian reference frame (i.e., an

[5] "Unsteady non-linear waves in sloping channels," by R. F. Dressler, Proceedings, Royal Soc. of London, Vol. 229A, March 1958, pp. 186-198.

accelerating coordinate system) every such wave problem can be replaced by an associated problem for a horizontal channel. Then the equations are transformed into the Euler-Poisson equation through the hodograph inversion method. Application of the Riemann method of integration yields an auxiliary function which is transformed into a Legendre function and then into the elliptic integral. The resulting plots given by Dressler enable the depth and one-dimensional velocity profiles at various times to be constructed.

The parameters can be non-dimensionalized by the following scheme. A circumflex (^) over a particular variable indicates a non-dimensional quantity:

$$\hat{x} \equiv \frac{x}{x_{o_{theo.}}}; \quad \hat{y} \equiv \frac{\theta_o}{z_o} y; \quad \hat{z} \equiv \frac{z}{z_o}; \quad \hat{t} \equiv \theta_o \sqrt{\frac{g}{z_o}}\, t;$$

$$\hat{u} \equiv \frac{\bar{u}}{u_{theo.\ max.}}; \quad \hat{v} \equiv \frac{\bar{v}}{\sqrt{g\, z_o}} \qquad \ldots\ldots\ldots\ldots\ldots\ldots (5)$$

The subscripts are self-explanatory in the above cases. Several illustrative profiles (in non-dimensional form) are given in Fig. 5 for times of 0, 0.3, 0.6, 1.0, 2.0, and 3.0.

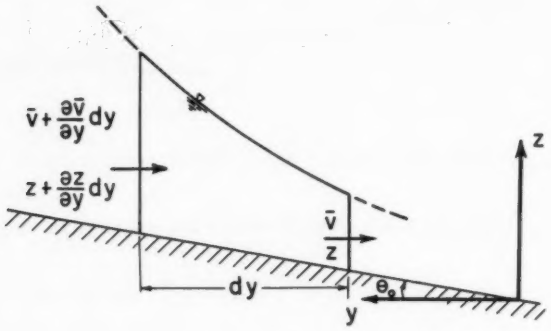

FIG. 4.—DERIVATION SKETCH

Superposition.—There is a natural breakdown of the total curb-opening inlet flow into two definite sections, labelled Zone I and Zone II, as indicated in Fig. 6. In the flow field a definite curve ($\overline{OB}$) is formed at which the water appears to be "sloughing off" and forming a crest. This curve is the boundary in the y-direction of the negative surge crest as it passes downstream due to the x-component of velocity. In other words, the information that the curb has terminated at the origin 0, is transmitted in the y-direction at a certain finite rate, which shall be derived. Superposed on this is a motion in the downstream direction at a rate governed by the incoming velocity distribution. The delineation of $\overline{OB}$ was visually observable in the experimental phase of the program only for certain configurations (θ_o equals 1 on 24 and 1 on 12 for all ϕ_o), although it was measurable by instrument for all positions investigated.

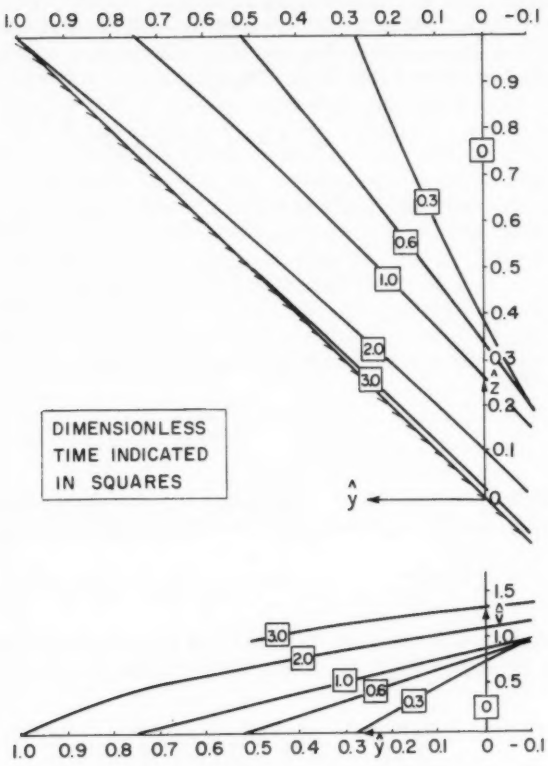

FIG. 5.—DEPTH AND VELOCITY PROFILES

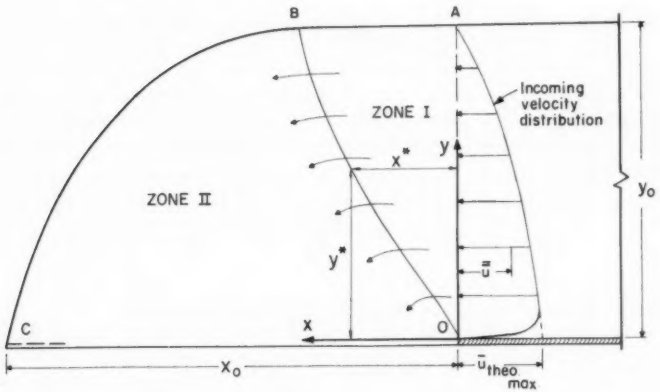

FIG. 6.—DELINEATION OF ZONES

Before Zones I or II can be determined, it is necessary to determine the movement of the crest of the negative surge in the transverse direction. Knowing the velocity of propagation of a small disturbance, $c = \sqrt{g z}$ one can write with respect to the crest itself (from Fig. 3)

$$c = \frac{dy^*}{dt} = \sqrt{g z^*} = \sqrt{g}\ \left(z_o - \theta_o y^*\right)^{1/2} \quad \ldots\ldots\ldots (6)$$

By integrating between the limits of 0 and y^*, and 0 and t, and rearranging the results, one obtains

$$y^* = \sqrt{g z_o}\, t - \frac{\theta_o g t^2}{4} \quad \ldots\ldots\ldots\ldots\ldots (7)$$

where $t \leq \dfrac{2\sqrt{z_o}}{\theta_o \sqrt{g}}$. By non-dimensionalizing, according to Eqs. 5, there results

$$\hat{y}^* = \hat{t} - \frac{1}{4}\hat{t}^2 \quad \ldots\ldots\ldots\ldots\ldots (8)$$

where $\hat{t} \leq 2$.

Zone I.—Now rewriting Eq. 2, expressing the one-dimensional absolute velocity, $\bar{u}$, in terms of the equivalent differential quantity, one finds that

$$\frac{dx^*}{dt} = C_o\,(z^*)^{1/2} = C_o\,\left(z_o - \theta_o y^*\right)^{1/2}$$

where in this case, the asterisk superscripts refer to measurements taken to the boundary of Zone I (Fig. 6). Substitution of Eq. 7 into the above leads to

$$\frac{dx^*}{dt} = C_o \sqrt{\theta_o}\left(\frac{z_o}{\theta_0} - \sqrt{g z_o}\, t + \frac{\theta_o g}{4} t^2\right)^{1/2}$$

By integration between the limits of 0 and x^*, and 0 and t, there results

$$x^* = \frac{C_o z_o}{\theta_o \sqrt{g}} + \frac{C_o}{g\sqrt{\theta_o}}\left[\left(\frac{z_o}{\theta_o} - \sqrt{g z_o}\, t + \frac{\theta_o g}{4} t^2\right)\left(\frac{\theta_o g}{2} t - \sqrt{g z_o}\right)\right] \quad \ldots (9)$$

Eqs. 7 and 9 give the parametric expressions for the line $\overline{OB}$. When the parameter t is eliminated from these two equations a linear relationship in x^* and y^* results:

$$x^* = \frac{C_o}{\sqrt{g}}\ y^* \quad \ldots\ldots\ldots\ldots\ldots (10)$$

From Eq. 7, when $y^* = y_o$, $t = 2\sqrt{z_o}/\left(\theta_o \sqrt{g}\right)$, and therefore,

$$x^* = x_B = \frac{C_o y_o}{\sqrt{g}} \quad \ldots\ldots\ldots\ldots\ldots (11)$$

Hence, it is a very simple matter to plot theoretically the line marking the downstream boundary of Zone I. The first superposition phase of the analytical solution for the curb-opening inlet has thus been completed. Since the definition for non-dimensionalizing the x-coordinate depends upon the theoretical length of x_o, Eqs. 10 and 11 will be made dimensionless after this length has been derived (Eq. 18 and Table 1).

In Zone I no change in upstream conditions is possible (for supercritical conditions), and the surface level and velocities at various points are easily calculated.

Zone II.—Upon the completion of the determination of Zone I, a method must be found for continuing the solution into the interior of Zone II. One way of doing this involves the description of the trajectory of a given fluid element. As it moves transversely across the channel it simultaneously translates in the longitudinal direction according to the nature of the incoming velocity dis-

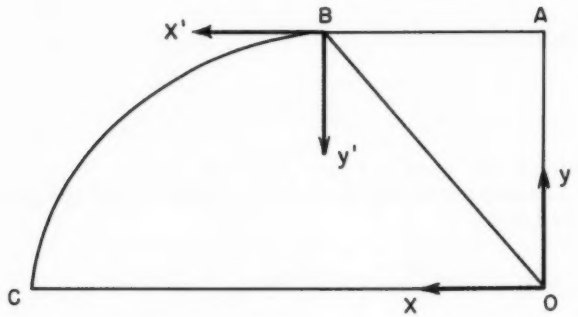

FIG. 7.—TRANSLATED COORDINATE SYSTEM

tribution. Combination of these two motions determines the complete velocity, depth fields and streamline picture.

The analytical definition of the limiting streamline in the zone under study is one of the more important parts of the solution. By the relatively simple result derived, the clear length of opening necessary for complete interception can be obtained immediately, knowing the upstream parameters of the flow.

From Dressler's exact solution of the hydraulic problem associated with the instantaneous dam failure, the last particle of flow is governed by a very simple equation influenced by gravity alone, that is, frictional and surface tension effects are neglected. At $t = 2\left(\sqrt{z_o}/\left(\theta_o \sqrt{g}\right)\right)$, one has $y = y_o$, and $x = C_o y_o/\sqrt{g}$, and the motion of this particle is given by

$$\ddot{y} = -g\theta_o \quad \ldots\ldots\ldots\ldots\ldots\ldots (12)$$

To simplify the solution of Eq. 12 with the necessary boundary conditions, it is convenient to define a new coordinate system as shown in Fig. 7 from a linear translation of the original system.

The equations of translation are quickly found to be

$$x' = x - \frac{C_o\, y_o}{\sqrt{g}} \quad ,$$

$$y' = y_o - y \quad ,$$

and

$$t' = t - \frac{2\sqrt{z_o}}{\theta_o \sqrt{g}} \quad .$$

Hence Eq. 12 can be rewritten as,

$$\ddot{y}' = g\, \theta_o .$$

The solution is readily obtained as,

$$y' = \frac{1}{2}\, g\, \theta_o\, t'^2 \quad \ldots\ldots\ldots\ldots\ldots\ldots (13)$$

using the condition that when $t' = 0$, $y' = \dot{y}' = 0$.

From Eq. 2, using the modified reference frame, with the relationship $z = \theta_o y'$, it is found that

$$u = \frac{dx'}{dt'} = C_o\, z^{1/2} = C_o\, (\theta_o\, y')^{1/2} \quad \ldots\ldots\ldots\ldots (14)$$

Substituting Eq. 13 into Eq. 14, and integrating between the limits of 0 and x', and 0 and t' gives the result

$$x' = C_o\, \theta_o\, \frac{\sqrt{g}}{2\sqrt{2}}\, t'^2 \quad \ldots\ldots\ldots\ldots\ldots (15)$$

By elimination of the parameter t'^2, between Eqs. 13 and 15, the expression is obtained

$$x' = \frac{C_o}{\sqrt{2\, g}}\, y' \quad \ldots\ldots\ldots\ldots\ldots\ldots (16)$$

which is a linear relationship in x' and y'. In terms of the original coordinate system,

$$x = \frac{C_o}{\sqrt{g}} \left(y_o + \frac{y_o - y}{\sqrt{2}} \right) \ldots\ldots\ldots\ldots\ldots (17)$$

At y = 0,

$$x = x_{o_{theo.}} = \frac{C_o\, y_o}{\sqrt{g}} \left(1 + \frac{1}{\sqrt{2}}\right) \quad \ldots\ldots\ldots\ldots (18)$$

The non-dimensional forms of Eqs. 17 and 18 are given in Table 1.

TABLE 1.—BOUNDARY EQUATIONS FOR ZONES I AND II

Line (1)	Analytical Solutions	
	Dimensional (2)	Non-dimensional (3)
$\overline{OA}$	$x = 0,\ (0 \leqslant y \leqslant y_o)$.	$\hat{x} = 0,\ (0 \leqslant y \leqslant 1)$.
$\overline{AB}$	$y = y_o,\ \left(0 \leqslant x \leqslant \frac{C_o\, y_o}{\sqrt{g}}\right)$.	$\hat{y} = 1,\ \left(0 \leqslant x \leqslant \frac{2}{2 + \sqrt{2}}\right)$.
$\overline{OB}$	$x^* = \frac{C_o}{\sqrt{g}}\, y^*,\ (0 \leqslant y^* \leqslant y_o)$. $x_B = \frac{C_o\, y_o}{\sqrt{g}}$.	$\hat{x} = \left(\frac{2}{2 + \sqrt{2}}\right) \hat{y},\ (0 \leqslant y \leqslant 1)$. $\hat{x}_B = \frac{2}{2 + \sqrt{2}}$.
$\overline{OC}$	$y = 0,\ \left[0 \leqslant x \leqslant \frac{C_o\, y_o}{\sqrt{g}} \left(2 + \frac{1}{\sqrt{2}}\right)\right]$.	$\hat{y} = 0,\ (0 \leqslant \hat{x} \leqslant 1)$.
$\overline{BC}$	$x = \frac{C_o}{\sqrt{g}} \left(y_o + \frac{y_o - y}{\sqrt{2}}\right)$, $(y_o \leqslant y \leqslant 0)$. $x_{o_{theo.}} = \frac{C_o\, y_o}{\sqrt{g}} \left(1 + \frac{1}{\sqrt{2}}\right)$.	$\hat{x} = \frac{2 + \sqrt{2}\ (1 - \hat{y})}{2 + \sqrt{2}}$, $(1 \leqslant \hat{y} \leqslant 0)$. $\hat{x}_{o_{theo.}} = 1$.

A comment may be made here which applies to all the streamlines in Zone II, including the boundary, since friction is not considered. As depth decreases, the velocity decreases in uniform, steady flow. It would seem, therefore, that some adjustment should be made for the downstream component of velocity. However, it is unlikely that the fluid would decrease immediately to uniform flow velocity (given by Manning's or Darcy's equation) for each incremental distance in the region under study; inertial effects would have to be considered. Hence in the short distances involved, the particles are assumed not to decrease significantly in velocity in the x-direction due to decrease in depth.

The delineation of the various intermediate streamlines in the interior of Zone II is unfortunately not so straightforward as the analysis presented for the boundaries of the two zones and the interior of Zone I, and a finite incremental solution seems to be the most practical.

TABLE 2.—ZONE II—INTERMEDIATE

$\hat{t}$ (1)	$\hat{x}_{ip}$ (2)	$\hat{y}_{ip}$ (3)	$\hat{z}_{ip}$ (4)	$\hat{u}_{ip}$ (5)	$\hat{v}_{ip}$ (6)	$\delta\hat{t}$ (7)	$\delta\hat{y}_1$ (8)	$\hat{y}_1$ (9)	$\hat{\bar{v}}_1$ (10)	$\hat{\bar{v}}_{1_{avg.}}$ (11)	$\delta\hat{y}_2$ (12)
	initial position values for P_i at time, $\hat{t}$						$\langle\hat{v}_{ip}\,\delta\hat{t}$	$\hat{y}_{ip} - \delta\hat{y}_1$	from Fig. 5 at $\hat{y}_1$ & $\hat{t} + \delta\hat{t}$	$\frac{1}{2}\left(\hat{\bar{v}}_{ip} + \hat{\bar{v}}_1\right)$	$\langle\hat{v}_{1_{avg.}}\,\delta\hat{t}$

Consider a transverse profile at an arbitrary time, $\hat{t}$ (Fig. 3). Assume the depths and velocities (in non-dimensional form) at various points as having previously been obtained. A particle, P_i, located on $\overline{OB}$, is then selected. This corresponds to any given desired streamline in the x-direction in Zone I depending upon the time assumed, for example, the streamline dividing the flow in half.

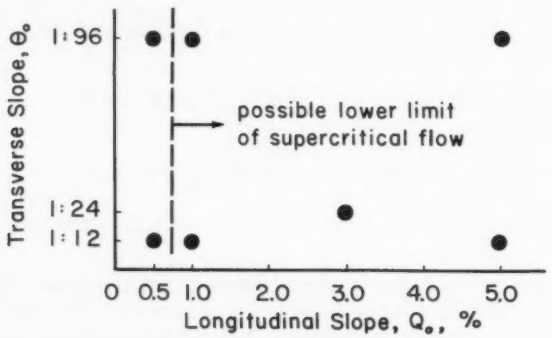

FIG. 8.—APPARATUS CONFIGURATIONS

Now a certain interval of time, $\delta\hat{t}$, is assumed to have elapsed. The velocity $\bar{v}_1$, at time $\hat{t} + \delta\hat{t}$, for the particle P_i, at the new position is found from Fig. 5. This allows an average of the two velocities $\left(\hat{\bar{v}}_{ip} \text{ and } \hat{\bar{v}}_1\right)$ to be taken, thus determining approximately the position of the particle. This process is continued until the position of P_i has stabilized for the assumed small interval of time. Two cycles are sufficient for practical application of the method.

The actual final position (in terms of $\hat{x}$ and $\hat{y}$) that the particular particle P_i, takes in $\delta\hat{t}$ can be found quite readily by determining the average downstream velocity, $\hat{u}_{avg.}$, during the time interval.

STREAMLINE DETERMINATION

$\hat{y}_2$ (13)	$\hat{\bar{v}}_2$ (14)	$\hat{\bar{v}}_{2_{avg.}}$ (15)	$\delta\hat{y}_{fp}$ (16)	$\hat{y}_{fp}$ (17)	$\hat{z}_{fp}$ (18)	$\hat{\bar{v}}_{fp}$ (19)	$\bar{u}_{fp}$ (20)	$\hat{\bar{u}}_{avg.}$ (21)	$\delta\hat{x}$ (22)	$\hat{x}_{fp}$ (23)
$\hat{y}_{ip} - \delta\hat{y}_2$	from Fig. 5 at $\hat{y}_2$ & $\hat{t} + \delta\hat{t}$	$\frac{1}{2}\left(\hat{\bar{v}}_{ip} + \hat{\bar{v}}_2\right)$	$\hat{\bar{v}}_{2_{avg.}}\,\delta\hat{t}$	$\hat{y}_{ip} - \delta\hat{y}_{fp}$	final position values for P_i at time, $\hat{t} + \delta\hat{t}$			$\frac{1}{2}\left(\hat{\bar{u}}_{ip} + \hat{\bar{u}}_{fp}\right)$	$k\,\bar{u}_{avg.}\,\delta\hat{t}$	$x_{ip} + \delta\hat{x}$

The iteration procedure is given in Table 2. Under the column $\delta\hat{x}$, a factor k ($k = 2/(2 + \sqrt{2})$ appears; this is because of the nature of the non-dimensional definitions $\hat{x}$ and $\hat{u}$.

If desired, it is possible to describe adequately any general experimental incoming velocity distribution, including the fact that the velocity approaches zero at the curb face, by means of suitable power expressions with arbitrary exponents. By a similar procedure to that developed previously, power series expressions can be obtained which determine the boundaries of Zones I and II. (In this case, closed form solutions cannot be obtained, and the pertinent differential equations are expanded by use of the binomial theorem and then integrated term by term in the convergent domain).[6]

COMPARISON OF THEORY AND EXPERIMENT

A matrix of apparatus configurations was investigated experimentally. This information is most easily and clearly presented in a plot such as Fig. 8. The solid circles indicate that the measurements were taken for these arrangements.

It is seen from this figure that the lower limit of supercritical flow possibly occurred between the longitudinal slopes[7] of 1/2% and 1%. Since the theory was initially predicated upon uniform and super-critical flow being maintained upstream from the inlet, this was of some concern with regard to the range of application of the theory.

A dimensionless plan of the inlet section is presented in Fig. 9. Zones I and II are delineated from the analytical methods previously developed, and from theory certain intermediate streamlines (at 25%, 50%, 75% and 90% of the total

6 "Hydrodynamics of Flow into Curb-Opening Inlets," by R. J. Wasley, Ph. D. Dissertation, Stanford Univ., Stanford, Calif., No., 1960.

7 "Hydrodynamics of Flow into Curb-Opening Inlets," by R. J. Wasley, Ph. D. Dissertation, Stanford Univ., Stanford, Calif., Nov., 1960.

flow) are plotted. The experimental data defining the boundaries of the flow are shown, with the exception of the data for the 1 on 96 transverse slopes; this slope introduced additional phenomena which invalidated the adequate representation of conditions by the present theory. Very shallow depths with small velocities, and consequences of such a flat cross-slope caused forces such as friction and surface tension to become more prominent.

The agreement between experiment and theory is quite good. The experimental intermediate streamlines, especially the 50% streamline, corresponding to the divisions given above, satisfactorily compare with theory. The depths

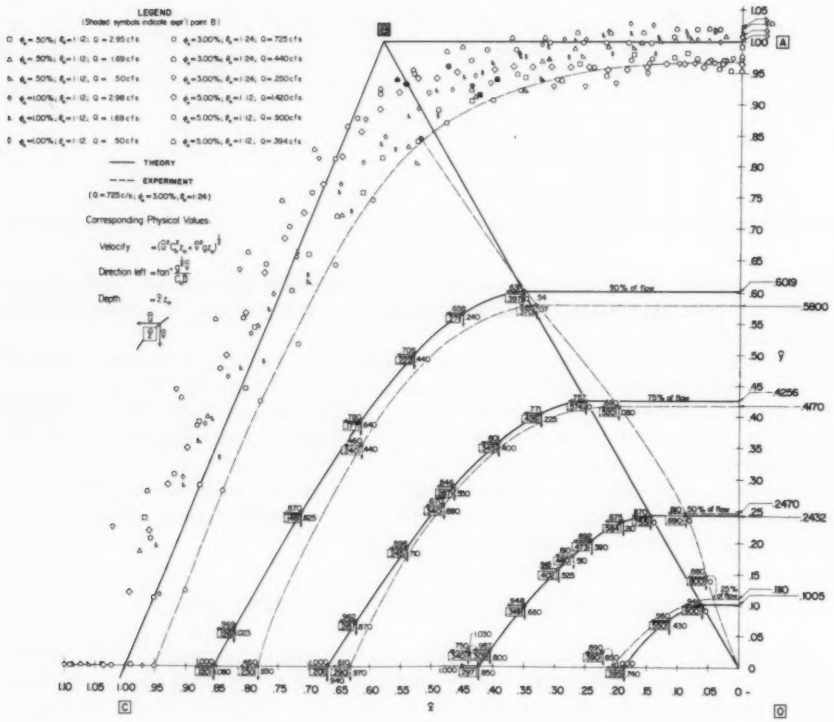

FIG. 9.—STUDY SECTION PLAN—THEORETICAL AND EXPERIMENTAL RESULTS

and velocities on the various experimental streamlines do not coincide with theory quite as well, but they are still fairly satisfactory, particularly in and near Zone I and in the area where $\hat{x}$ and $\hat{y}$ are reasonably small. The several formulas necessary to convert the non-dimensional theoretical results in Fig. 9 to the actual corresponding physical values are given in the plot itself and are self-explanatory.

It is seen that the theoretical boundary streamline creates a sudden change in direction at point B. However, it is clear from the fact that the 90% stream-

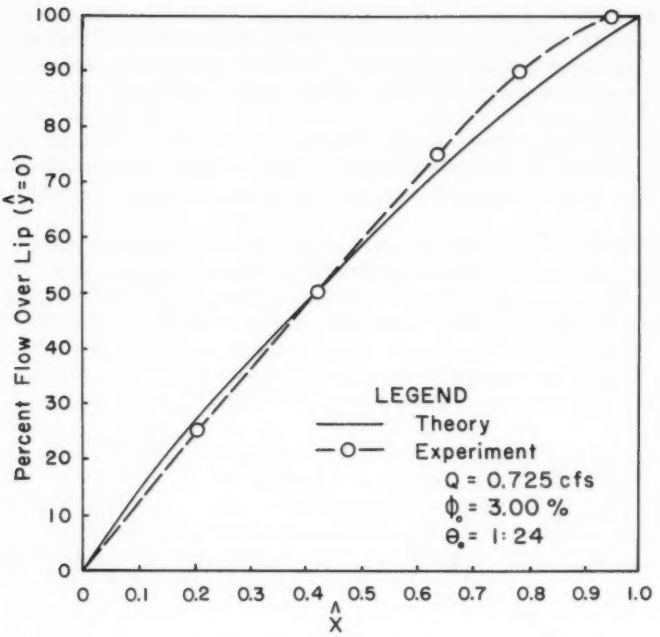

FIG. 10.—DISTRIBUTION OF FLOW ALONG LIP—THEORETICAL AND EXPERIMENTAL RESULTS

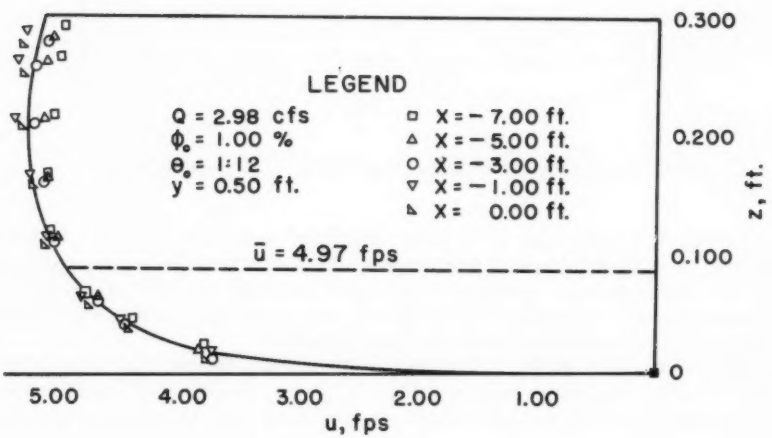

FIG. 11.—TYPICAL SUPERPOSITION OF VELOCITY PROFILES

line is relatively a considerable distance from this boundary, that no practical significance should be attached to this.

It is desirable for practical purposes to determine the distribution of flow at the lip of the inlet in order to locate the position where some certain percentage of flow has been intercepted. This distribution is plotted in Fig. 10 (for $\bar{y} = 0$) and compared with the experimental results as shown ($Q = 0.725$ cfs, $\phi_o = 3.00\%$, and $\theta_o = 1{:}24$). The variation is almost linear - both theoretically and experimentally. Such a situation could conceivably be used advantageously. If merely a good estimate of this quantity is desired, then to consider this an exact linear relationship (knowing x_o) would be more than adequate.

It was stated that one of the assumptions used in the development of the analytical approach was the consideration of uniform flow upstream from the region under study. A typical superposition of velocity profiles at several positions (x = 0 ft, -1.00 ft, -3.00 ft, -5.00 ft, and -7.00 ft) for a given configuration

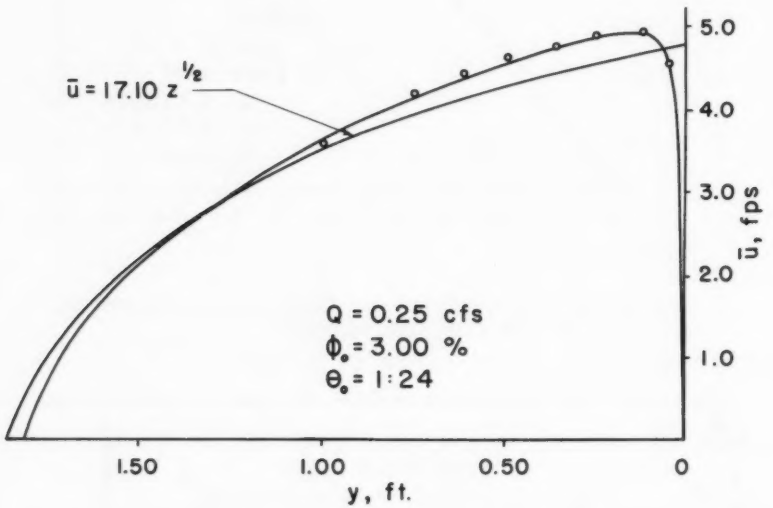

FIG. 12.—TYPICAL TRANSVERSE VELOCITY DISTRIBUTION

($\phi_o = 1.00\%$, $\theta_o = 1{:}12$, and y = 0.50 ft) and flow rate (Q = 2.98 cfs) is shown in Fig. 11; this illustrates that successive longitudinal profiles of velocity and depths for this particular point were essentially identical. For all positions, configurations, and flow rates investigated, this situation existed, thus indicating that the uniform flow requirement was satisfied.

It was mentioned that Eq. 2, although quite simple, defined the actual experimental velocity distribution adequately. A typical transverse distribution is given in Fig. 12 for Q = 0.25 cfs, $\phi_o = 3.00\%$, and $\theta_o = 1{:}12$, which indicates that agreement is quite good.

Surface fluctuation of high frequency (probably caused by turbulence effects) was noticed in all experimental runs made; in addition, surface tension phe-

nomena were observable, particularly in the shallower transverse slope apparatus configurations. However, no problems were encountered in the actual measurement of depths or velocities of flow. It was relatively easy to repeat readings to the limit of the accuracy (0.001 ft) of the depth-measuring point gage. For velocity determination, Pitot probe results were duplicable to within about 2% in most cases (the most critical situation having a maximum error of less than 5%).

The work covered a sufficient range of slopes (both transverse and longitudinal) to describe adequately most practical situations. It is quite certain that the theory developed in this paper is applicable to longitudinal slopes greater than 5%. It is also evident that the analysis is satisfactory for ϕ_o = 0.5% (see Fig. 9), but below this slope, the theoretical results may be inaccurate. The steeper cross-slopes were best when compared with theory; this is reasonable because of the assumptions in the analytical approach.

The range of flow rates investigated was from 0.0032 to 2.98 cfs. This covers the practical variation of flows in most situations. The quantity of flow does not invalidate the theory except if it becomes so small as to decrease the velocity to the point where frictional and surface tension effects become significant.

The analysis is simple and straightforward, depending only on knowledge of the upstream parameters Q, ϕ_o, θ_o, and f in its use, and is quite satisfactory within the specified ranges. It is readily possible to obtain any theoretical information on the depths and velocities (with directions) in the inlet section and the flow distribution along the inlet lip (for use in partial interception computations) from Figs. 9 and 10.

ACKNOWLEDGMENTS

The writer is indebted to John K. Vennard and Byrne Perry under whose direction this research was conducted. Discussions with Carl F. Izzard, Chief, Division of Hydraulic Research, Bureau of Public Roads, provided much useful background information. The assistance of F. G. Baker, J. Duncan, R. L. Street, and Y. Wang is also acknowledged. Financial support for this research was provided by the U. S. Department of Commerce, Bureau of Public Roads.

APPENDIX.—NOTATION

The following symbols have been adopted for use in this paper:

C_o = a coefficient defined by $\left(\frac{8 g \phi_o}{f}\right)^{1/2}$, in $\sqrt{\text{ft}}$ per sec;

c = absolute celerity of wave in still water, in feet per second, defined by $\sqrt{g z}$;

d = vertical depth of water, in ft, defined by $z \cos \phi_o \cos \theta_o$;

f = the Darcy friction factor;

g = the acceleration of gravity, in ft per sec per sec;

P_i = an arbitrary particle;

Q = rate of flow, in cfs;

R = the hydraulic radius, in ft;

t = time, in sec;

$\overline{u}$, $\overline{v}$ = the x- and y-components of velocity (average in vertical), respectively, in fps;

$\overline{\overline{u}}$ = the x-component of velocity (average of section), in fps;

x, y, z = the coordinate axes and distances measured parallel thereto;

x_o, y_o, z_o = maximum distances, in ft;

γ = specific weight of water, in lb per cu ft;

θ_f = the friction slope, defined by $\frac{f\overline{u}^2}{8gR}$;

θ_o = the transverse slope;

ρ = the density of water, in slugs per cu ft;

ϕ_o = the longitudinal slope, in %;

$( )^*$ = quantity measured to surge crest or line $\overline{OB}$;

$(\hat{})$ = dimensionless quantity;

$( )'$ = quantities in translated coordinate system; and

$(\dot{})$ = time differentiation

Journal of the
ENGINEERING MECHANICS DIVISION
Proceedings of the American Society of Civil Engineers

STABILITY OF FRAMES IN THE PRESENCE OF PRIMARY BENDING MOMENTS

By E. F. Masur,[1] I. C. Chang,[2] and L. H. Donnell[3]

SYNOPSIS

A systematic method of analyzing the stability of frames against sidesway buckling is developed. Two possible avenues of approach are presented: (1) a slope-deflection equation method based on equilibrium considerations; and (2) a moment distribution procedure. These techniques are well-known in connection with the analysis of the stability of frames subjected to loads at the joints only; the present paper represents an extension to the general case in which primary bending moments occur prior to buckling.

INTRODUCTION

If a framed structure of the type shown in Fig. 1 is subjected to increasing loads, its carrying capacity may be defined as the highest point in a load-displacement diagram. Collapse is said to occur when that branch of the diagram has been reached on which the load magnitude decreases with increasing deflections.

A linear, elastic, first-approximation analysis of the structural response does not exhibit such a maximum. Actual collapse is due to factors not in-

Note.—Discussion open until January 1, 1962. To extend the closing date one month, a written request must be filed with the Executive Secretary, ASCE. This paper is part of the copyrighted Journal of the Engineering Mechanics Division, Proceedings of the American Society of Civil Engineers, Vol. 87, No. EM 4, August, 1961.

[1] Prof. of Engrg. Mechanics, Univ. of Michigan, Ann Arbor, Mich.

[2] Stress Analyst, Scientific Design Co., New York, N. Y.

[3] Senior Research Scientist, Inst. of Science and Tech., Univ. of Michigan, Ann Arbor, Mich.

cluded in this type of analysis; among these are chiefly inelasticity and the second order effects associated with "buckling" instability, or a combination of both. These combined effects are difficult to analyze, although some progress has been made in recent years.[4] The usual approach is to assess the effects of plasticity and of elastic instability separately and then to devise some technique of estimating their interaction.

The present paper is concerned with elastic instability alone. The problem has been investigated extensively in the past; however, in almost all previous investigations of the subject, the actual loading system consists of, or is replaced by one consisting of, forces that are applied at the joints only. The un-

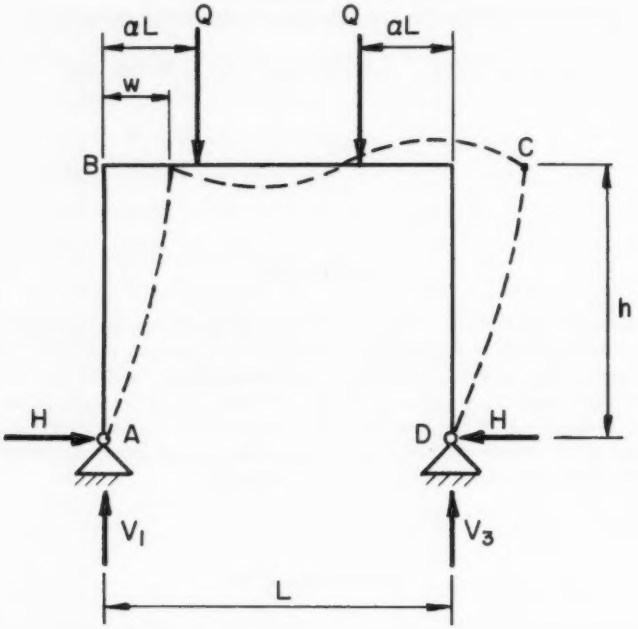

FIG. 1.—TYPICAL FRAME

buckled structure is therefore assumed to be in its virginal state, that is, its members are straight and no "primary" bending moments are present. The replacement of the actual loading system by one that is (for each member) statically equivalent to it is usually justified by the assumption that very small errors are thus introduced. This assumption is fortified by a result of E.

4 "The Stability of Tall Buildings," by R. H. Wood, Proceedings, ICE, Vol. 11, 1958, p. 69; discussion by M. R. Horne, et al., of "The Stability of Tall Buildings," by R. H. Wood, Vol. 12, 1959, p. 502.

Chwalla[5,6] who has made an exact study of an example, including the effect of primary bending moments. Unfortunately, Chwalla's work is almost the only one to date of which the writers are aware; moreover, it is unsystematic and complicated. A schematic discussion of the problem has been presented by A. H. Chilver,[7] who replaces the actual structure by a much simpler one thought to be equivalent. The present study seems to confirm the relatively insignificant effect of primary bending moments on the elastic stability of structures of the type shown in Fig. 1. Nevertheless, the results presented herein are considered to be of potential value, in the sense that they may represent a first step toward a more comprehensive plastic instability analysis, for which primary bending moments may not be considered negligible a priori. Similar doubts, even as applied to the elastic case, have recently been expressed by E. Guillard,[8] F. ASCE.

Two avenues of approach are presented. These are: (1) an equilibrium analysis leading to a set of "slope-deflection equations" and (2) a moment-distribution technique. Both of these methods can be seen to be extensions of classical methods that do not take the effect of primary bending moments into account and that are treated comprehensively elsewhere.[6] Of course these two formulations are not the only ones possible. For example, in analogy with more conventional problems of structural analysis, a solution may be obtained through the use of the conditions of compatible deformations. This type of procedure is described more fully elsewhere,[9] but, together with other possible lines of attack, has been omitted here for sake of brevity.

SLOPE-DEFLECTION METHOD

In what follows a brief resume is given of the development of the standard slope-deflection equations. Although this subject is treated exhaustively in standard treatises,[6] a cursory summary is considered necessary in order to make the present discussion reasonably self-contained.

A typical member connecting joints i and j is shown in Fig. 2. It is subjected to an axial force P_{ij}, which is considered positive in compression. It is also subjected to a lateral load $q_{ij}(x)$, which is positive if its direction is clockwise relative to the x-axis pointing from i to j. The rotation of joint i is θ_i. If ρ_{ij} and β_{ij} are, respectively, the bar rotation and the slope of the deflected beam at joint i relative to the deflected cord (i, j), then the continuity of the structure requires that

$$\theta_i = \beta_{ij} + \rho_{ij} = \beta_{ih} + \rho_{ih} = \ldots \quad \ldots\ldots\ldots\ldots (1)$$

if all terms are defined to be positive if clockwise.

---

5 "Die Stabilitat lotrecht belasteter Rechteckramen," by E. Chwalla, Der Bauingenieur, Vol. 19, 1938, p. 69.

6 Buckling Strength of Metal Structures, by F. Bleich, McGraw-Hill Book Co., Inc., New York, 1952.

7 "Buckling of a Simple Portal Frame," by A. H. Chilver, Journal of the Mechanics of Physical Solids, Vol. 5, 1956, p. 18.

8 Discussion by Eugene Guillard of "Influence of Partial Base Fixity on Frame Stability," by T. V. Galambos, Proceedings, ASCE, Vol. 86, No. ST 5, May, 1960, p. 153.

9 "On the Buckling Strength of Frames," by I. C. Chang, thesis presented to the Illinois Inst. of Tech., in Chicago, Ill., in 1958, in partial fulfillment of the requirements for the degree of Doctor of Philosophy.

The bending moment (also positive clockwise) acting on the bar (i, j) at joint i is M_{ij}. According to elementary beam theory, the bending moments and joint rotations, in view of Eq. 1, are related by

$$M_{ij} = K(\theta_i + C\,\theta_j) - \overline{K}\,\rho_{ij} + M^f_{ij} \quad \ldots\ldots\ldots \quad (2a)$$

and

$$\overline{K} = K(1 + C) \quad \ldots\ldots\ldots\ldots\ldots\ldots \quad (2b)$$

in which subscripts have been retained only when their omission may lead to ambiguities. If the bar in question is prismatic, that is, if its modulus of elasticity E and moment of inertia I are independent of x, then

$$K = \frac{E\,I}{L}\,\phi\,\frac{\sin\phi - \phi\cos\phi}{2 - 2\cos\phi - \phi\sin\phi} \quad \ldots\ldots\ldots \quad (3a)$$

$$C = \frac{\phi - \sin\phi}{\sin\phi - \phi\cos\phi} \quad \ldots\ldots\ldots\ldots \quad (3b)$$

and

$$\phi^2 = \frac{P\,L^2}{E\,I} \quad \ldots\ldots\ldots\ldots\ldots \quad (3c)$$

In these equations K represents the stiffness coefficient, while C may be interpreted as the "carry-over factor." Both are tabulated as functions of the

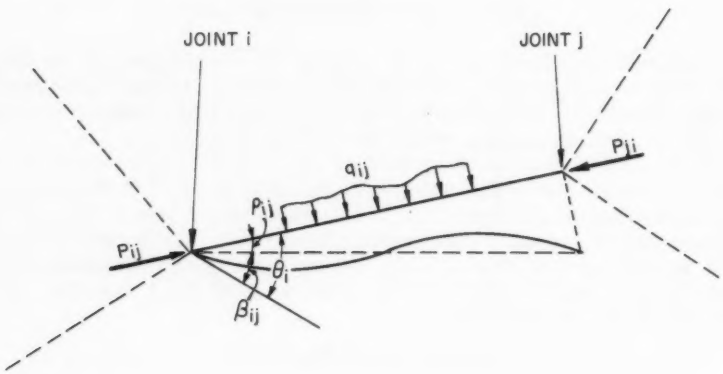

FIG. 2.—TYPICAL MEMBER

dimensionless factor ϕ in another publication,[10] although the notation used there is slightly different from the present notation. For the case of tension, that is, when P is negative, ϕ becomes imaginary and the trigonometric functions in Eqs. 3 are replaced by their hyperbolic equivalents. For $\phi = 0$ the values of K and C approach the conventional $4\,E\,I/L$ and 1/2, respectively.

[10] "Extended Tables of Stiffness and Carry-Over Factor for Structural Members Under Axial Load," by E. E. Lundquist and W. D. Kroll, Wartime Report L-255, N.A.C.A. (Originally 4B24, 1944).

In Eq. 2 the term M^f represents a "fixed-end moment." This can be expressed in the form

$$M_{ij}^f = -K(F_{ij} + C\,F_{ji}) \quad \ldots\ldots\ldots\ldots\ldots\ldots \quad (4a)$$

and

$$F_{ij} = \frac{1}{P}\int_0^L q_{ij}(x)\left[\frac{\sin\phi\left(1-\frac{x}{L}\right)}{\sin\phi} - \left(1-\frac{x}{L}\right)\right]dx \quad \ldots\ldots \quad (4b)$$

Two special cases may be considered here:

(a) $q(x) = q_o$ = constant:

$$F_{ij} = -F_{ji} = \frac{q_o L}{2P}\left(\frac{2}{\phi}\tan\frac{\phi}{2} - 1\right) \quad \ldots\ldots\ldots\ldots \quad (5a)$$

(b) a concentrated force of magnitude Q applied at a distance αL from joint i:

$$F_{ij} = \frac{Q}{P}\left[\frac{\sin\phi\,(1-\alpha)}{\sin\phi} - (1-\alpha)\right] \quad \ldots\ldots\ldots\ldots \quad (5b)$$

The moment equations of equilibrium at joint i require that

$$\sum_j M_{ij} = 0 \quad (i = 1, 2, \ldots) \quad \ldots\ldots\ldots\ldots\ldots\ldots \quad (6)$$

in which the summation extends over all the bars connected at joint i. The number of equations so obtained is equal to the number of unknown joint rotations θ_i. There is an equation of equilibrium against rotation for each bar; the number of equations so obtained equals the number of bar shears. Finally, two force equations of equilibrium per joint correspond to the number of unknown axial bar forces plus the number of independent bar rotations that the kinematic constraints of the structure permit.

In the present paper this is applied to the example shown in Fig. 1; this example has been chosen in order to afford a comparison between the method of analysis described in the present paper and the numerical results obtained elsewhere.[5] Complete symmetry of both the structure and the loading system is assumed.

From the equations of equilibrium of the structure as a whole, it follows that the axial forces in the bars are given by

$$P_{AB} = Q\left(1 - 2\frac{w}{L}\right) \quad \ldots\ldots\ldots\ldots\ldots \quad (7a)$$

$$P_{CD} = Q\left(1 + 2\frac{w}{L}\right) \quad \ldots\ldots\ldots\ldots\ldots \quad (7b)$$

and

$$P_{BC} = H \quad \ldots\ldots\ldots\ldots\ldots\ldots \quad (7c)$$

In Eqs. 7, w represents the sidesway of the cross beam and is assumed to be positive to the right. From the symmetry of the problem w = 0 in the present case; nevertheless, the term is included in Eqs. 7 for the purpose of later comparison with nonsymmetric configurations. The redundant horizontal re-

action is designated by H. From Eq. 6 it follows, in view of Eqs. 2, the condition of symmetry, and the kinematics of the structure that

$$\theta_B = -\theta_C = -\frac{M_B^f}{\tilde{K}_{AB} + K_{BC}(1 - C_{BC})} \quad \left(\tilde{K} = K(1 - C^2)\right) \ldots\ldots (8)$$

The equilibrium of the left column requires that

$$\tilde{K}_{AB}\left(\theta_B - \frac{w}{h}\right) = H\,h - P_{AB}\,w \ldots\ldots\ldots\ldots (9)$$

in which both sides represent M_{BA}. Again $w = 0$ in the present case.

Eqs. 8 and 9 are combined to eliminate the joint rotation θ_B. When Eqs. 3, 4, 5(b), and 7 are substituted this leads to the following relationship between H and the applied load Q:

$$\frac{H^2}{Q^2}(1 - \phi \cot \phi)\cos\frac{\Psi}{2} + \cos\frac{\Psi}{2} - \cos\Psi\,(1 - \alpha) + \frac{\Psi\,h\,H}{Q\,L}\sin\frac{\Psi}{2} = 0 \ldots (10a)$$

$$\phi^2 = \frac{Qh^2}{E\,I} \ldots\ldots\ldots\ldots\ldots\ldots (10b)$$

and

$$\Psi^2 = \frac{H\,L^2}{E\,I'} \ldots\ldots\ldots\ldots\ldots\ldots (10c)$$

In Eqs. 10, I and I' are used for the moments of inertia of the columns and of the cross beam, respectively. Eqs. 10 can be simplified greatly by considering that Ψ is usually a very small quantity. When the appropriate trigonometric expressions are expanded in a Taylor series near $\Psi = 0$, and only the lowest terms are included, this leads to the approximate relation

$$\frac{Q\,L^2}{2\,E\,I'}\,\alpha(1 - \alpha) = H\left[\frac{h\,L}{2\,E\,I'} + \frac{1}{Q}(1 - \phi \cot \phi)\right] \ldots\ldots\ldots (10d)$$

From Eq. 10(d) H can be determined explicitly in terms of Q.

Up to this point the analysis is conventional and agrees with similar discussions given elsewhere.[5,6] The question arises as to whether the equilibrium configuration so obtained is stable or not. In the present paper, instability is postulated if, in addition to the configuration just obtained, there also exists one which is adjacent to it while the loads retain their magnitude and direction and their position relative to the moving frame. (This definition of instability is not open to question here. It is inherent in most classical treatments since Euler and has been discussed exhaustively by H. Ziegler,[11] who has reconfirmed its validity as well as its limitations.) The existence of such a condition implies one of two possibilities:

(1) the load deflection curve has reached a maximum point, with collapse imminent;

(2) there exists a bifurcation of the load-deflection relationship, which, in the present example, signifies the possibility of impending sidesway.

The first case, although of potential interest in problems involving symmetry as in the present example, is usually of primary importance only if such

11 "On the Concept of Elastic Stability," by H. Ziegler, Advances in Applied Mechanics, Vol. 4, Academic Press, Inc., New York, 1956, p. 351.

symmetry is not present. For the symmetrical example under consideration, the problem of general interest is that of the bifurcation of the equilibrium configuration, when an asymmetric configuration (sidesway) is imposed on the existing state of the structure; this occurs when the load Q reaches its critical value.

For this adjacent state of equilibrium Eqs. 2 and 6 continue to be valid; however, the moments M are replaced by $M + \Delta M$, the rotations ρ by $\rho + \Delta\rho$, and so forth. Furthermore, the coefficients K and C also change and must be replaced by $K + \Delta K$ and $C + \Delta C$, as will be demonstrated later. If these new terms are then inserted in Eqs. 2 and 6, if the original Eqs. 2 and 6 are subtracted from the ensuing relationships, and if all terms of order higher than the first in the incremental terms are deleted, the incremental equations of moment equilibrium take the form

$$\sum_j \Delta M_{ij} = 0 \quad \ldots\ldots\ldots\ldots\ldots\ldots \quad (11)$$

In Eq. 11 the incremental moments ΔM are expressed by

$$\Delta M_{ij} = K\left(\Delta\theta_i + C\,\Delta\theta_j\right) - \overline{K}\,\Delta\rho + \Delta G_{ij} \quad \ldots\ldots\ldots\ldots (12a)$$

and

$$\Delta G_{ij} = \Delta M^f_{ij} + \theta_i\,\Delta K + \theta_j\,\Delta(C\,K) - \rho\,\Delta\overline{K} \quad \ldots\ldots\ldots\ldots (12b)$$

Eqs. 12, together with appropriate incremental equations of bar equilibrium, represent the condition of neutral equilibrium as outlined above. The terms ΔG account for the effect of the prebuckling deformations and, hence, of the primary bending moments; they vanish if these effects are ignored, in which case the analysis becomes identical with the analysis proposed in the standard literature.

In Eqs. 12 the terms ΔK, ΔM^f, for example, represent the change in the stiffness factor, fixed-end bending moment, and so forth, associated with the change in the axial force in the individual bars resulting from the change in the equilibrium configuration. That is, after linearization,

$$\Delta K = K'\,\Delta P \quad \ldots\ldots\ldots\ldots\ldots\ldots (13a)$$

$$\Delta C = C'\,\Delta P \quad \ldots\ldots\ldots\ldots\ldots\ldots (13b)$$

and

$$\Delta F = F'\,\Delta P \quad \ldots\ldots\ldots\ldots\ldots\ldots (13c)$$

in which $K' = dK/dP = (dK/d\phi)(d\phi/dP)$; the expression for ΔF is needed in view of Eqs. 4.

Expressions for K', C', for example, appearing in Eqs. 13, are obtained by differentiating Eqs. 3 with respect to ϕ. When ϕ is eliminated from the resulting formulas through the use of Eqs. 3, then, after some manipulation, the following set of expressions is obtained:

$$K' = \frac{K}{2P}\left(1 - C^2\,\frac{K\,L}{E\,I}\right) \quad \ldots\ldots\ldots\ldots\ldots (14a)$$

$$C' = \frac{1+C}{2P}\left[1 - C\,K(1-C)\,\frac{L}{E\,I}\right] \quad \ldots\ldots\ldots\ldots (14b)$$

$$\overline{K}' = \frac{\overline{K}}{2P}\left(2 - \frac{C K L}{E I}\right) \quad \ldots\ldots\ldots\ldots\ldots\ldots (14c)$$

$$(C K)' = \frac{K}{2P}\left(1 + 2C - \frac{C K L}{E I}\right) \quad \ldots\ldots\ldots\ldots\ldots\ldots (14d)$$

and

$$\widetilde{K}' = \frac{\widetilde{K}}{2P}\left(\frac{1 - 3C}{1 - C} + C^2 \frac{K L}{E I}\right) \quad \ldots\ldots\ldots\ldots\ldots\ldots (14e)$$

Eqs. 14 were first introduced elsewhere.[12] An expression for ΔM^f, that appears in Eqs. 12, can be obtained similarly; this is done by considering Eqs. 4 and by differentiating the expression for F with respect to ϕ. The result depends of course on the individual loading case, but the effect of this term is in general small. It often vanishes altogether; this is, for example, true in the present case because, as will be shown later, $\Delta P = 0$ for the cross bar during buckling.

In most cases, the axial force in the column is small compared with the Euler force associated with a simply supported column. With ϕ thus approaching zero, the expressions in Eqs. 14 may be approximated, near $\phi = 0$, by

$$\frac{P K'}{K} = \frac{-\phi^2}{30} \pm \ldots \quad \ldots\ldots\ldots\ldots\ldots\ldots (15a)$$

$$\frac{P \overline{K}'}{\overline{K}} = \frac{-\phi^2}{60} \pm \ldots \quad \ldots\ldots\ldots\ldots\ldots\ldots (15b)$$

$$\frac{P \widetilde{K}'}{\widetilde{K}} = \frac{-\phi^2}{15} \pm \ldots \quad \ldots\ldots\ldots\ldots\ldots\ldots (15c)$$

and

$$\frac{P C'}{(1 - C^2)} = \frac{+\phi^2}{30} \pm \ldots \quad \ldots\ldots\ldots\ldots\ldots\ldots (15d)$$

Some of the terms given in Eqs. 14 and 15 have been tabulated[9] as functions of ϕ.

If one end of the bar, for example, joint j, is hinged the equivalent expressions for Eqs. 2 and 12 become somewhat simpler and are given by

$$M_{ij} = \widetilde{K}(\theta_i - \rho) \quad \ldots\ldots\ldots\ldots\ldots\ldots (16a)$$

and

$$\Delta M_{ij} = \widetilde{K}\left(\Delta\theta_i - \Delta\rho\right) + \widetilde{K}'\left(\theta_i - \rho\right) \Delta P \quad \ldots\ldots\ldots (16b)$$

in which $\widetilde{K}'$ given in Eqs. 14 or 15.

In view of Eqs. 13 the terms ΔG appearing in Eqs. 12 contain ΔP representing the change in the axial force in the corresponding bar. This axial force P may be found from the reaction if the equilibrium configuration of the structure is taken into consideration, the latter being uniquely expressed in terms of the bar rotations ρ. In turn, some of these reactions may be established by means of the equations of equilibrium for the whole structure; they are, therefore, functions of the bar rotations ρ as well as of the remaining (that is, "re-

12 "Post-Buckling Strength of Redundant Trusses," by E. F. Masur, Transactions, ASCE, Vol. 119, 1954, p. 699.

dundant") reactions R. If the bar rotations ρ and the redundant reactions R are used as independent variables the incremental bar forces may then be expressed in the form

$$\Delta P = \sum \left(\frac{\partial P}{\partial \rho}\right)\Delta\rho + \sum\left(\frac{\partial P}{\partial R}\right)\Delta R \quad \ldots\ldots\ldots\ldots \quad (17)$$

in which the summations extend over the unknown rotations and redundant reactions, respectively.

In the present case, the kinematics of the structure shown in Fig. 1 implies that $\rho_{AB} = \rho CD = w/h$, whereas $\rho_{BC} = 0$. The only redundant reaction in the present case is H. It follows therefore, by applying the incremental process to Eqs. 7 (with Q held constant) that

$$\Delta P_{AB} = -\Delta P_{CD} = -\frac{2\,Q\,\Delta w}{L} \quad \ldots\ldots\ldots\ldots (18a)$$

and

$$\Delta P_{BC} = \Delta H \quad \ldots\ldots\ldots\ldots\ldots\ldots (18b)$$

Incremental equations of equilibrium for the two columns are obtained from Eq. 9 and from an equivalent equation for the bending moment M_{CD}. With w = 0 this leads to

$$\tilde{K}_{AB}\left(\Delta\theta_B - \frac{\Delta w}{h}\right) - h\,\Delta H + Q\,\Delta w\left(1 - \frac{2\,\theta_B\,\tilde{K}'_{AB}}{L}\right) = 0 \quad \ldots\ldots (19a)$$

$$\tilde{K}_{CD}\left(\Delta\theta_C - \frac{\Delta w}{h}\right) + h\,\Delta H + Q\,\Delta w\left(1 + \frac{2\,\theta_C\,\tilde{K}'_{CD}}{L}\right) = 0 \quad \ldots\ldots (19b)$$

in which the first equation refers to the left column and the second equation to the right column.

The incremental joint equations of equilibrium corresponding to Eq. 11 are found similarly. In view of Eqs. 12, 13, 16, and 18 this leads eventually to the system of equations

$$\left(\tilde{K}_{AB} + K_{BC}\right)\Delta\theta_B + C_{BC}\,K_{BC}\,\Delta\theta_C - \frac{\tilde{K}_{AB}\,\Delta w}{h} - \frac{2\,\tilde{K}'_{AB}\,Q\,\theta_B\,\Delta w}{L} + \left[\frac{dM^f_{BC}}{dP} + K'_{BC}\,\theta_B + \left(C_{BC}\,K_{BC}\right)'\theta_C\right]\Delta H = 0 \ldots (20a)$$

and

$$\left(\tilde{K}_{CD} + K_{BC}\right)\Delta\theta_C + C_{BC}\,K_{BC}\,\Delta\theta_B - \frac{\tilde{K}_{CD}\,\Delta w}{h} + \frac{2\,\tilde{K}'_{CD}\,Q\,\theta_C\,\Delta w}{L} + \left[\frac{dM^f_{CB}}{dP} + K'_{BC}\,\theta_C + \left(C_{BC}\,K_{BC}\right)'\,\theta_B\right]\Delta H = 0 \quad \ldots\ldots (20b)$$

of which Eq. 20(a) refers to joint B and Eq. 20(b) to joint C.

Eqs. 19 and 20 are four linear homogeneous equations in the four unknowns $\Delta\theta_B$, $\Delta\theta_C$, ΔH, and Δw. As usual, a nontrivial solution is possible if and only if the determinant of the coefficients vanishes; this represents the characteristic equation of neutral equilibrium.

In the present example, the determinant splits into two (2 x 2) determinants by virtue of the symmetry of the problem $\left(\tilde{K}_{AB} = \tilde{K}_{CD},\ \theta_B = -\theta_C,\right.$ and

so forth). The two cases represented by these two subdeterminants are as follows:

(1) $\Delta\theta_B = -\Delta\theta_C$ and $\Delta w = 0$. This means that the symmetry of the configuration is retained and the load-deflection diagram has reached its highest point. In most structural problems of practical significance the critical value of Q so obtained is much higher than the one found from the second case; this condition will therefore not be pursued further.

(2) $\Delta\theta_B = \Delta\theta_C = \Delta\theta$ and $\Delta H = 0$. In that case

$$\left(\tilde{K}_{AB} + K_{BC}\right)\Delta\theta - \left(\frac{\tilde{K}_{AB}}{h} + 2\,Q\,\theta_B\,\frac{\tilde{K}'_{AB}}{L}\right)\Delta w = 0 \quad \ldots\ldots\ldots (21a)$$

and

$$\tilde{K}_{AB}\,\Delta\theta - \left(\frac{\tilde{K}_{AB}}{h} + 2\,Q\,\theta_B\,\frac{\tilde{K}'_{AB}}{L - Q}\right)\Delta w = 0 \quad \ldots\ldots\ldots (21b)$$

The vanishing of the determinant of this subsystem corresponds to

$$\left(\frac{\tilde{K}_{AB}}{h} + 2\,Q\,\theta_B\,\frac{\tilde{K}'_{AB}}{L}\right) r - Q = 0 \quad \ldots\ldots\ldots\ldots (22a)$$

and

$$r = \frac{\overline{K}_{BC}}{\left(\tilde{K}_{AB} + \overline{K}_{BC}\right)} \quad \ldots\ldots\ldots\ldots\ldots\ldots (22b)$$

in which r may be interpreted as a "moment distribution factor" at joint B associated with an antisymmetric deformation. The term θ_B in Eqs. 22 is found from Eq. 8 and represents the effect of the primary bending moment for the example under consideration; if it is omitted, the analysis agrees with that described elsewhere.[6]

If in Eqs. 22 the appropriate expressions for the stiffness factors and their derivatives are substituted, and if Eq. 8 is considered, the characteristic equation eventually takes the form

$$\phi \cot \phi - \frac{2\,Q\,h}{H\,L}\left(1 - \frac{\Psi}{2}\cot\frac{\Psi}{2}\right) + \frac{H\,h}{Q\,L}\left(2 - \phi\cot\phi - \phi^2 \csc^2\phi\right) = 0 \quad \ldots (22c)$$

Eq. 22(c) must be solved jointly with Eqs. 10 governing the value of H. It is interesting to note that, except for a slight difference in the second term, which accounts for the presence of a small axial force in the cross beam, Eq. 22(c) is identical with that given by Chwalla.[5] However, Chwalla's work involves the integration of several differential equations and the satisfaction of the associated boundary conditions. The last term represents the effect of the primary bending moments because H = 0 if the loads are applied at the joints, that is, if $\alpha = 0$.

Numerical values have been obtained for the special case I = I' and L = h. If $\alpha = 1/3$ the critical force Q is given by $\phi^2 = 1.775$ as against $\phi^2 = 1.816$ for $\alpha = 0$. It is seen, as already pointed out by Chwalla, that the introduction of primary bending moments results in a very small reduction of the critical load. It would, of course, be hasty to predict that the relative insignificance of this reduction applies to all problems of practical interest. In particular, when the primary bending moments are such that the elastic limit of the material is ex-

ceeded, the effect of the primary bending moments may become far more pronounced. (This is clearly true in the present example unless the members are assumed to be unrealistically slender.) Conversely, it is not to be ruled out that primary bending moments may actually increase the stability of the structure. This is demonstrated in the next section; attention is also called to the well-known fact that the lateral stability of beams is increased under certain circumstances if their prebuckling deformation is taken into consideration.

MOMENT DISTRIBUTION

The form of the equations developed in the previous section suggests that a moment distribution technique may be developed that permits the establishment of the solution through successive approximating steps. (Similarly, a solution based on compatibility conditions corresponds to an "angle-change distribution" method. No advantage is apparent in the application of such a method to the present problem; moreover, its convergence is less rapid and, in some cases, open to question altogether.) For the simplified problem (that is, in the absence of primary bending moments) this was first introduced by G. Winter, F. ASCE,[13] P. T. Hsu, B. Koo, for the single-story frame and was extended by E. F. Masur, M. ASCE,[14] to multiple stories. In Winter's paper[13] the magnitude of the load is assumed and the horizontal force necessary to produce a sidesway is computed by means of moment distribution. So long as this force is positive, that is, in the direction of the assumed sidesway, the frame is stable; by repeated trials the critical load, which corresponds to sidesway without lateral force, can be obtained through interpolation. In Masur's work[14] the process is generalized to investigate the positive definiteness of a matrix. Again, interpolative techniques are employed, together with the establishment of upper and lower bounds to aid in the solution of the problem.

In the present paper, the technique introduced by Winter[13] is extended to the case in which primary bending moments are present. Further extensions are possible, and fairly obvious, for the multi-story building, to which the boundedness principles of Masur[14] can be shown to apply also. A rectangular frame like the one shown in Fig. 1 will be treated first; in that case it is permissible to ignore the effect of the horizontal reaction H on the stiffness of the beam BC, although such an effect could readily be included in the treatment.

To start with, the magnitude of the force Q is assumed and the associated rotations, moments, and so forth, are determined by standard methods, as reviewed previously. It is convenient to restate Eqs. 2, that, with the simplifications just mentioned, take the form

$$M_{ij}^{b} = \frac{4\,E\,I}{L}\left(\theta_i + \frac{1}{2}\,\theta_j\right) + M_{ij}^{f} \quad \ldots\ldots\ldots\ldots (23a)$$

and

$$M_{ij}^{c} = K\left(\theta_i + C\,\theta_j\right) \quad \ldots\ldots\ldots\ldots\ldots (23b)$$

---

13 "Buckling of Trusses and Rigid Frames," by G. Winter, P. T. Hsu, B. Koo, and M. H. Loh, Cornell Univ. Experiment Sta., Bulletin No. 36, 1948.

14 "On the Lateral Stability of Multi-Story Bents," by E. F. Masur, Proceedings Separate No. 672, ASCE, Vol. 81, 1955.

in which the superscripts b and c refer to beams and columns, respectively, and in which the effect of symmetry (that is $\rho = 0$) has been included.

If now the structure undergoes a virtual sidesway Δw, the joint rotations θ, the stiffness factor K, and the carry-over factor C change their values slightly. Therefore, similar to Eqs. 12,

$$\Delta M_{ij}^{b} = \frac{4\,E\,I}{L}\left(\Delta\theta_i + \frac{1}{2}\,\Delta\theta_j\right) \ldots\ldots\ldots\ldots\ldots (24a)$$

and

$$\Delta M_{ij}^{c} = K\left(\Delta\theta_i + C\,\Delta\theta_j\right) + \theta_i\,\Delta K + \theta_j\,\Delta(C\,K) - \frac{\overline{K}}{h}\,\Delta w \ \ldots\ldots (24b)$$

in which ΔK and $\Delta(C\,K)$ are obtainable from Eqs. 13, 14, and 18. Because Eqs. 23 imply

$$\theta_i = \frac{1}{\tilde{K}}\left(M_{ij}^{c} - C\,M_{ji}^{c}\right) \ldots\ldots\ldots\ldots\ldots (25)$$

it follows from Eq. 24(b) that

$$\Delta M_{ij}^{c} = K\left(\Delta\theta_i + C\,\Delta\theta_j\right) + \Delta M_{ij}^{cf} \ldots\ldots\ldots\ldots (26a)$$

and

$$\Delta M_{ij}^{cf} = \pm\frac{2\,Q}{L}\left[\left(\frac{K'}{K} - \frac{C\,C'}{1-C^2}\right)M_{ij}^{c} + \frac{C'}{1-C^2}\,M_{ji}^{c}\right]\Delta w - \frac{\overline{K}}{h}\,\Delta w \ \ldots (26b)$$

in which the positive and negative signs refer to the right and left column, respectively.

When the additional moments from the first of Eqs. 24 and from Eqs. 26 are substituted in the equations of equilibrium (Eq. 11), the resulting system of equations is similar to the conventional slope-deflection equations, with the term ΔM_{ij}^{cf} representing a fixed-end moment applied at the top and bottom of each column. It is therefore possible to solve this system through a sequence of successive approximations. In particular, the moment distribution technique is most useful because it permits the determination of the additional moments (and hence, of the additional shears) without the actual determination of the additional joint rotations. Owing to the linearity of the system, the results depend linearly on the magnitude of Δw. The latter is therefore arbitrary and may, if convenient, be equated to unity.

The proposed procedure is therefore as follows:

(1) Assume a value of Q and find all stiffness factors and bending moments by conventional methods.

(2) Assume a sidesway of arbitrary magnitude, say, $\Delta w = 1$. This is equivalent to the application of a fixed-end bending moment given by Eqs. 26 to the columns at each joint. It is noted that, in the absence of primary bending moments, this reduces to the procedure suggested by Winter.[13] It is also noted that no fixed-end bending moments are applied to the beams in the present case.

(3) Balance the joints and determine the final bending moments ΔM_{ij}^{c} in the columns, using, of course, stiffness factors that are modified by the presence of the assumed axial forces.

(4) Compute the additional column shears from

$$h\,\Delta H_{ij}^{c} = \Delta M_{ij}^{c} + \Delta M_{ji}^{c} + Q\,\Delta w \ldots\ldots\ldots\ldots (27)$$

(5) Check whether the horizontal force ΔF given by

$$\Delta F = - \sum \Delta H_{ij}^{c} \quad \ldots\ldots\ldots\ldots\ldots\ldots \quad (28)$$

is positive, negative, or zero; this implies stable, unstable, or neutral equilibrium, respectively. The summation in Eq. 28 extends over all the columns in the structure.

Two special cases call for a slight modification of the procedure:

(a) If one of the column joints (say, joint j) is hinged, then the equivalent of Eqs. 26 becomes

$$\Delta M_{ij}^{c} = \tilde{K} \Delta \theta_i + \Delta M_{ij}^{cf} \quad \ldots\ldots\ldots\ldots\ldots\ldots (29a)$$

and

$$\Delta M_{ij}^{cf} = \pm \frac{2Q}{L} \frac{\tilde{K}'}{\tilde{K}} M_{ij}^{c} \Delta w - \frac{\tilde{K}}{h} \Delta w \quad \ldots\ldots\ldots\ldots (29b)$$

while ΔM_{ji}^{c}, of course, vanishes.

(b) If joint j is fixed, then

$$\Delta M_{ij}^{c} = K \Delta \theta_i + \Delta M_{ij}^{cf} \quad \ldots\ldots\ldots\ldots\ldots\ldots (29c)$$

and

$$\Delta M_{ij}^{cf} = \pm \frac{2Q}{L} \frac{K'}{K} M_{ij}^{c} \Delta w - \frac{\overline{K}}{h} \Delta w \ldots\ldots\ldots\ldots (29d)$$

In the present example, the initial value of ϕ was assumed to be equal to 1.33, or, equivalently, $Q = 1.769\ E\ I/h^2$; then, with $\alpha = 1/3$, $M_{BC}^{f} = - M_{CB}^{f} = - 0.222\ Q\ L = - 0.393\ E\ I/h$ for $h = L$. Because $\tilde{K}_1 = 2.630\ E\ I/h$ for this value of ϕ, and in view of the symmetry of the initial deformation, the primary bending moments

$$M_{BA} = - M_{CD} = - \frac{2.630}{2.630 + 2.000} M_{BC}^{f} = 0.223\ E\ I/h$$

are obtained by means of moment distribution (or otherwise). From Chang's table[9] and by Eqs. 29(a) and 29(b) it follows that

$$\Delta M_{BA}^{f} = \Delta M_{CD}^{f} = [(0.300)(0.223) - 2.630] \frac{E\ I}{h^2} \Delta w;$$

after moment distribution and in consideration of the antisymmetry of the deformation the additional moments are

$$\Delta M_{BA} = \Delta M_{CD} = \frac{6.000}{6.000 + 2.630} \Delta M_{BA}^{f} = - 1.784 \frac{E\ I}{h^2} \Delta w.$$

From Eq. 27, the additional column shears are

$$\Delta H_{AB} = \Delta H_{CD} = \left(-1.784 \frac{E\ I}{h^2} + Q \right) \frac{\Delta w}{h} = - 0.015 \frac{E\ I}{h^2} \frac{\Delta w}{h}.$$

By Eq. 28, the force F is positive; the structure is, therefore, stable and the assumed value of Q is too low.

An error estimate may now be obtained conveniently by setting $F = 0$ and by solving Eqs. 27 and 28 for Q, using the values of the additional bending mo-

ments that were found previously. The value of $Q = 1.784\ E\ I/h^2$ so determined, as proved for the simplified case presented by Masur,[14] represents an upper bound to the actual critical load; hence,

$$1.769\ \frac{E\ I}{h^2} \leqq Q_{cr} \leqq 1.784\ \frac{E\ I}{h^2}.$$

The next trial value of Q should therefore lie between these two values.

As another example of the effect of primary bending moments the gabled frame shown in Fig. 3 is considered; for the sake of simplicity all members are assumed to have the same E I values. Again the moment distribution technique described earlier in this section is applied, although a few modifications are necessary.

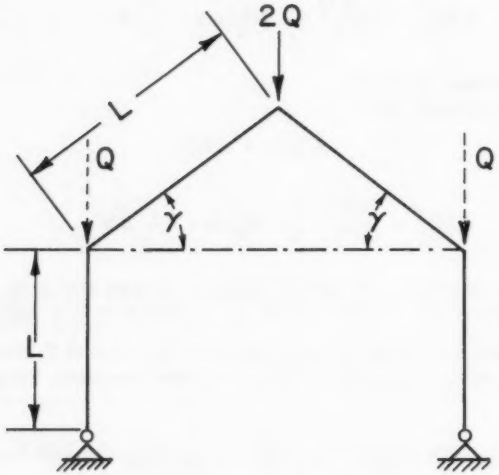

FIG. 3.—GABLE FRAME

To demonstrate the effect of the position of the loads on their critical value the problem is first analyzed under the assumption that the loads are applied at the eaves as shown in dashed lines. In that case, no primary bending moments appear and the type of analysis proposed by Winter[13] can be carried out without difficulty. Because of the symmetry of the structure the problem is again divided into possible modes of buckling:

(1) a buckling configuration that retains symmetry, and
(2) an antisymmetric configuration involving sidesway of the roof structure.

In the first case the critical value of Q can be shown to be determined by the equation

$$\phi^2 = \frac{4\ \tilde{K}}{\tilde{K} + \frac{4\ E\ I}{L}} \left[1 + 3\ \mathrm{csec}\ \gamma + 3 \left(1 + \frac{E\ I}{\tilde{K}\ L} \right) \mathrm{csec}^2\ \gamma \right] \quad \ldots\ldots\ldots (30)$$

in which ϕ is given by Eqs. 3 with reference to either column and $\tilde{K}$ is the associated stiffness coefficient. In the second case the critical load satisfies the relationship

$$\phi^2 = \frac{3\tilde{K}}{\tilde{K} + \frac{3EI}{L}} \quad \ldots\ldots\ldots\ldots\ldots\ldots \quad (31)$$

It is easy to see that the antisymmetric mode is associated with a smaller value of Q and is therefore critical; the latter is independent of γ and assumes the value of $1.39\,\frac{EI}{L^2}$.

As the second approximation to the actual problem, the force is assumed to be applied at the top of the roof; however, the effect of the primary bending moments is to be ignored. This may be visualized by imagining an inextensible cross cable attached to the structure as shown in the figure. In that case the structure is under purely axial stress before buckling if the effect of the change in length of the members is ignored.

Again two modes of instability are possible, of which the one associated with the smaller buckling load involves sidesway. It is governed by the relationship

$$\phi^2 = \frac{\tilde{K}_1 \tilde{K}_2 \frac{L}{EI}}{\tilde{K}_1 + \tilde{K}_2} \quad \ldots\ldots\ldots\ldots\ldots\ldots \quad (32)$$

in which $\tilde{K}_1$ and $\tilde{K}_2$ refer to the column and the rafter, respectively. This leads to the critical load $Q = 1.10\ EI/L^2$, that represents a substantial reduction from the value found previously.

If the cross cable used previously is removed the problem is drastically modified through the development of prebuckling deformations and bending moments. The analysis is lengthy and is therefore not reproduced here for the sake of conserving space. It follows roughly the outline of the analysis of the rectangular frame, the chief modification being the inclusion of the initial rotations of the columns as well as the somewhat more complicated kinematics (that is, two degrees of freedom). Also, the change in the axial force magnitude in the rafters during buckling must be included. The results of the analysis indicate that the structure has been stiffened considerably as a result of the prebuckling deformations. In fact, the first trial solution indicates that the critical load lies between $1.25\ EI/L^2$ and $1.38\ EI/L^2$.

It is interesting to note that this seems to violate a principle of Rayleigh, according to which the relaxation of geometric constraints cannot increase the smallest solution of an eigenvalue problem. Actually this contradiction is more apparent than real; two different neutral equilibrium configurations are being compared here, and the problem falls therefore outside the pale of the Rayleigh principle. (A similar "contradiction" exists in that a shallow spherical cap or a shallow arch can be stiffened against snap-through by relaxing its boundary conditions in such a way that it may undergo certain types of symmetric prebuckling deformations.) The reason for the increase in the stability of a gabled frame seems to lie in the fact that as a result of the initial deformations the load in the rafters is carried only partially in direct compression, the other part being taken up in shear. (There is at least some question as to whether these results are entirely reliable. The assumed inextensibility of the

structural members represents an idealization whose implications should be investigated further. Certainly some obvious contradictions may arise. For example, if the structure shown in Fig. 1 were loaded by a concentrated force at the center of the cross beam the analysis presented here would apply with small modifications. If now, in addition, a column were added to the structure directly under the load, then (in view of the assumed inextensibility of this column) the entire load would be carried by the center column irrespective of its cross section. It follows, therefore, that the buckling load against sidesway would be increased, because the outside columns would be initially stress free; this finite increase would take place for an arbitrarily weak center column--a result that is patently absurd.) However, as in the previous example elastic buckling is highly unlikely for conventional slenderness ratios.

CONCLUSIONS

It appears that, with the techniques introduced in this paper (and especially with the moment distribution procedure described in the previous section), the labor involved in determining the elastic buckling load of the actual problem has not been increased significantly over that involved in the "simplified" problem. It is, therefore, open to question whether the customary neglect of the effect of primary bending moments is, in fact, justifiable from the point of view of economy of computing labor.

It is true that, for the examples considered, primary bending moments affect the stability of the structure only very little; whether this is always true, however, is not clear. In any event, the stability of a partially plastic structure is certain to be intimately related to the presence of primary bending moments. It is suggested that the tools described here may be useful in evaluating this important problem.

ACKNOWLEDGMENTS

This investigation was supported by the Office of Ordnance Research, United States Army, and the National Science Foundation.

Journal of the
ENGINEERING MECHANICS DIVISION
Proceedings of the American Society of Civil Engineers

ANALYSIS OF FRAMES LOADED INTO THE PLASTIC RANGE

By Morris Ojalvo,[1] M. ASCE and Le-Wu Lu,[2] A. M. ASCE

SYNOPSIS

A precise method of analyzing plane frames stressed into the inelastic range is presented. The method involves the determination of a "compatible" moment and rotation at a joint by the intersection of two moment versus end-rotation curves of the adjoining members. The effects of initial residual stresses and instability of beam-columns are considered in the analysis. It is shown how the behavior of frames may be predicted after the attainment of the ultimate loads. Throughout the paper the frames are assumed to fail by excessive bending in the plane of loading. A complete example is included to illustrate the technique developed.

INTRODUCTION

Two assumptions that are commonly made in the analysis of rigid frames, and that reduce the problem to a linear one in structural analysis, are that (a) the material follows Hooke's Law and (b) the deformations of the loaded structure are small in comparison with the dimensions. The latter assumption is cited to justify the formulation of the equilibrium equations on the basis of the undeformed structure.

Note.—Discussion open until January 1, 1962. To extend the closing date one month, a written request must be filed with the Executive Secretary, ASCE. This paper is part of the copyrighted Journal of the Engineering Mechanics Division, Proceedings of the American Society of Civil Engineers, Vol. 87-8, No. EM 4, August, 1961.

[1] Assoc. Prof., Dept. of Civ. Engrg., Ohio State Univ., Columbus, Ohio.
[2] Research Assoc., Fritz Engrg. Lab., Lehigh Univ., Bethlehem, Pa.

Other publications[3,4] consider the inelastic behavior of the structure but make no provisions for the effects of the deformations or the effects of the axial loads on the moment-curvature relationship of the members. Other studies that consider axial load and deformation effects are limited to cases in which the stresses do not exceed the proportional limit in any part of the structure. Two papers[5,6] fall into this category of elastic analysis. They are primarily concerned with the determination of the sidesway buckling load of symmetrical frames when the loads are not applied directly to the joints.

A third method of analysis,[7,8,9] takes into account both inelastic action and deformations, but in a somewhat restricted way. It ignores the effect of axial load on the moment-curvature relationship, and although the displacements of the joints and the deflections at points of concentrated load are considered, the

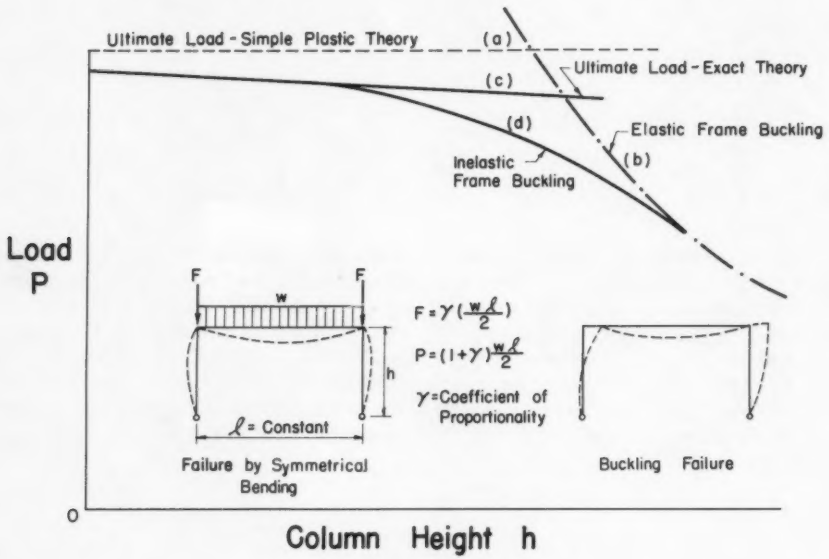

FIG. 1.—LOAD-CARRYING CAPACITY OF FRAMES

3 "Theory of Inelastic Bending with Reference to Limit Design," by A. Hrennikoff, Transactions, ASCE, Vol. 113, 1948, p. 213.

4 "Elastic-Plastic Design of Single-Span Beams and Frames," by H. A. Sawyer, Jr., ASCE Proceedings Separate No. 851, Vol. 181, December, 1955.

5 "Die Stabilitat Lotrecht Belasteter Rechteckrahmen," by E. Chwalla, Der Bauingenieur, Vol. 19, 1938, p. 69.

6 "Stability of Frames in the Presence of Primary Bending Moments," by E. F. Masur, L. H. Donnell, and I. C. Chang, presented at the 1960 Conf. on Structural Mechanics at Purdue Univ. in Lafayette, Ind.

7 "Analysis of Frames with Non-Linear Behavior," by A. H. Ang, Proceedings, ASCE, Vol. 186, No. EM 3, June, 1960, p. 1.

8 "The Analysis of Partially Plastic Redundant Steel Frames," by B. Rawlings, Australian Journal of Applied Science, Vol. 7, No. 1, 1956, p. 10.

9 "The Elasto-Plastic Analysis of Two Experimental Portal Frames," by J. W. Roderick, The Structural Engineer, Vol. 38, No. 8, August, 1960, p. 245.

influence of the displacements at intermediate points is not fully taken into account.

In spite of the good correlation with experimental results that other methods provide,[3,4,5,8,9] the interest in the buckling of frames loaded into the inelastic range has made it desirable to develop a more precise method. The present method will consider inelastic action, axial load effects, and the exact shape of the loaded structure. The scope of the method presented here may be seen by referring to Fig. 1. A symmetrical frame having beam and column elements of specified cross sections is subjected to symmetrical loading as shown. For a specified beam length and varying column heights, the curves give the ultimate load according to the different modes of failure assumed and according to the methods used in the computation of the curves. (In Fig. 1 the load P is equal to half of the total applied loads. It is equivalent to the axial force carried by each column.)

At the specified column height on the chart of Fig. 1, line (a) gives the carrying capacity according to simple plastic theory. This theory assumes failure by symmetrical bending without sidesway. It ignores the reduction in the moment capacity of the columns due to axial load and due to the secondary moments in the columns resulting from their deformations.

Curve (b) assumes purely elastic behavior, with failure caused by sidesway buckling as shown in the right sketch of Fig. 1. Points on this curve are determined by the methods presented elsewhere.[5,6]

Curve (c) gives the ultimate load according to the theory developed in this paper. Failure occurs by excessive symmetrical bending deformations; this mode of failure would occur when a lateral restraint at an upper joint prevents sidesway motion. As will be indicated in an example, the ultimate load is the largest for which an equilibrium configuration of the frame can be found.

Curve (d) gives the true ultimate load of the frame when it is not laterally restrained. A procedure is developed elsewhere[10] for determining a point on this curve. The method may be summarized as follows:

(1) Assume a value for the load.

(2) Perform an exact analysis according to the method described in the present paper. The analysis will give the bending stiffnesses of the frame members for the assumed loading.

(3) Perform a stability analysis to determine whether positive work is required to deform the frame into an adjacent anti-symmetrical shape. This may be performed by the methods outlined elsewhere[11] (where only elastic frames are considered), using the stiffnesses of the partially plastic members (computed in step (2)) in the analysis.

(4) If step (3) indicates a higher or lower buckling load than the one assumed in step (1), a lower or higher load, respectively, is assumed until the analysis of step (3) and the assumed load in step (1) are identical.

DEVELOPMENT OF THE METHOD

Notation.—The letter symbols adopted for use in this paper are defined and arranged alphabetically, for convenience of reference, in the Appendix.

---

[10] "Stability of Elastic and Partially Plastic Frames," by L. W. Lu, thesis presented to Lehigh Univ. in Bethlehem, Pa., in 1960, in partial fulfillment of the requirements for the degree of Doctor of Philosophy.

[11] Theory of Elastic Stability, by S. Timoshenko, McGraw-Hill Book Co., Inc., New York, 1936.

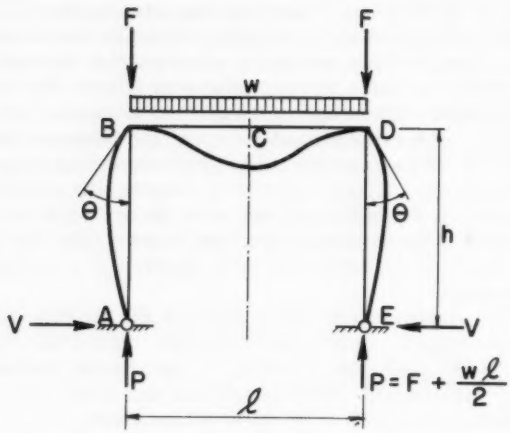
F
F
w
B
C
D
θ
θ
h
V
A
E
V
P
P = F + wℓ/2
ℓ

FIG. 2.

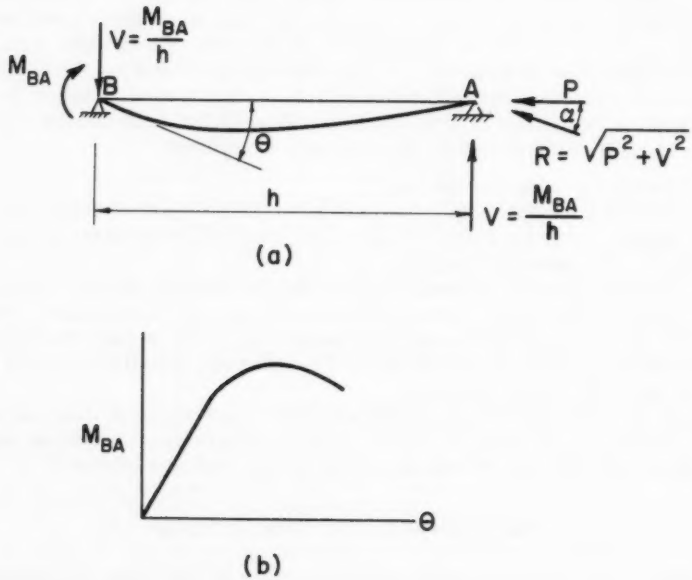
V = M_BA / h
M_BA
B
A
P
α
θ
R = √(P² + V²)
h
V = M_BA / h
(a)
M_BA
θ
(b)

FIG. 3.

The theoretical analysis is subject to the following limitations:

(1) The frame is symmetrical.
(2) The loading is symmetrical.
(3) The members are prismatic.
(4) Only deformations due to flexure are considered.
(5) The members of the structure are made up of columns that have no loads applied to them except possibly at their ends, and beams that have negligibly small axial loads in them. Although allowance for the axial loads in the beams may be made by a trial procedure, the present analysis ignores these effects because of their small influence on the structural behavior. The effect of axial load in the columns is more critical and it is, therefore, taken into account.
(6) The method is non-historic. It is necessary to specify that during the loading there is no strain reversal of material stressed beyond the elastic limit.

A typical structure, shown in Fig. 2, will be used as an illustration of the proposed method. The frame is symmetrical about a vertical axis passing

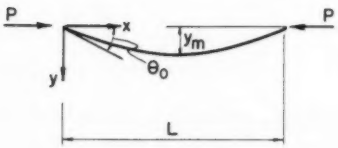

FIG. 4.—COLUMN DEFLECTION CURVE

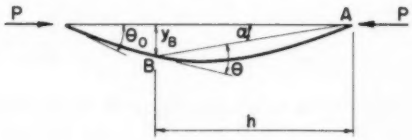

FIG. 5.

through point C. It is desirable at first to consider the columns and the beam of the frame separately.

In Fig. 3(a) the column element BA is shown with axial load P and moment M_{BA} applied to end B. Fig. 3(b) shows how the rotation of end B varies as M_{BA} is slowly increased while the axial load P is maintained constant. A procedure by which the curve in Fig. 3(b) may be obtained follows from the fact that a column such as BA may be considered as a segment of a column deflection curve. The column deflection curve is defined as the shape that a compressed member (identical to the column member except in length) will take when held in a bent configuration by axial loads applied to the ends. Such a column deflection curve is shown in Fig. 4. It may be identified by the angle θ_0 of the initial tangent. An infinite number of column deflection curves are possible for a single cross section and axial load. For each value of θ_0, the column deflection curve will have a different shape. If θ_0 is small so that the stresses in the column deflection curve do not exceed the proportional limit, the curve is a sine wave and its half wave length is determined by the Euler column formula:

$$L = \pi \sqrt{\frac{E\,I}{P}} \quad \ldots\ldots\ldots\ldots\ldots \quad (1)$$

As θ_o becomes larger, y_m increases. When the proportional limit is exceeded over some part of the column, the length shortens. The bending moment at any section is equal to P y. It will be noticed that the segment AB of the column deflection curve in Fig. 5 resembles the column AB in Fig. 3(a). The only difference between the two curves is that the component of the reaction at A in Fig. 3(a) along the direction AB is P, whereas in Fig. 5 it is P cos α. This difference will be examined.

In Fig. 3(a) the angle between the reactive forces at A and the direction AB is:

$$\tan \alpha = \frac{V}{P} = \frac{M_{BA}}{P\,h} \quad \ldots\ldots\ldots\ldots\ldots \quad (2)$$

In Fig. 5 the same angle is given by:

$$\tan \alpha = \frac{y_B}{h} = \frac{M_{BA}}{P\,h} \quad \ldots\ldots\ldots\ldots\ldots \quad (3)$$

It is seen that the angles between the total thrust at A and the direction AB are the same for the segment of the column deflection curve and the actual column.

Next the magnitude of these thrusts will be examined. In Fig. 3(a) the thrust is:

$$R = \sqrt{P^2 + V^2} \quad \ldots\ldots\ldots\ldots\ldots \quad (4)$$

When V is equal to 20% of P, R exceeds P by only 2%. With V equal to 10% of P, R exceeds P by 1/2%; and for smaller ratios of V to P, R approaches P very rapidly. The preceding consideration makes it possible to consider the segment of Fig. 5 equivalent to the column of Fig. 3(a) for all practical cases.

There remains the problem of constructing several column deflection curves for the actual column load. A numerical integration procedure that is based on the moment-curvature (M-θ) relationship of the column is best used here because it is easily adaptable to different cross sections and material properties. The moment-curvature relationship is first determined for the actual axial load, material properties, and column cross section. General methods for determining the M-θ curve and performing the integration for the column deflection curve are outlined elsewhere.[12] For rolled steel wide-flange sections with residual stresses due to uneven cooling, another publication[13] provides information for the determination of the M-θ curve. The integration gives the slope and deflections at intervals along the column deflection curve corresponding to the interval of length used for the integration. It has been noted[14] that with stresses below the proportional limit, the numerical integration gives lengths and maximum ordinates that are in error by less than 0.13%. In the comparisons given elsewhere[14] an interval of length equal to four times the radius of gyration of the section was used.

---

12 Ibid., p. 51.

13 "Plastic Deformation of Wide-Flange Beam Columns," by R. L. Ketter, E. L. Kaminsky, and L. S. Beedle, Transactions, ASCE, Vol. 120, 1955, p. 1028.

14 "Restrained Columns," by M. Ojalvo, thesis presented to Lehigh Univ. in Bethlehem, Pa., in 1960, in partial fulfillment of the requirements for the degree of Doctor of Philosophy.

After several column deflection curves have been computed, the moment-rotation curve (M-θ curve) of Fig. 3(b) may be determined from them. Point B is located on each column deflection curve at a horizontal distance h from one end of the curve (Fig. 5). The moment corresponding to M_{BA} is P y_B while the angle θ is the slope of the tangent at B plus y_B/h. Each column deflection curve is thus seen to furnish the coordinates of a point on the M-θ curve in Fig. 3(b).

Beam member BD can now be considered for the purpose of determining an M_{BD} -θ relation analogous to the M_{BA} -θ relation for the column. The construction of an M_{BD} -θ curve for the beam proceeds from the fact that the shear as well as the slope must be zero at the center of the beam. (When the center section of the beam is fully plastified (formation of a plastic hinge), the M_{BD} -θ curve becomes simply a straight line parallel to the θ axis; Fig. 10 for example.) The deformed shape of the beam in Fig. 6 will be referred

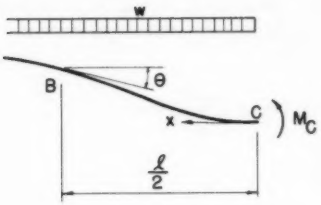

FIG. 6.—BEAM DEFLECTION CURVE

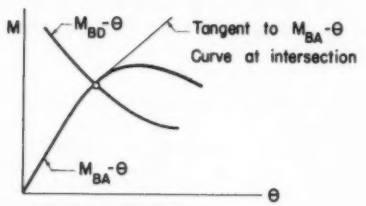

FIG. 7.

to as a beam deflection curve. If one assumes an arbitrary internal bending moment at C (Fig. 6) the bending moment at distance x measured from C is:

$$M_x = - M_C + \frac{w\,x^2}{2} \quad \ldots\ldots\ldots\ldots\ldots \quad (5)$$

A positive bending moment is one that causes tensile stresses on the outside of the frame. By using an integration procedure similar to that used for the columns it is possible to construct several beam deflection curves, each for a different value of the center moment M_C. For each beam deflection curve:

$$M_{BD} = - M_C + \frac{w\,l^2}{8} \quad \ldots\ldots\ldots\ldots\ldots \quad (6)$$

The value of θ at x equal to 1/2 is determined from the numerical integration. Each beam deflection curve, therefore, provides the coordinates of a point on the beam curve M_{BD} -θ in Fig. 7. Because the axial load in the beam is small, a moment-curvature relation for zero axial load may be used for numerical integration without the introduction of an appreciable error. A further refinement to this part of the procedure would require that an estimate be made of V and that a slightly more appropriate M-θ curve be used for the beam curve integration.

When the two M-θ curves, one for the column and one for the beam, are plotted as in Fig. 7 the intersection will give the moment and rotation at B (or D) for the equilibrium configuration of the structure. In other words, of all the combinations of moment and rotation at B that are possible in the column and of all the combinations that are possible for the beam, the correct one is the one that is simultaneously compatible for the beam and the column. Once the correct M and θ at B are determined, it is possible to obtain the forces in the rest of the frame by statics. Deflections may be determined by interpolation from column and beam deflection curves yielding values near the correct values of M and θ.

The stiffness of member BA is given by:

$$K_{BA} = \frac{\Delta M_{BA}}{\Delta \theta} \quad \ldots\ldots\ldots\ldots\ldots \quad (7)$$

On the basis of the Engesser concept of inelastic buckling, in which no unloading is assumed to take place at the instant of buckling, the stiffness of the col-

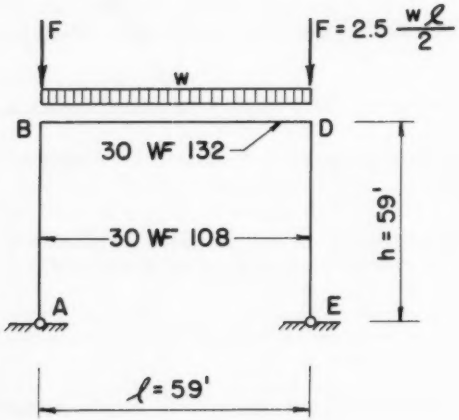

FIG. 8.—ILLUSTRATIVE EXAMPLE

umn is given by the slope of the tangent to the column M-θ curve at its intersection with the beam M-θ curve (Fig. 7). The stiffness K_{BD} (or K_{DB}) for the member BD may be determined in the usual manner by considering the effective flexural rigidity (reduced due to yielding) of all the sections. Detailed procedure for computation can be found elsewhere.[10]

ILLUSTRATIVE EXAMPLE

The behavior of the portal frame shown in Fig. 8 will be investigated in this section by using the procedure described above. The dimensions and member

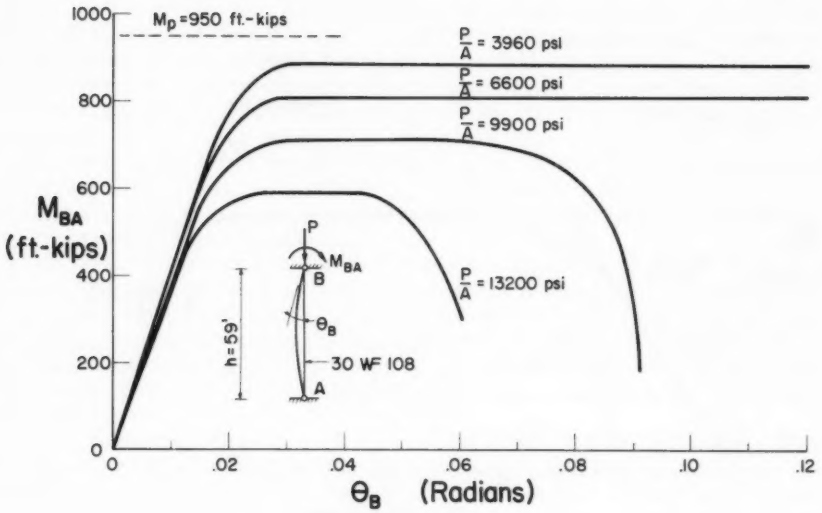

FIG. 9.—M_{BA} VS. θ_B CURVES OF THE COLUMN

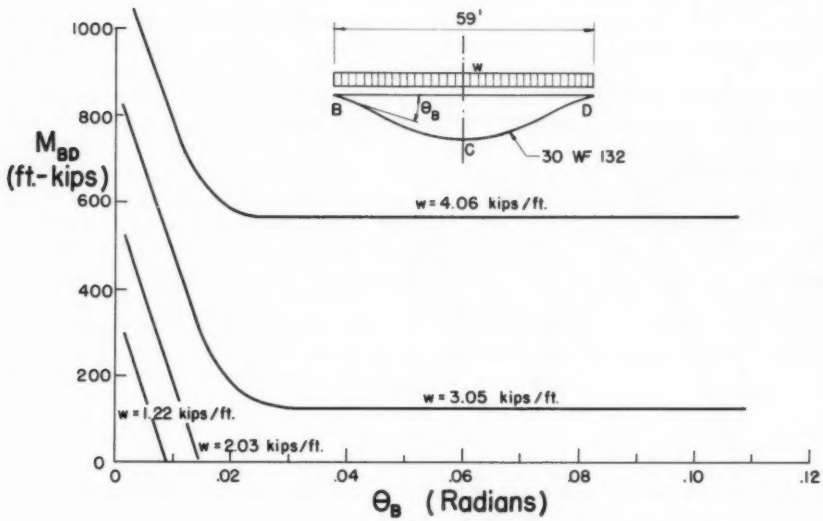

FIG. 10.—M_{BC} VS. θ_B CURVES OF THE BEAM

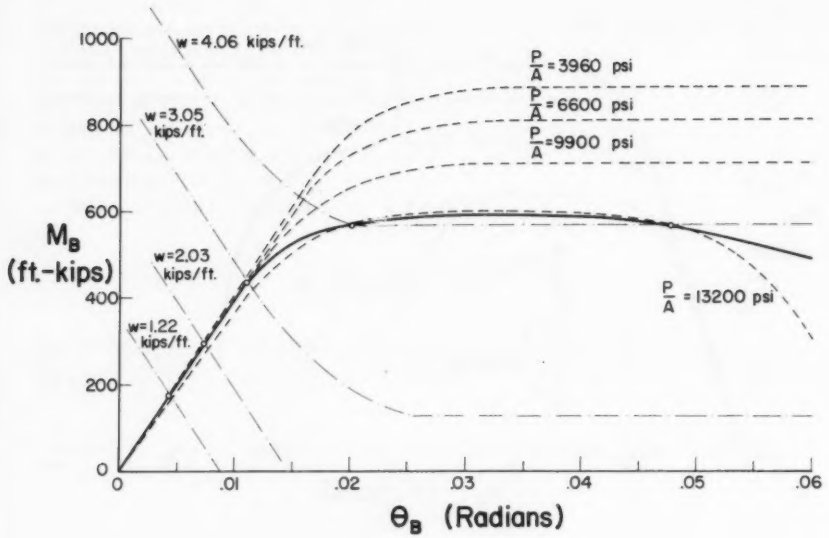

FIG. 11.—MOMENT VS. JOINT ROTATION RELATIONSHIP

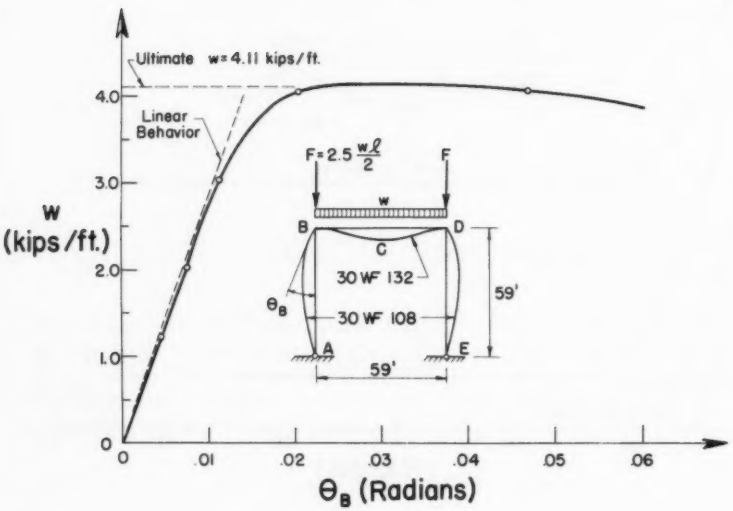

FIG. 12.—LOAD VS. JOINT ROTATION RELATIONSHIP

sizes of the frame were chosen arbitrarily. The stress-strain diagram for the rolled steel members is assumed to be ideally elastic-plastic with a yield stress level at 33,000 psi. The M-ϕ curves that were used in the computations were taken from another source.[13] These curves assumed a well defined residual stress pattern in which a maximum residual stress of about 10,000 psi occurred at the tips of the flanges. Fig. 9 shows M_{BA} -θ curves obtained elsewhere.[14] The M_{BD} -θ curves for the beam (Fig. 10) were taken from another publication.[10]

The ratio of the force F applied directly to the column top to the distributed load w l/2 on the beam, γ, is arbitrarily maintained at 2.5. Solutions for several values of w, corresponding to several stages in the proportional loading of the structure, will be obtained.

The values of w that are considered are w = 1.22, 2.03, 3.05 and 4.06 kips per ft. The corresponding average compressive stresses in the columns are P/A = 3960, 6600, 9900, and 13,200 psi. (The axial forces in the columns, corresponding to these values of stresses, are 0.12, 0.2, 0.3 and 0.4 P_y, in which P_y is the axial yield load ($P_y = A\ \sigma_y$) of the column member.) By combining the curves of Figs. 9 and 10, values of θ and M_B are obtained for each value of w (Fig. 11).

It will be noticed from Fig. 11 that intersections of beam and column M-θ curves occur in pairs until the load reaches a certain maximum value for the frame. At this maximum load the beam and column M-θ curves become tangent. For a frame that is restrained against a premature sidesway buckling failure, a higher load would produce no intersection and thus indicate that the capacity of the frame has been exhausted. For the frame of Fig. 8, the maximum value of w is estimated to be 4.11 kips per ft. The maximum value of w according to simple plastic theory is 4.94 kips per ft, indicating a reduction of 16.8% of the load-carrying capacity due to beam-column action. Fig. 12, which shows the rotation of the joint at B with increasing load, gives a graphic indication of the non-linearity of the structural action.

It is of interest to know whether the ability of the structure to support load diminishes suddenly after the load attains its maximum value or whether the structure's load-carrying capacity is maintained until the deformations become very large. This information is obtainable from the second intersections of the M-θ curves which trace the load deformation characteristics after the maximum load has been reached. Fig. 11 indicates that the unloading will be gradual as long as the M-θ curve for the column has a long flat portion at or near the maximum moment. It is known from a study of M-θ curves for rolled steel wide-flange columns that this will generally be true when the slenderness ratio remains below 60 and the average compressive stress is less than 40% of the yield stress of the steel (it is assumed here that the column does not fail except by excessive bending in its plane).[14]

CONCLUSIONS

A new method of elasto-plastic analysis for rigid frames has been developed in this paper. It is based on the graphical determination of a moment and rotation at a joint by the intersection of two moment-rotation curves of the adjoining members. In constructing these moment-rotation curves, the effects of initial residual stresses and the instability of beam-columns may be included

in the calculations. It is expected that the proposed method would yield results more precise than those obtained by other currently available methods.

The chief importance of the method is that it provides information by which the problem of sidesway buckling of frames in the plastic range may be investigated. It can also be used to determine the carrying capacity of a frame subjected to high axial forces in the columns, but restrained against sidesway

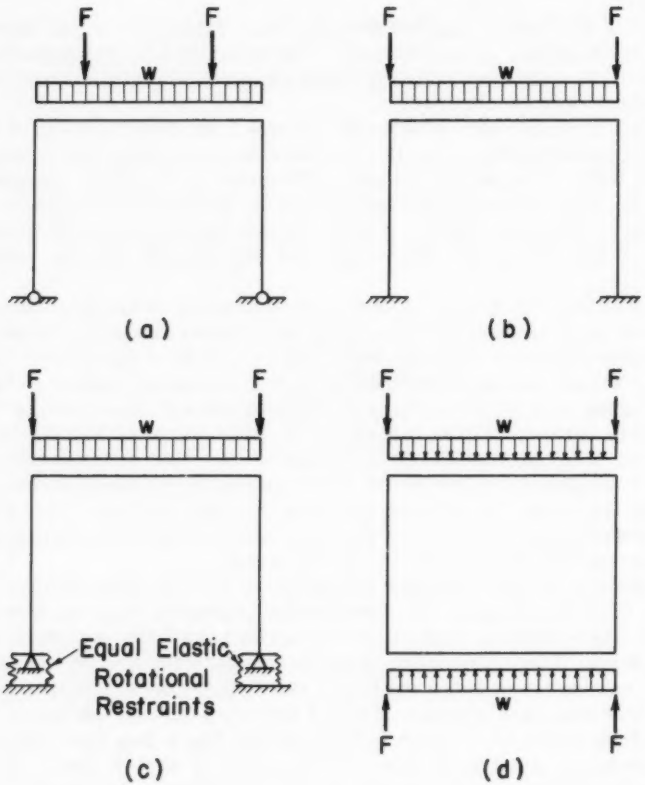

FIG. 13.

movement. It is also of interest when it is desirable to study the behavior of a frame after the attainment of the ultimate load.

The method described herein has been illustrated by reference to a pinned-base symmetrical frame. It is equally valid to the solution of the several symmetrical frames shown in Fig. 13. In each case appropriate sets of moment-

rotation curves of the beam and column are first constructed, the joint moments are then determined by the intersection of these curves.

ACKNOWLEDGMENTS

This study is part of the general investigations "Welded Continuous Frames and Their Components" currently (1961) being carried out at the Fritz Engineering Laboratory of the Cvili Engineering Department of Lehigh University under the general direction of Lynn S. Beedle, F. ASCE. The investigation is sponsored jointly by the Welding Research Council and the Department of the Navy, with funds furnished by the American Institute of Steel Construction, American Iron and Steel Institute, Office of Naval Research, Bureau of Ships, and Bureau of Yards and Docks.

The writers express special thanks to Theordore V. Galambos, A. M. ASCE, and George C. Driscoll, Jr., M. ASCE, for their constructive suggestions that have been incorporated in this paper.

APPENDIX.—NOTATION

A = area of a column cross section (sq in.);

E = modulus of elasticity (kips per sq in.);

F = concentrated load applied to the top of a column (kips);

h = column length (ft);

I = moment of inertia about axis of bending $\left(\text{in.}^4\right)$;

K_{BA}, K_{BD} = stiffness of frame member $\left(\frac{\text{ft-kips}}{\text{radian}}\right)$;

L = half wave length of a column deflection curve (in.);

M, M_C, M_x = internal bending moments (ft-kips);

M_{BA}, M_{BD} = joint moments (ft-kips);

P = axial load in column (kips);

R = resultant thrust in column (kips);

V = shear in column, horizontal reactive force at frame support (kips);

l = span length (ft);

w = distributed load on the beam (kips/ft);

x, y = coordinates;

y_B = deflection at B on a column deflection curve (in.);

y_m = maximum deflection of a column deflection curve (in.);

θ, θ_B, θ_C = rotation of a joint (radians);

θ_o = initial slope on a column deflection curve (radians);

ϕ = curvature of a member (radians/in.);

Δ = symbol indicating a small increment;

α = arctan y_B/h or Arctan V/P (radians); and

γ = coefficient of proportionality.

Journal of the
ENGINEERING MECHANICS DIVISION
Proceedings of the American Society of Civil Engineers

ANALYSIS OF NONCOPLANAR ELASTIC RINGS

By D. H. Pletta,[1] F. ASCE, W. C. Liessner,[2] and Yen-Ming Yeh[3]

SYNOPSIS

The six scalar equations required to determine the components of the indeterminate moments and forces in loaded or distorted elastic rings are derived using vector algebra. Simple sign conventions and easily remembered formulas for "elastic areas" result. The equations may be transformed to the column analogy or to the shear and torsion analogy for the analysis of coplanar rings, or to a corresponding analogy using a single elastic centroid in space for noncoplanar rings. The analysis of a superelevated helical beam is illustrated, using cylindrical rather than cartesian coordinates. The expressions are easily converted to any orthogonal coordinate system.

INTRODUCTION

The analysis of irregularly shaped elastic rings stressed by either applied loads or by distortions is based on either the classical analysis of least work or on the more modern concepts based on satisfying statics and geometry. By using the latter method Hardy Cross, F. ASCE, developed the column analogy[4]

Note.—Discussion open until January 1, 1962. To extend the closing date one month, a written request must be filed with the Executive Secretary, ASCE. This paper is part of the copyrighted Journal of the Engineering Mechanics Division, Proceedings of the American Society of Civil Engineers, Vol. 87, No. EM 4, August, 1961.

[1] Prof. and Head, Engrg. Mechanics Dept., Virginia Polytechnic Inst., Blacksburg, Va.

[2] Engr., Sperry Gyroscope Co., Great Neck, N. Y.; formerly Instr., Engrg. Mechanics Dept., Virginia Polytechnic Inst., Blacksburg, Va.

[3] Engr., Amman and Whitney, Cons. Engrs., New York, N. Y.; formerly Graduate Asst., Engrg. Mechanics Dept., Virginia Polytechnic Inst., Blacksburg, Va.

[4] "The Column Analogy," by Hardy Cross, Bulletin 215, Univ. of Illinois Engrg. Experiment Sta., 1930.

for coplanar rings stressed by forces or displacements lying in the same plane, or by moments or rotations acting about axes perpendicular thereto. James P. Michalos, F. ASCE and Frank Baron, F. ASCE extended the method in their shear and torsion analogy[5] to coplanar rings stressed by moments or rotations acting about axes lying in the same plane, or by forces and displacements acting perpendicular thereto. They also extended the method to cover elastic rings curved in space.[5] The special case of a helical beam without superelevation was analyzed by Alan C. Holmes.[6] In all threee of these studies the analysis was based on a scalar rather than on a vector approach. Other studies on more general noncoplanar rings, such as pipe lines curved or segmental in space, have been made by John E. Brock[7,8] using matrix analysis.

Equations based on a vector or matrix derivation must, of course, be expanded to the more familiar scalar versions when the actual computations are made. Nevertheless, the vector derivation presented herein is considerably shorter and the standard vector sign convention easier to follow than that usually adopted in scalar derivations. Furthermore, the equations in vector form are more easily expressed in the coordinate system most suitable for a particular ring. For example, cylindrical coordinates would usually be more appropriate for a helical beam. Other than this, however, the final resulting scalar equations do not differ from the more familiar scalar analyses[4,5,6] but those derived herein do present expressions for a single elastic centroid or neutral point in space.

The elastic axis of the ring considered herein, can have any arbitrary shape in space, and the modulus of elasticity and cross section can vary in any manner along the ring. The analysis herein is restricted to the case in which (a) the effect of deflections due to longitudinal strain can be neglected, or superimposed, (b) the deflections are small, (c) the curvature per depth ratio is large, and (d) do buckling occurs. The ring can be loaded in any arbitrary manner by either forces and moments, distorted at any point by relative displacements or small rotations, or distorted throughout by temperature changes, shrinkage, etc.

ANALYSIS

Consider any continuous, noncoplanar ring, subject to the restrictions previously listed, in equilibrium and loaded in any arbitrary manner. If the structure is made statically determinate by cutting it at some point A (Fig. 1), the ends and tangents to the elastic axis at A will undergo a relative linear and angular displacement due to the applied forces and moments. These loads will produce a statical force $\overrightarrow{V_S}$ and moment $\overrightarrow{M_S}$ which act on the cross section of each elemental length ds of the ring whose position vector is $\vec{\rho}$.

Continuity can be restored by applying equal and opposite reactive forces $\overrightarrow{V_C}$ and moments $\overrightarrow{M_C}$ at the ends C of rigid brackets connected to the cut ends of

5 "Laterally Loaded Plane Structures and Structures Curved in Space," by James P. Michalos and Frank Baron, Transactions, ASCE, Vol. 117, 1952, p. 279.

6 "Analysis of Helical Beams Under Symmetrical Loading," by Alan C. Holmes, Proceedings, ASCE, Vol. 83, No. ST 6, November, 1957.

7 "Matrix Analysis of Flexible Elements," by John E. Brock, Proceedings, First U. S. Natl. Congress of Applied Mechanics, 1952, p. 285.

8 "A Matrix Method for Flexibility Analysis of Piping Systems," by John E. Brock, Transactions, ASME, Journal of Applied Mechanics, Vol. 74, 1952, p. 501.

the ring at A. The brackets are coincident at no load. The origin of the coordinate system is located in any arbitrary manner at end C of these brackets. The restoring reactions will produce a restoring force $\overrightarrow{V_r}$ and moments $\overrightarrow{M_r}$ on the cross section of each elemental length ds of the ring. Hence the final moments and forces acting on a cross section of ds are

$$\overrightarrow{M} = \overrightarrow{M_S} - \overrightarrow{M_r} \quad \ldots\ldots\ldots\ldots\ldots\ldots \quad (1a)$$

and

$$\overrightarrow{V} = \overrightarrow{V_S} - \overrightarrow{V_r} \quad \ldots\ldots\ldots\ldots\ldots\ldots \quad (1b)$$

and the requirements of both statics and geometry are satisfied.

If, instead of being subjected to actual loads, the ring is distorted by subjecting the two cut ends at point A in Fig. 1 to a linear displacement, or by subjecting the tangents to the elastic axis, there to a small relative angular

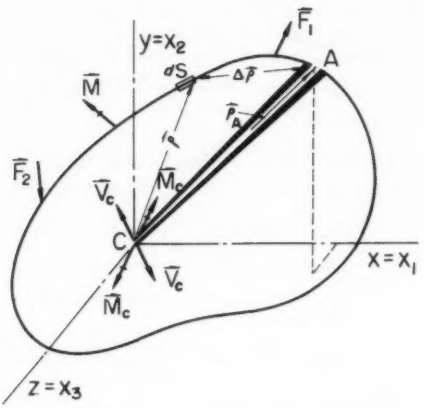

FIG. 1.—LOADED RING WITH REDUNDANTS APPLIED AT THE ORIGIN TO RESTORE CONTINUITY

displacement, the forces $\overrightarrow{V_r}$ and moments $\overrightarrow{M_r}$ would then be the only ones that develop and

$$\overrightarrow{M} = \overrightarrow{M_r} \quad \ldots\ldots\ldots\ldots\ldots\ldots \quad (2a)$$

and

$$\overrightarrow{V} = \overrightarrow{V_r} \quad \ldots\ldots\ldots\ldots\ldots\ldots \quad (2b)$$

The ends and tangents at A can be displaced in any prescribed manner by applying a suitable force $\overrightarrow{V_c}$ and moment $\overrightarrow{M_c}$ at C.

Sign Convention.—The rectangular components parallel to the coordinate axes of the moments $\overrightarrow{M}$, forces $\overrightarrow{V}$, rotations $\overrightarrow{d\theta}$, and displacements $\overrightarrow{\delta}$ will be considered positive if the vectors which represent them act in the direction of the positive axes, provided such components act on the front face of a cross section of the ring. Normally rotations do not obey the law of operation of a

vector even though they possess magnitude and direction. When such rotations are infinitesimal they can be treated as vectors. The right hand rule is used to determine the direction of $\overrightarrow{d\theta}$ and $\overrightarrow{M}$.

The front face of an element is defined as the cross section normal to the elastic axis farthest counter clockwise around the ring when viewed from the

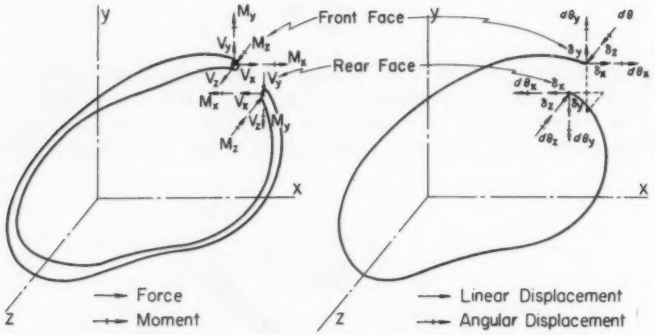

(a) Postive Resisting Forces and Moments

(b) Postive Relative Linear and Angular Displacements

FIG. 2.

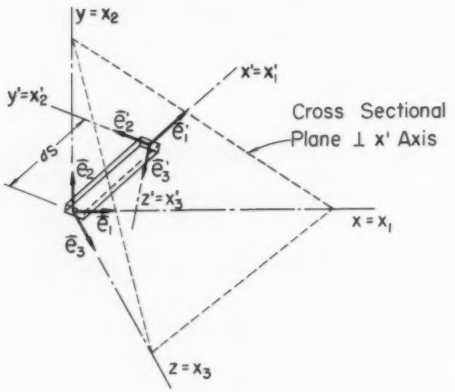

FIG. 3.

positive end of a coordinate axis. Fig. 2 illustrates the positive directions of the vector quantities and positions of the front and rear faces.

Direction Cosines.—The orientation of any differential length ds along the elastic axis x_1' or of the principal axes x_2' and x_3' of the rings cross section

perpendicular to the elastic axis, can be specified most conveniently by means of direction cosines. Fig. 3 indicates the relative orientation of these axes as well as the unit vectors in the two rectangular coordinate systems. The axes associated with the element will herein be considered as the primed x', y', z' system and the arbitrarily chosen axes x, y, and z as the unprimed set.

For any vector, such as one for moment, its three orthogonal components in the primed coordinate system may be related to its three orthogonal components in the unprimed system in index rotation as

$$M_i' = b_{ij} M_j \quad i, j = x, y, z \text{ or } 1, 2, 3 \quad \ldots\ldots\ldots \quad (3)$$

in which M_i' is the moment vector $\overrightarrow{M}$ with components in the primed coordinate system; M_j denotes the moment vector $\overrightarrow{M}$ with components in the unprimed coordinate system; and b_{ij} represents the direction cosine for the angle between the x_i' and x_j' axes. The vectors and direction cosines are expressed in the index notation. An unrepeated index (such as i given previously) represents a range convention and indicates the number of components (such as x', y', z' or, briefly, 1', 2', 3'). A repeated index (such as j) implies summation over the range of that index (such as x, y, z). Hence, Eq. 3 can be expanded into

$$M_1' = b_{xx} M_x + b_{xy} M_y + b_{xz} M_z \quad \ldots\ldots\ldots \quad (4a)$$

and

$$M_2' = b_{yx} M_x + b_{yy} M_y + b_{yz} M_z \quad \ldots\ldots\ldots \quad (4b)$$

$$M_3' = b_{zx} M_x + b_{zy} M_y + b_{zz} M_z \quad \ldots\ldots\ldots \quad (4c)$$

Eqs. 4 can be written in transposed form as

$$M_i = b_{ji} M_j \quad \ldots\ldots\ldots\ldots\ldots\ldots\ldots \quad (5a)$$

or

$$M_x = b_{xx} M_1' + b_{yx} M_2' + b_{zx} M_3' \quad \ldots \quad \ldots\ldots \quad (5b)$$

The slender elemental ring segment ds, when subjected to bending moments M_2' and M_3' and a twisting moment M_1', will undergo angle changes as follows provided the curvature/depth ratio is large

$$d\theta_1' = \frac{M_1' \, ds}{G j'} = \frac{M_1' \, ds}{K_1'} \quad \ldots\ldots\ldots\ldots\ldots \quad (6a)$$

$$d\theta_2' = \frac{M_2' \, ds}{E I_2'} = \frac{M_2' \, ds}{K_2'} \quad \ldots\ldots\ldots\ldots \quad (6b)$$

$$d\theta_3' = \frac{M_3' \, ds}{E I_3'} = \frac{M_3' \, ds}{K_3'} \quad \ldots\ldots\ldots\ldots \quad (6c)$$

or

$$d\theta_1' = \lambda_{ij}' M_j' \, ds \quad \ldots\ldots\ldots\ldots\ldots\ldots \quad (6d)$$

in which

$$\lambda'_{ij} = \begin{bmatrix} \frac{1}{K'_1} & 0 & 0 \\ 0 & \frac{1}{K'_2} & 0 \\ 0 & 0 & \frac{1}{K'_3} \end{bmatrix} = \text{a stiffness matrix} \quad \ldots\ldots\ldots \quad (7)$$

Herein, $G J'$, $E I'_2$, and so forth, are related to the element's stiffness. The term J' is not a polar moment of inertia, except for a ring of circular cross section.

Elemental angle changes $d\theta_i$ may be related as was the moment vector M_i in Eq. 3 and 5. Then

$$d\theta_i = b_{ji}\, d\theta'_j = b_{ji}\, \lambda'_{jk}\, M'_k\, ds = b_{ji}\, \lambda'_{jk}\, b_{k1}\, M_1 ds \quad \ldots\ldots\ldots\ldots \quad (8)$$

when Eq. 8 is expanded in x, y, and z, three scalar equations similar to the following result, but only one is shown herein as

$$d\theta_x = \left\{ \begin{matrix} b_{xx} \frac{1}{K'_1} \left\{ \begin{matrix} b_{xx} M_x \\ b_{xy} M_y \\ b_{xz} M_x \end{matrix} \right. \\ b_{yx} \frac{1}{K'_2} \left\{ \begin{matrix} b_{yx} M_x \\ b_{yy} M_y \\ b_{yz} M_z \end{matrix} \right. \\ b_{zx} \frac{1}{K'_3} \left\{ \begin{matrix} b_{zx} M_x \\ b_{zy} M_y \\ b_{zz} M_z \end{matrix} \right. \end{matrix} \right\} ds$$

$$= M_x\, ds \left\{ \frac{b^2_{xx}}{K'_1} + \frac{b^2_{yx}}{K'_2} + \frac{b^2_{zx}}{K'_3} \right\} + M_y\, ds \left\{ \frac{b_{xx} b_{xy}}{K'_1} + \frac{b_{yx} b_{yy}}{K'_2} + \frac{b_{zx} b_{xy}}{K'_3} \right\}$$

$$+ M_z\, ds \left\{ \frac{b_{xx} b_{xz}}{K'_1} + \frac{b_{yx} b_{yz}}{K'_2} + \frac{b_{zx} b_{zz}}{K'_3} \right\} \ldots (9)$$

If the terms in brackets are denoted by $1/K_{xx}$ and ds/K_{xx} by dA_{xx}, etc.,

$$d\theta_x = \frac{M_x\, ds}{K_{xx}} + \frac{M_y\, ds}{K_{xy}} + \frac{M_z\, ds}{K_{xz}} = M_x\, dA_{xx} + M_y\, dA_{xy} + M_z\, dA_{xz} \ldots\ldots \quad (10)$$

Eq. 8 may, then, be written as

$$d\theta_i = \frac{M_j\, ds}{K_{ij}} = M_j\, dA_{ij} \quad \ldots\ldots\ldots\ldots\ldots \quad (11)$$

The $1/K_{ij}$ terms may be regarded as widths of elastic areas ds long. The relationship of these nine K_{ij} terms in terms of b_{ij} and K_i are listed in Eq. 41, Appendix I. It can be shown that $K_{ij} = K_{ji}$ and so only six elastic areas are needed. The expressions derived herein for dA_{ij} differ considerably from those proposed originally by Michalos and Baron,[5] essentially because of their simpler functional relationships to the direction cosines.

Statical and Correction Reactions.— The reactions $\overrightarrow{V_c} = (V_c)_i$ and $\overrightarrow{M_c} = (M_c)_i$, applied at the ends C of the rigid bracket of Fig. 1 which coincide with the origin of the coordinate system, will produce on a cross section of the element ds, a restoring force $\overrightarrow{V_r} = \overrightarrow{V_c}$ and a moment which may be expressed in vector form as

$$\overrightarrow{M_r} = \overrightarrow{M_c} - \overrightarrow{\rho} \times \overrightarrow{V_c} \quad \ldots\ldots\ldots\ldots\ldots\ldots\ldots \quad (12)$$

or, in index notation as

$$(M_r)_i = (M_c)_i - c_{ijk}\, \rho_j\, (V_c)_k \quad \ldots\ldots\ldots\ldots \quad (13)$$

in which c_{ijk} is a permutation symbol for a vector cross product; $c_{ijk} = +1$ if i, j, k can be permuted to 1, 2, 3 by an even number of interchanges; $c_{ijk} = -1$ if the permutations are odd; and $c_{ijk} = 0$ if any 2 indices are the same.

Eq. 12 or 13 may be expanded in scalar form and the parenthesis dropped for sake of simplicity to yield Eq. 43 of Appendix I.

Corrective Angle Changes.—The statical moment $\overrightarrow{M_s} = (M_s)_i$ and correction moments $(M_r)_i$ both produce differential angle changes $(d\theta_s)_i$ and $(d\theta_r)_i$ at the element ds and are unequal in general. Their sum over a closed loop will be

$$\int d\theta_i = \int (d\theta_s)_i - \int (d\theta_r)_i = 0 \quad \ldots\ldots\ldots\ldots \quad (14)$$

if continuity is restored. Substituting Eqs. 11 and 13

$$\int (d\theta_s)_i = \int (d\theta_r)_i \quad \ldots\ldots\ldots\ldots\ldots\ldots\ldots \quad (15a)$$

$$\int (M_s)_j\, dA_{ij} = \int (M_r)_j\, dA_{ij}$$

$$= \int \left[(M_c)_j - c_{jkl}\, \rho_k\, (V_c)_l \right] dA_{ij} \quad \ldots\ldots \quad (15b)$$

and

$$P_i = A_{ij} (M_c)_j + C_{ij} (V_c)_j \quad \ldots\ldots\ldots\ldots \quad (15c)$$

If, now, the parenthesis for individual vectors are dropped for sake of simplicity, Eqs. 15 expands into three equations of the following type as

$$\int (M_{sx}\, dA_{xx} + M_{sy}\, dA_{xy} + M_{sz}\, dA_{xz}) = M_{cx} \int dA_{xx} + M_{cy} \int dA_{xy} + M_{cz} \int dA_{xz}$$
$$+ V_{cz} \int (x\, dA_{xy} - y\, dA_{xx})$$
$$+ V_{cy} \int (z\, dA_{xx} - x\, dA_{xz})$$
$$+ V_{cx} \int (y\, dA_{xz} - z\, dA_{xy}) \quad \ldots\ldots\ldots\ldots\ldots \quad (16a)$$

or

$$P_x = M_{cx}\, A_{xx} + M_{cy}\, A_{xy} + M_{cz}\, A_{xz} + V_{cx}\, C_{xx}\, V_{cy}\, C_{xy} + V_{cz}\, C_{xz} \ldots (16b)$$

The left hand side of Eq. 15 represents a relative angle change between the rigid brackets at C due to the statical moment $(M_s)_j$ and will be considered as a load P_i on the elastic areas A_{ij}. The equations for P_i, listed as the first three Eqs. 44 of Appendix I, and the A_{ij}, C_{ij} terms are defined in Tables 1(a), 1(b), and 1(d), respectively.

Corrective Displacements.—The differential angle changes $\overrightarrow{d\theta}$ at the element ds produce linear displacements at the origin C of Fig. 1 such that

$$\overrightarrow{d\delta}_c = \overrightarrow{\rho} \times \overrightarrow{d\theta} \quad \ldots\ldots\ldots\ldots\ldots\ldots \quad (17a)$$

or

$$d(\delta_c)_i = c_{ijk}\, \rho_j\, d\theta_k \quad \ldots\ldots\ldots\ldots\ldots\ldots \quad (17b)$$

If continuity is restored at C (and A)

$$\int d(\delta_c)_i = 0 = \int d(\delta_{cs})_i - \int d(\delta_{cr})_i \quad \ldots\ldots\ldots \quad (18)$$

If Eqs. 17 and 11 are substituted in Eq. 18

$$\int c_{ijk}\, \rho_j\, (M_s)_m\, dA_{km} = \int c_{ijk}\, \rho_j\, (M_c)_m\, dA_{km} \quad \ldots\ldots\ldots\ldots \quad (19a)$$

$$\int c_{ijk}\, \rho_j\, dP_k = \int c_{ijk}\, \rho_j\, dA_{km} \left[(M_c)_m - c_{mno}\, \rho_n\, (V_c)_o \right] \ldots\ldots \quad (19b)$$

and

$$D_i = C_{ji}\, (M_c)_j + J_{ij}\, (V_c)_j \quad \ldots\ldots\ldots\ldots\ldots\ldots \quad (19c)$$

Expansion of Eqs. 19 yields the last three of Eqs. 44 of Appendix I. The individual integrals for C_{ij}, J_{ij}, and D_i are defined in Tables 1(b), 1(c), and 1(e), respectively.

The left hand side of Eq. 19 represents a relative displacement of the ends of the rigid bracket at C due to the statical moments $(M_s)_m$ and will be considered as a moment D_i on the elastic areas A_{ij}.

The P_i and D_i terms represent displacements at the origin C and may result from actual distortions such as those accompanying shrinkage, support settlement or rotation, temperature changes, etc., as well as applied loads. If a rotation $(P_A)_i$ occurs at some specific point A in the ring

$$P_i = (P_C)_i = (P_A)_i \quad \ldots\ldots\ldots\ldots\ldots\ldots \quad (20)$$

and

$$D_i = (D_C)_i = (D_A)_i + c_{ijk}\, (\rho_A)_j\, (P_A)_k \quad \ldots\ldots\ldots \quad (21)$$

If only linear distortions occur, such as those for temperature changes then

$$D_i = \alpha\ L_i\, \Delta T \quad \ldots\ldots\ldots\ldots\ldots\ldots \quad (22)$$

in which α is the coefficient of thermal expansion; L_i denotes the projected length of the ring along the i^{th} axis; and ΔT represents the temperature change.

FINAL EQUATIONS AND ANALOGIES

The six equations for P_i and D_i (Eqs. 44, Appendix I) represent relationships between these angle changes and displacements at C, due to the statical

moment $(M_S)_i$, in terms of the restoring forces $(V_C)_i$ and moments $(M_C)_i$ at C and the area elastic areas A_{ij} and their first (C_{ij}) and second (J_{ij}) moments. If certain of the C_{ij} terms are made to vanish by locating the origin of the unprimed system properly, the six equations may be simplified somewhat. The equations then reduce to several popular analogies[4,5] and become simpler for coplanar structures.

Column Analogy.—Consider a coplanar ring, symmetrical about and lying in the xy plane and loaded by forces (or displacements) in that plane, or by moments (or rotations) about the z axis. Let the z' axis coincide with the z axis. Then $z = 0, b_{xz} = b_{zx} = b_{yz} = b_{zy} = 0, b_{zz} = 1$, and $b_{xy} = -b_{yx}$. Since bending takes place about only the z' or z axis, $M_x = M_y = 0$. Hence, all terms of Eq. 44, Appendix I, vanish except those overlined with solid lines. If the remaining three equations are further simplified by setting $C_{zx} = C_{zy} = 0$, correcting the J_{ij} terms accordingly, and substituting solutions for M_{cz}, V_{cy}, and V_{xc} in the last of Eqs. 43 of Appendix I, the familiar column analogy equation appears.

Shear and Torsion Analogy.—Consider a coplanar ring lying in and symmetrical about the xy plane and loaded with forces or displacements along the z axis, or by moments or rotations about the x and y axes. Then, $z = 0$, $b_{xz} = b_{zx} = b_{yz} = b_{zy} = 0, b_{zz} = 1$, and $b_{xy} = -b_{yx}$ as before, but now $M_z = 0$. Hence, all terms of the six equations vanish except those overlined with dotted lines. Letting $C_{xz} = C_{yz} = 0$, correcting the J_{ij} P_i, and D_i terms accordingly, and combining terms in the first two of Eqs. 43, Appendix I, the result are found to be identical with the shear and torsion analogy of Baron and Michalos.[5]

Noncoplanar Rings.—When Baron and Michalos developed their analysis for noncoplanar rings, they set all C_{ij} except the C_{ii} terms equal to zero. In this way they located three elastic centroids, one in each coordinate plane. These did not coincide with the projection of any single point in space. They did simplify the six equations so that each now had but four terms, but the J_{ij}, P_i, and D_i had to be corrected for the transfer of the axes.

A similar simplification was developed[9] by setting the three $C_{ii} = 0$ and correcting the J_{ij}, P_i, and D_i accordingly. This amounts physically to locating a single elastic centroid or neutral point in space, and reducing the six equations so that each now has but five terms. Physically, this restriction means that a restoring moment M_{cx} at C produces no displacement of C along the x axis, that a force V_{cx} produces no rotation about the x axis, etc.

In general, the labor of locating the origin at the centroid of the elastic areas, and of correcting the J_{ij} "moment of inertia" terms by analogous parallel axis theorem computations, etc., is seldom worth the effort. This is especially true now that computers are available to solve simultaneous equations.

TABULAR SOLUTIONS

The final analysis of any ring, coplanar or noncoplanar, is most readily accomplished by tabulating all computations for each segment into which the ring is divided, assuming that the entire operation has not been previously programmed on a computer. Tables 1(a) to 1(e) illustrate the manner of deter-

9 "A General Procedure for Analysis of Elastic Rings in Space," by Walter C. Liessner, thesis presented to Virginia Polytechnic Inst., at Blacksburg, in October, 1957, as partial fulfillment of the requirements for the degree of Master of Science.

TABLE 1(a) & TABLE 1(b)

Line	Element	Length	x	y	z	$\frac{1}{K_{xx}}$	$\frac{1}{K_{xy}}$	$\frac{1}{K_{xz}}$	$\frac{1}{K_{yy}}$	$\frac{1}{K_{yz}}$	$\frac{1}{K_{zz}}$	δA_{xx}	δA_{xy}	δA_{xz}	δA_{yy}	δA_{yz}	δA_{zz}
1																	
2																	
3																	
4																	
5																	
6																	
7																	
8																	
9																	
10																	
	Shear Torsion Analogy										Σ						
	Column Analogy											A_{xx}	A_{xy}	A_{xz}	A_{yy}	A_{yz}	A_{zz}

Line	$y\delta A_{xz}$	$z\delta A_{xy}$	$x\delta A_{yz}$	$z\delta A_{xx}$	$x\delta A_{xz}$	$x\delta A_{xy}$	$y\delta A_{xx}$	$y\delta A_{yz}$	$z\delta A_{yy}$	$z\delta A_{xz}$	$x\delta A_{zz}$	$y\delta A_{zz}$	$z\delta A_{yz}$	$x\delta A_{yy}$	$y\delta A_{xy}$
1															
2															
3															
4															
5															
6															
7															
8															
9															
10															
Σ															
=	√√	√	√	√√	√	√√	√	√√	√	√√	√	√√	√	√√	√
	C_{xx} = √√-√	C_{yy} = √-√	C_{zz} = √-√√	C_{xy} = √√-√		C_{xz} = √√-√		C_{yx} = √√-√		C_{zy} = √√-√		C_{zx} = √√-√		C_{yz} = √√-√	

TABLE 1(c)

Line	$(I_{xy})_{xy}$ $+z^2\delta A_{xy}$	$(I_{yz})_{xy}$ $+zx\delta A_{yz}$	$(I_{xz})_{xy}$ $+yz\delta A_{xz}$	$(I_z)_{xy}$ $+xy\delta A_{zz}$	$(I_{yz})_{yz}$ $+x^2\delta A_{yz}$	$(I_{xz})_{yz}$ $+xy\delta A_{xz}$	$(I_{xy})_{yz}$ $+xz\delta A_{xy}$	$(I_x)_{yz}$ $+yz\delta A_{xx}$	$(I_{xz})_{xz}$ $+y^2\delta A_{xz}$	$(I_{xy})_{xz}$ $+yz\delta A_{xy}$	$(I_{yz})_{xz}$ $+xy\delta A_{yz}$	$(I_y)_{xz}$ $+xz\delta A_{yy}$
1												
2												
3												
4												
5												
6												
7												
8												
9												
10												
Σ												
=												
	$J_{xy} =$			$= J_{yx} =$	$J_{yz} =$			$= J_{zy} =$	$J_{zx} =$			$= J_{xz} =$

Line	$(I_y)_x$ $+z^2\delta A_{yy}$	$(I_z)_x$ $+y^2\delta A_{zz}$	$(I_{yz})_x$ $+yz\delta A_{yz}$	$(I_z)_y$ $+x^2\delta A_{zz}$	$(I_x)_y$ $+z^2\delta A_{xx}$	$(I_{xz})_y$ $+xz\delta A_{xz}$	$(I_x)_z$ $+y^2\delta A_{xx}$	$(I_y)_z$ $+x^2\delta A_{yy}$	$(I_{xy})_z$ $+xy\delta A_{xy}$	M_{sx}	M_{sy}	M_{sz}
1												
2												
3												
4												
5												
6												
7												
8												
9												
10												
Σ												
=												
	$J_{xx} =$			$J_{yy} =$			$J_{zz} =$					

TABLE 1(d)

Line	$M_{sx}\delta A_{xx}$	$M_{sy}\delta A_{xy}$	$M_{sz}\delta A_{xz}$	$M_{sx}\delta A_{xy}$	$M_{sy}\delta A_{yy}$	$M_{sz}\delta A_{yz}$	$M_{sx}\delta A_{xz}$	$M_{sy}\delta A_{yz}$	$M_{sz}\delta A_{zz}$	x_s	y_s	z_s
1												
2												
3												
4												
5												
6												
7												
8												
9												
10												
Σ												
=	✓	✓	✓	✓	✓	✓	✓	✓	✓			
	P_x = ✓ + ✓ + ✓ =			P_y = ✓ + ✓ + ✓ =			P_z = ✓ + ✓ + ✓ =					

TABLE 1(e)

Line	$z_s M_{sx} \delta A_{xy}$	$z_s M_{sy} \delta A_{yy}$	$z_s M_{sz} \delta A_{yz}$	$y_s M_{sx} \delta A_{xz}$	$y_s M_{sy} \delta A_{yz}$	$y_s M_{sz} \delta A_{zz}$
1						
2						
3						
4						
5						
6						
7						
8						
9						
10						
Σ						
=	✓	✓	✓	✓	✓	✓
	$\Sigma z_s \delta P_y =$ ✓ = ✓ + ✓ + ✓			$\Sigma y_s \delta P_z =$ ✓ ✓ = ✓ + ✓ + ✓		
	$D_x =$ ✓✓ − ✓ =					

Line	$x_s M_{sx} \delta A_{xz}$	$x_s M_{sy} \delta A_{yz}$	$x_s M_{sz} \delta A_{zz}$	$z_s M_{sx} \delta A_{xx}$	$z_s M_{sy} \delta A_{xy}$	$z_s M_{sz} \delta A_{xz}$
1						
2						
3						
4						
5						
6						
7						
8						
9						
10						
Σ						
=	✓	✓	✓	✓	✓	✓
	$\Sigma x_s \delta P_z =$ ✓ = ✓ + ✓ + ✓			$\Sigma z_s \delta P_x =$ ✓✓ = ✓ + ✓ + ✓		
	$D_y =$ ✓✓ − ✓ =					

Line	$y_s M_{sx} \delta A_{xx}$	$y_s M_{sy} \delta A_{xy}$	$y_s M_{sz} \delta A_{xz}$	$x_s M_{sx} \delta A_{xy}$	$x_s M_{sy} \delta A_{yy}$	$x_s M_{sz} \delta A_{yz}$
1						
2						
3						
4						
5						
6						
7						
8						
9						
10						
Σ						
=	✓	✓	✓	✓	✓	✓
	$\Sigma y_s \delta P_x =$ ✓ = ✓ + ✓ + ✓			$\Sigma x_s \delta P_y =$ ✓✓ = ✓ + ✓ + ✓		
	$D_z =$ ✓✓ − ✓ =					

mining the coefficients of the six Eqs. 44 of Appendix I. This table differs from that presented by Michalos and Baron[5] because the centroidal corrections are ignored, because some subscripts are interchanged to conform to the index notation used herein, and because the signs of some terms vary. These sign changes result from adherence herein to the right hand rule used in vector analysis.

Tabular solutions in other than cartesian coordinates follow similar patterns. The problem subsequently illustrated lends itself to cylindrical coordinates but requires a double transformation between three sets of orthogonal coordinate systems.

Although the summations involved in tabular solutions are not as precise as integrals, the results are invariably quite accurate, especially when a ring

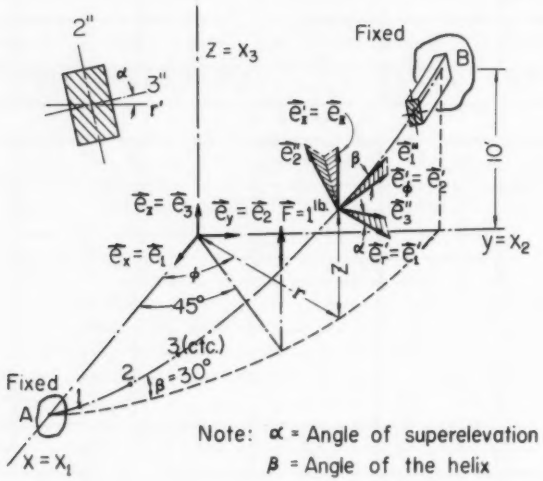

FIG. 4.—UNIT VECTOR ORIENTATIONS FOR A SUPER-ELEVATED HELICAL BEAM

is broken into at least ten segments. Tabular solutions are decidedly simpler than those involving integrals when the cross sections of the ring vary, or when the elastic axis cannot be expressed in convenient functional form.

Cylindrical Coordinates.—Consider a helical beam fixed at both ends and superelevated as shown in Fig. 4.

Let a_{ij} = the direction cosines between the (primed) cylindrical (r', ϕ', z') and (unprimed) fixed cartesian (x, y, z) coordinate systems, therefore

$$a_{ij} = \begin{array}{c} \begin{matrix} \vec{e}_x & \vec{e}_y & \vec{e}_z \end{matrix} \\ \left[\begin{array}{ccc} \cos\phi & \sin\phi & 0 \\ -\sin\phi & \cos\phi & 0 \\ 0 & 0 & 1 \end{array}\right] \end{array} \begin{matrix} \vec{e}'_r \\ \vec{e}'_\phi \\ \vec{e}_z \end{matrix} \quad \ldots\ldots\ldots \quad (23)$$

and b_{ij} is the direction cosines between the (double primed) principal rorsional and bending elastic axes (1", 2", 3") and the (primed) cylindrical (r', ϕ', z') coordinate system, therefore

$$b_{ij} = \begin{array}{c} \begin{array}{ccc} \vec{e}'_r & \vec{e}'_\phi & \vec{e}'_z \end{array} \\ \left[\begin{array}{ccc} 0 & \cos\beta & \sin\beta \\ -\sin\alpha & -\cos\alpha\sin\beta & \cos\alpha\cos\beta \\ \cos\alpha & -\sin\alpha\sin\beta & \sin\alpha\cos\beta \end{array}\right] \end{array} \begin{array}{c} \vec{e}''_1 \\ \vec{e}''_2 \\ \vec{e}''_3 \end{array} \quad \ldots\ (24)$$

Then

$$d\theta_i = a_{ji}\, d\theta'_j = a_{ji}\, b_{kj}\, d\theta''_k = a_{ji}\, b_{kj}\, \lambda''_{kl}\, M''_l\, ds$$
$$= a_{ji}\, b_{kj}\, \lambda''_{kl}\, b_{lm}\, M'_m\, ds = a_{ji}\, dA'_{jk}\, M'_k \quad \ldots\ (25)$$

The dA'_{jk} terms in Eq 25 are identical with those of Eqs. 41, Appendix I, provided the expansion is now conducted with j in terms of a 1", 2", and 3" instead of x', y', and z' and k in terms of r', ϕ', and z' instead of x, y, and z and provided moments are expressed in the primed coordinate system. The vector $d\theta_i$ may also be expressed in terms of the components of the moment vector in the unprimed (x, y, z) system as

$$d\theta_i = a_{ji}\, b_{kj}\, \lambda''_{kl}\, b_{lm}\, a_{mn}\, M_n\, ds = a_{ji}\, dA'_{jk}\, a_{kl}\, M_l \quad \ldots\ (26)$$

Now

$$\int d\theta_i = 0 = \int \left(d\theta_s\right)_i - \left(d\theta_r\right)_i = P_i - \int \left(d\theta_r\right)_i \quad i = x, y, z \quad \ldots\ (27)$$

So

$$P_i = \int \left(d\theta_s\right)_i = \int a_{ji} \left(d\theta_s\right)'_i = \int a_{ji}\, dA'_{jk} \left(M_s\right)'_k \quad \ldots\ (28)$$

and

$$\int \left(d\theta_r\right)_i = \int a_{ji}\, dA'_{jk} \left(M_r\right)'_k = \int a_{ji}\, dA'_{jk}\, a_{kl} \left(M_r\right)_l$$
$$= \int a_{ji}\, dA'_{jk}\, a_{kl} \left[\left(M_c\right)_l - c_{lmn}\, \rho_m \left(V_c\right)_n\right]$$
$$= \int a_{ji}\, dA'_{jk}\, a_{kl} \left(M_c\right)_l - \int a_{ji}\, dA'_{jk}\, a_{kl}\, c_{lmn}\, \rho_m \left(V_c\right)_n \quad \ldots\ (29)$$

Hence

$$P_i = A_{ij} \left(M_c\right)_j + C_{ij} \left(V_c\right)_j \quad \ldots\ (30)$$

Similarly, the displacement vector $\left(d\,\delta_c\right)_i$ may be expressed as

$$\int \left(d\,\delta_c\right)_i = 0 = \int \left(d\,\delta_{cs}\right)_i - \int \left(d\,\delta_{cr}\right)_i = D_i - \int \left(d\,\delta_{cr}\right)_i \quad i = x, y, z \quad \ldots\ (31)$$

So

$$D_i = \int \left(d\,\delta_{cs}\right)_i = \int c_{ijk}\, \rho_j \left(d\theta_s\right)_k = \int c_{ijk}\, \rho_j\, a_{lk}\, dA'_{lm} \left(M_s\right)'_m \quad \ldots\ (32)$$

and

$$\int \left(d\,\delta_{cr}\right)_i = \int c_{ijk}\, \rho_j \left(d\theta_r\right)_k = \int c_{ijk}\, \rho_j\, a_{lk}\, dA'_{lm}\, a_{mn} \left(M_c\right)_n$$
$$- \int c_{ijk} \rho_j\, a_{lk}\, dA'_{lm}\, a_{mn}\, c_{npq}\, \rho_p \left(V_c\right)_q \quad \ldots\ (33)$$

and

$$\int \left(d\,\delta_{cr}\right)_i = C_{ji} \left(M_c\right)_j + J_{ij} \left(V_c\right)_j \quad \ldots\ (34)$$

Eqs. 25, 28, 29, 32, and 33 could be adapted to Table 1(a) to e after their expansion. However, the repetitious nature of many of the terms makes it worthwhile to rearrange these tables so that the A_{ij}, C_{ij}, and J_{ij} coefficients can be more readily computed. Tables 2 and 3 define such terms and show

TABLE 2

Line	$\Sigma\mu(z, \phi)$	Value of $\Sigma\mu(z, \phi)\ \delta A'_{ij}$					
		$\delta A'_{rr}$	$\delta A'_{r\phi}$	$\delta A'_{rz}$	$\delta A'_{\phi\phi}$	$\delta A'_{\phi z}$	$\delta A'_{zz}$
0	1	--	--	--	C_{400}	C_{500}	C_{600}
1	$\Sigma\cos\phi$	--	C_{201}	C_{301}	C_{401}	C_{501}	C_{601}
2	$\Sigma\sin\phi$	--	$C_{2\ 2}$	C_{302}	C_{402}	C_{502}	C_{602}
3	$\Sigma\cos^2\phi$	C_{103}	C_{203}	C_{303}	C_{403}	C_{503}	C_{603}
4	$\Sigma\sin^2\phi$	C_{104}	C_{204}	C_{304}	C_{404}	C_{504}	C_{604}
5	$\Sigma\cos\phi\sin\phi$	C_{105}	C_{205}	C_{305}	C_{405}	C_{505}	C_{605}
6	$\Sigma z\cos\phi$	--	C_{206}	C_{306}	C_{406}	C_{506}	--
7	$\Sigma z\sin\phi$	--	C_{207}	C_{307}	C_{407}	C_{507}	--
8	$\Sigma z\cos^2\phi$	C_{108}	C_{208}	C_{308}	C_{408}	C_{508}	--
9	$\Sigma z\sin^2\phi$	C_{109}	C_{209}	C_{309}	C_{409}	C_{509}	--
10	$\Sigma z\cos\phi\sin\phi$	C_{110}	C_{210}	C_{310}	C_{410}	C_{510}	--
11	$\Sigma z^2\cos^2\phi$	C_{111}	C_{211}	--	C_{411}	--	--
12	$\Sigma z^2\sin^2\phi$	C_{112}	C_{212}	--	C_{412}	--	--
13	$\Sigma z^2\cos\phi\sin\phi$	C_{113}	C_{213}	--	C_{413}	--	--

how they are combined to form the coefficients of the final matrix (Eqs. 44 Appendix I).

ILLUSTRATIVE EXAMPLE

(1) A superelevated helical beam is fixed at two ends 90° apart and loaded with an upward unit vertical load at its midpoint. Determine the variation in bending and twisting moments along its elastic axis if $\alpha = 5°$, $\beta = 30°$, h = 10 ft,

r = 11.03 ft, $K_1'' = K_2'' = 10^5$ k-ft^2, and $K_3'' = 30^5$ k-ft^2. (2) Determine the stiffness factor about the y axis at A. (a) If the direction cos b_{ij} are evaluated and sub-

TABLE 3

$$A_{xx} = C_{103} - 2C_{205} + C_{404}$$

$$A_{xy} = C_{105} + C_{203} - C_{204} - C_{405}$$

$$A_{xz} = C_{301} - C_{502}$$

$$A_{yy} = C_{104} + 2C_{205} + C_{403}$$

$$A_{yz} = C_{302} + C_{501}$$

$$A_{zz} = C_{600}$$

$$C_{xx} = - C_{110} - C_{208} + C_{209} + C_{410} + r\,(C_{305} - C_{504})$$

$$C_{xy} = C_{108} - 2C_{210} + C_{409} + r\,(C_{505} - C_{303})$$

$$C_{xz} = r\,(C_{201} - C_{402})$$

$$C_{yx} = - C_{109} - 2C_{210} - C_{408} + r\,(C_{304} + C_{505})$$

$$C_{yy} = C_{110} + C_{208} - C_{209} - C_{410} - r\,(C_{305} + C_{503})$$

$$C_{yz} = r\,(C_{202} + C_{401})$$

$$C_{zx} = - C_{307} - C_{506} + r\,C_{602}$$

$$C_{zy} = C_{306} - C_{507} - r\,C_{601}$$

$$C_{zz} = r\,C_{500}$$

$$J_{xx} = C_{112} + 2C_{213} + C_{411} - 2r\,(C_{309} + C_{510}) + r^2\,C_{604} - C_{211}$$

$$J_{xy} = - C_{113} + C_{212} + C_{413} + r\,(2C_{310} + C_{508} - C_{509}) - r^2\,C_{605}$$

$$J_{xz} = r^2\,C_{502} - r\,(C_{207} + C_{406})$$

$$J_{yy} = C_{111} - 2C_{213} + C_{412} - 2r\,(C_{308} - C_{510}) + r^2\,C_{603}$$

$$J_{yz} = r\,(C_{206} - C_{407}) - r^2\,C_{501}$$

$$J_{zz} = r^2\,C_{400}$$

stituted in Eqs. 41, Appendix I, the K_{ij} terms can be computed. Letting the axes $r' = x_1'$, $\phi' = x_2'$, and $z' = x_3'$ and using 1, 2, and 3 instead of x, y, and x

TABLE 4(a) & TABLE 4(b)

Element No.	Length Ft.	Values $\times 10^{-5}$					
		$\frac{1}{K'_{rr}}$	$\frac{1}{K'_{r\phi}}$	$\frac{1}{K'_{rz}}$	$\frac{1}{K'_{\phi\phi}}$	$\frac{1}{K'_{\phi z}}$	$\frac{1}{K'_{zz}}$
1 to 10		0.33840	0.028943	-0.050129	1.0	0.002193	0.99620
		A'_{rr}	$A'_{r\phi}$	A'_{rz}	$A'_{\phi\phi}$	$A'_{\phi z}$	A'_{zz}
1 to 10	2.0	0.67680	0.057886	-0.100258	2.0	0.004386	1.99240
Σ (1- 10)	20.0	6.76800	0.57886	-1.00258	20.0	0.04386	19.92400

Ele-ment No.	z	ϕ	cosϕ	sinϕ	$\cos^2\phi$	$\sin^2\phi$	cosϕsinϕ	z cosϕ
1	0.5'	4.5°	0.99692	0.07846	0.99385	0.00616	0.07822	0.49846
2	1.5	13.5	0.97237	0.23345	0.94550	0.05450	0.22700	1.45856
3	2.5	22.5	0.92388	0.38268	0.85355	0.14644	0.35355	2.30970
4	3.5	31.5	0.85264	0.52250	0.72699	0.27301	0.44550	2.98424
5	4.5	40.5	0.76041	0.64945	0.57822	0.42179	0.49385	3.42185
6	5.5	49.5	0.64945	0.76041	0.42179	0.57822	0.49385	3.57198
7	6.5	58.5	0.52250	0.85264	0.27301	0.72699	0.44550	3.39625
8	7.5	67.5	0.38268	0.92388	0.14644	0.85355	0.35355	2.87010
9	8.5	76.5	0.23345	0.97237	0.05450	0.94550	0.22700	1.98433
10	9.5	85.5	0.07846	0.99692	0.00616	0.99385	0.07822	0.74537
		$\Sigma\mu$ (z, ϕ)	6.37276	6.37276	5.00001	5.00001	3.19624	23.24084

Element No.	z sinϕ	z $\cos^2\phi$	z $\sin^2\phi$	z cosϕsinϕ	$z^2\cos^2\phi$	$z^2\sin^2\phi$	z^2cosϕsinϕ
1	0.03923	0.49692	0.00308	0.03911	0.24846	0.00154	0.01955
2	0.35018	1.41826	0.08175	0.34050	2.12740	0.12263	0.51076
3	0.95670	2.13389	0.36611	0.88388	5.33471	0.91527	2.20969
4	1.82875	2.54448	0.95552	1.55927	8.90569	3.34433	5.45743
5	2.92253	2.60201	1.89804	2.22232	11.70906	8.54118	10.00046
6	4.18226	2.31982	3.18023	2.71617	12.75904	17.49130	14.93895
7	5.54216	1.77454	4.95947	2.89578	11.53451	30.71554	18.82256
8	6.92910	1.09833	6.40166	2.65163	8.23747	48.01243	19.88721
9	8.26515	0.46324	8.03678	1.92950	3.93757	68.31270	16.40079
10	9.47074	0.05848	9.44157	0.74307	0.55558	89.69492	7.05921
$\Sigma\mu$ (z, ϕ)	40.48680	14.90997	35.09021	15.98123	65.34949	267.15184	95.30661

TABLE 4(c)

Element	z (2)	ø (3)	cos ø (4)	sin ø (5)	M'_{sr} * (6)	$M'_{s\phi}$ * (7)	$M'_{sr}\delta A'_{rr}$ (8)	$M'_{s\phi}\delta A'_{r\phi}$ (9)	$\delta\theta'_r$ (8)+(9) = (10)	$M'_{sr}\delta A'_{r\phi}$ (11)	$M'_{s\phi}\delta A'_{\phi\phi}$ (12)
6	5.5	49.5°	0.64945	0.76041	0.86541	-0.03397	0.58571	-0.00197	0.58374	0.05010	- 0.06794
7	6.5	58.5°	0.52250	0.85264	2.57495	-0.30476	1.74273	-0.01764	1.72509	0.14905	- 0.60952
8	7.5	67.5°	0.38268	0.92388	4.22096	-0.83960	2.85675	-0.04860	2.80815	0.24433	- 1.67920
9	8.5	76.5°	0.23345	0.97237	5.76318	-1.62538	3.90052	-0.09409	3.80643	0.33361	- 3.25076
10	9.5	85.5°	0.07846	0.99692	7.16343	-2.64268	4.84821	-0.15297	4.69524	0.41466	- 5.28536
B	1	90	0	1.0	7.79931	3.23069					

Element	$\delta\theta'_\phi$ (11)+(12) = (13)	$M'_{sr}\delta A'_{rz}$ (14)	$M'_{s\phi}\delta A'_{\phi z}$ (15)	$\delta\theta'_z = \delta P_z$ (14)+(15) = (16)	$\delta\theta'_r \cos\phi$ (17)	$-\delta\theta'_\phi \sin\phi$ (18)	$\delta\theta_x = \delta P_x$ (17)+(18) = (19)	$\delta\theta'_r \sin\phi$ (20)	$\delta\theta'_\phi \cos\phi$ (21)	$\delta\theta_y = \delta P_y$ (20)+(21) = (22)
6	- 0.01784	-0.08677	- 0.000149	-0.086919	0.37911	+0.01357	0.39268	0.44388	- 0.01159	0.43229
7	- 0.46047	-0.25816	- 0.001337	-0.259497	0.90136	+0.39262	1.29398	1.47088	- 0.24060	1.23028
8	- 1.43487	-0.42319	- 0.003682	-0.426872	1.07462	+1.32565	2.40027	2.59439	- 0.54910	2.04529
9	- 2.91715	-0.57782	- 0.007129	-0.584949	0.88861	+2.83655	3.72516	3.70126	- 0.68101	3.02025
10	- 4.87070	-0.71821	- 0.011591	-0.729801	0.36839	+4.85570	5.22409	4.68078	- 0.38216	4.29862
Σ	- 9.70103	-2.06415	- 0.023888	-2.088038	3.61209	+9.42409	13.03618	12.89119	- 1.86446	11.02673

Element	$r\sin\phi\,\delta P_z$ (23)	$z\,\delta P_y$ (24)	δD_x (23)-(24) = (25)	$z\,\delta P_x$ (26)	$r\cos\phi\,\delta P_z$ (27)	δD_y (26)-(27) = (28)	$r\cos\phi\,\delta P_y$ (29)	$r\sin\phi\,\delta P_x$ (30)	δD_z (29)-(30) = (31)	
6	- 0.72902	2.37760	- 3.10662	2.15974	-0.62264	2.78238	3.09668	3.29353	- 0.19685	
7	- 2.44047	7.99682	- 10.43729	8.41087	-1.49553	9.90640	7.09032	12.16939	- 5.07907	
8	- 4.34999	15.33968	- 19.68967	18.00203	-1.80181	19.80384	8.63309	24.45970	- 15.82561	
9	- 6.27372	25.67213	- 31.94585	31.66386	-1.50622	33.17008	7.77700	39.95324	- 32.17624	
10	- 8.02491	40.83690	- 48.86181	49.62886	-0.63158	50.26044	3.72008	57.44423	- 53.72415	
Σ	-21.81811	92.22313	-114.04124	109.86536	-6.05778	115.92314	30.31717	137.32009	-107.00292	

* $M'_{sr} = Fr\sin(\phi - 45)$, $M'_{s\phi} = -Fr\left\{1 - \cos(\phi - 45)\right\}$, F = 1 lb., r = 11.03 ft.

TABLE 4(d) & TABLE 4(e)

Line	$\Sigma\mu\ (z, \phi)$	Value of $\Sigma\mu\ (z, \phi)\ A_{ij}$ for					
		$\delta A'_{rr}$	$\delta A'_{r\phi}$	$\delta A'_{rz}$	$\delta A'_{\phi\phi}$	$\delta A'_{\phi z}$	$\delta A'_{zz}$
0	10				20.0	0.04386	19.92400
1	$\Sigma \cos\phi$		0.36889	-0.63893	12.74552	0.02795	12.69709
2	$\Sigma \sin\phi$		0.36889	-0.63893	12.74552	0.02795	12.69709
3	$\Sigma \cos^2\phi$	3.38401	0.28943	-0.50130	10.00002	0.02193	9.96202
4	$\Sigma \sin^2\phi$	3.38401	0.28943	-0.50130	10.00002	0.02193	9.96202
5	$\Sigma \cos\phi \sin\phi$	2.16322	0.18501	-0.32046	6.39248	0.01402	6.36819
6	$\Sigma z \cos\phi$		1.34530	-2.33013	46.48168	0.10193	46.30505
7	$\Sigma z \sin\phi$		2.34358	-4.05921	80.97360	0.17758	80.66590
8	$\Sigma z \cos^2\phi$	10.09107	0.86306	-1.49487	29.81994	0.06540	29.70662
9	$\Sigma z \sin^2\phi$	23.74905	2.03120	-3.51814	70.18042	0.15391	69.91373
10	$\Sigma z \cos\phi \sin\phi$	10.81610	0.92507	-1.60228	31.96246	0.07009	31.84100
11	$\Sigma z^2 \cos^2\phi$	44.22853	3.78276		130.69898		130.20232
12	$\Sigma z^2 \sin^2\phi$	180.80837	15.46408		534.30368		532.27333
13	$\Sigma z^2 \cos\phi \sin\phi$	64.50351	5.51682		190.61322		189.88889

Values of P_i and D_i for			Values of A_{ij}, C_{ij}, and J_{ij}					
$\theta_{Ay} = 1$	F = 1 lb.		M_{cx}	M_{cy}	M_{cz}	V_{cx}	V_{cy}	V_{cz}
0	13.03618	=	13.01401	- 4.22926	- 0.66688	18.53794	84.10533	- 136.51423
+ 1	11.02673	=	- 4.22926	+ 13.75405	- 0.61098	- 60.79383	- 19.02111	144.65194
0	- 2.088038	=	- 0.66688	- 0.61098	19.92400	144.00618	- 142.55661	0.48378
0	-114.04124	=	18.53794	- 60.79383	144.00618	1610.59329	- 673.29126	- 535.14220
0	115.92314	=	84.10533	- 19.02111	-142.55661	- 673.29126	1814.00991	- 881.70057
+ 11.03	-107.00292	=	-136.51423	144.65194	0.48378	- 535.14220	- 881.70057	2433.21800
Values of Redundants $(M_c)_i$ and $(V_c)_i$ for	F = 1		-2.3723662	5.63370	-0.62629	0.0204479	-0.0670804	-0.53167838
	$\theta_{Ay} = 1$		0.0801448	0.3491825	-0.4658233	0.036428832	-0.030226093	-0.014577164

TABLE 4(f)

Element	V_{cx} = 0.0204479		V_{cy} = -0.0670804	V_{cz} = -0.5316783	M_{cx} = -2.372366	M_{rx} =
	z (1)	x = r cos ø (2)	y = r sin ø (3)	yV_{cz} (4)	zV_{cy} (5)	$M_{cx} - yV_{cz} + zV_{cy}$ = (6)
A	0	11.03	0	0	0	-2.372366
1	0.5	10.99603	0.86541	-0.460120	-0.033540	-1.945786
2	1.5	10.72524	2.57495	-1.369045	-0.100621	-1.103942
3	2.5	10.19040	4.22096	-2.244193	-0.167701	-0.295874
4	3.5	9.40462	5.76318	-3.064158	-0.234781	+0.457011
5	4.5	8.38732	7.16343	-3.808641	-0.301862	+1.144402
5.5	5.0	7.79898	7.79898	-4.146549	-0.335402	1.438781
6	5.5	7.16343	8.38732	-4.459357	-0.368942	1.718049
7	6.5	5.76318	9.40462	-5.000233	-0.436023	2.191844
8	7.5	4.22096	10.19040	-5.418015	-0.503103	2.542546
9	8.5	2.57495	10.72524	-5.702378	-0.570183	2.759829
10	9.5	0.86541	10.99603	-5.846351	-0.637264	2.836721
B	10.0	0	11.03	-5.864413	-0.670804	2.821243

Element	M_{cy} = 5.633700		M_{ry} =	M_{cz} = -0.626290		M_{rz} =
	xV_{cz} (7)	zV_{cx} (8)	$M_{cy} + xV_{cz} - zV_{cx}$ = (9)	xV_{cy} (10)	yV_{cx} (11)	$M_{cz} - xV_{cy} + yV_{cx}$ = (12)
A	-5.864413	0	-0.230713	-0.739897	0	0.113607
1	-5.846351	0.010224	-0.222875	-0.737618	0.017696	0.129024
2	-5.702378	0.030672	-0.099350	-0.719453	0.052652	0.145815
3	-5.418015	0.051120	+0.164565	-0.683576	0.086310	0.143596
4	-5.000233	0.071568	0.561899	-0.630866	0.117845	0.122421
5	-4.459357	0.092016	1.082327	-0.562625	0.146477	0.082812
5.5	-4.146549	0.102240	1.384911	-0.523159	0.159473	0.056342
6	-3.808641	0.112463	1.712596	-0.480526	0.171503	0.025739
7	-3.064158	0.132911	2.436631	-0.386594	0.192305	-0.047391
8	-2.244193	0.153359	3.236148	-0.283144	0.208372	-0.133774
9	-1.369045	0.173807	4.090848	-0.172729	0.219309	-0.234252
10	-0.460120	0.194255	4.979325	-0.058052	0.224846	-0.343392
B	0	0.204479	5.423221	0	0.225540	-0.400740

TABLE 4(g)

Element	$\cos\phi$ (1)	$\sin\phi$ (2)	$M_{rx}\sin\phi$ (3)	$M_{ry}\cos\phi$ (4)	$M_{rx}\cos\phi$ (5)	$M_{ry}\sin\phi$ (6)	M_{rz} (7)	From Table IV c M'_{sr} (8)	From Table IV c $M'_{s\phi}$ (9)	$M''_{r1} = b_{13}(7) + b_{12}[(4)-(3)]$ =(10)	$M''_{s1} = b_{12}(9)$ =(11)
A	1	0	0	-0.23071	-2.37237	0	0.11361	0	0	-0.14300	0
1	0.99692	0.07846	-0.15267	-0.21219	-1.93979	-0.01749	0.12902	0	0	+0.00430	0
2	0.97237	0.23345	-0.25772	-0.09660	-1.07344	-0.02319	0.14582	0	0	+0.21244	0
3	0.92388	0.38268	-0.11323	+0.15204	-0.27335	+0.06298	0.14360	0	0	+0.30153	0
4	0.85264	0.52250	+0.23879	+0.47910	+0.38967	+0.29359	0.12242	0	0	+0.26933	0
5	0.76041	0.64945	0.74323	+0.82301	+0.87021	+0.70292	0.08281	0	0	+0.11050	0
5.5	0.70707	0.70707	1.01732	0.97923	+1.01732	0.97923	0.05634	0	0	-0.00482	0
6	0.64945	0.76041	1.30642	1.11231	+1.11579	1.30235	0.02574	0.86541	-0.03397	-0.15524	- .02942
7	0.52250	0.85264	1.86885	1.27314	1.14524	2.07757	-0.04739	2.57495	-0.30476	-0.53959	- .26393
8	0.38268	0.92388	2.34901	1.23841	0.97298	2.98981	-0.13377	4.22096	-0.83960	-1.02870	- .72712
9	0.23345	0.97237	2.68357	0.95501	0.64428	3.97782	-0.23425	5.76318	-1.62538	-1.61410	-1.40763
10	0.07846	0.99692	2.82798	0.39068	0.22257	4.96399	-0.34339	7.16343	-2.64268	-2.28246	-2.28864
B	0	1	2.82124	0	0	5.42822	-0.40074	7.79931	-3.23069	-2.64365	-2.79787

Element	$M''_1 =$ (11) - (10) =(12)	$M''_{r2} = b_{21}[(5)+(6)] + b_{22}[(4)-(3)] + b_{23}(7)$ =(13)	$M''_{s2} =$ $b_{21}(8) + b_{22}(9)$ =(14)	$M''_2 =$ (14) - (13) =(15)	$M''_{r3} = b_{31}[(5)+(6)] + b_{32}[(4)-(3)] + b_{33}(7)$ =(16)	$M''_{s3} =$ $b_{31}(8) + b_{32}(9)$ =(17)	$M''_3 =$ (17) - (16) =(18)
A	0.14300	0.41970	0	-0.41970	-2.34470	0	+2.34470
1	-0.00430	0.31654	0	-0.31654	-1.93705	0	+1.93705
2	-0.21244	0.14133	0	-0.14113	-1.08847	0	+1.08847
3	-0.30153	0.01010	0	-0.01010	-0.21029	0	+0.21029
4	-0.26933	-0.07363	0	+0.07363	+0.67942	0	-0.67942
5	-0.11050	-0.10541	0	+0.10541	+1.56991	0	-1.56991
5.5	+0.00482	-0.10644	0	+0.10644	+1.99486	0	-1.99486
6	+ .12582	-0.09188	-0.05851	+0.03337	+2.41933	0.86359	-1.55574
7	+ .27566	-0.02506	-0.07263	-0.04757	+3.23292	2.57842	-0.65450
8	+ .30158	+0.09237	+0.05030	-0.04207	+3.98599	4.24147	+0.25548
9	+ .20647	+0.25603	+0.30727	+0.05124	+4.66214	5.81206	+1.14992
10	- .000618	+0.46568	+0.69193	+0.22625	+5.24710	7.25131	+2.00421
B	- .15422	+0.58638	+0.92938	+0.34300	+5.50024	7.91038	+2.41015

$b_{11}=0$, $b_{12}=0.86603$, $b_{13}=0.5$, $b_{21}=-0.08716$, $b_{22}=-0.49809$, $b_{23}=0.86273$, $b_{31}=0.99619$, $b_{32}=-0.04358$, $b_{33}=0.07548$

indices for both the double primed and primed axes, it is found, for example that

$$K'_{11} = \frac{b^2_{11}}{K''_1} + \frac{b^2_{21}}{K''_2} + \frac{b^2_{31}}{K''_3} = \left(0 + \frac{\cos^2\beta}{1} + \frac{\sin^2\beta}{3}\right) 10^{-5} = 0.33840 \left(10^{-5}\right)$$

The beam is divided into ten equal segments to keep each $\delta A'_{ij}$ term constant for each segment. Tables 4 (a), (b), and (d) show the computations required

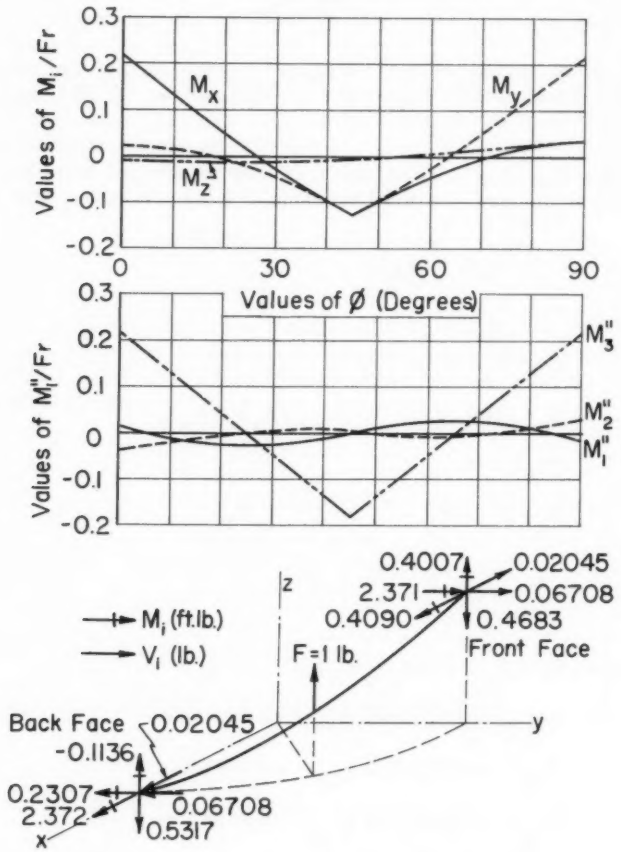

FIG. 5.

to determine the coefficients of Table 2 and the terms of Table 3. These final A_{ij}, C_{ij}, and J_{ij} coefficients, and the P_i and D_i terms found in Table 4 (c) are shown in Table 4 (e) as they would be substituted in Eqs. 44, Appendix I.

Solution of these six equations yields the redundants $(M_c)_i$ and $(V_c)_i$. Final substitution of these values in Tables 4(f) and (g) yields the restoring moments $(M_r)_i$. The final moments and shears are found by using Eqs. 1. Results for moment are plotted in Fig. 5 in terms of M_i/Fr and M_i''/Fr versus ϕ, and the values of V_i and M_i are shown on the ends of the helical beam. (b) The stiffness factor about the y axis at A is defined as the moment at A required to rotate the helical beam about the y axis at A through a unit angle with all other end rotations kept equal to zero. Thus, this stiffness factor may be expressed as

$$S_{Ay} = M_{Ay}\Big]_{\theta_{Ay}=1} \quad \ldots\ldots\ldots\ldots\ldots (35)$$

in which

$$M_{Ay}\Big]_{\theta_{Ay}=1} = M_{cy}\Big]_{\theta_{Ay}=1} + x\,V_{cz}\Big]_{\theta_{Ay}=1} - z\,V_{cx}\Big]_{\theta_{Ay}=1} \quad \ldots (36)$$

The values for $M_{cy}\big]_{\theta\,Ay=1}$, and so forth, may be obtained from Eqs. 44 after the P_i and D_i terms are evaluated in terms of θ Ay = 1. Using Eqs. 26 and 27.

$$P_i = (P_c)_i = (P_A)_i \quad \ldots\ldots\ldots\ldots\ldots\ldots\ldots\ldots (37)$$

So

$$P_y = \theta_{yA} = 1 \quad \ldots\ldots\ldots\ldots\ldots\ldots\ldots\ldots\ldots (38a)$$

and

$$P_x = P_z = 0 \quad \ldots\ldots\ldots\ldots\ldots\ldots\ldots\ldots\ldots (38b)$$

Since $$D_i = (D_c)_i = (D_A)_i + c_{ijk}\,(\rho_A)_j\,(P_A)_k$$

$$(D_A)_i = 0, \quad \ldots\ldots\ldots\ldots\ldots\ldots\ldots\ldots\ldots (39a)$$

and

$$P_x = P_z = 0 \quad \ldots\ldots\ldots\ldots\ldots\ldots\ldots\ldots\ldots (39b)$$

$$D_z = +x_A\,P_y - y_A\,P_x = x_A = +r = 11.03$$

and

$$D_x = D_z = 0$$

Solving Eq. 44 with $P_y = 1$ and $D_z = 11.03$, (Table 4 (e))

$$V_{cx} = +0.03642883 \quad M_{cx} = +0.0801448$$

$$V_{cy} = -0.03022609 \quad M_{cy} = +0.3491825$$

$$V_{cz} = -0.01457716 \quad M_{cz} = -0.4658233$$

Then

$$M_{Ay} = 0.3492 + 11.03\,(-0.01458) + 0 = +0.1884 = S_{Ay}$$

All values for the preceding $(V_c)_i$, $(M_c)_i$, and S_{Ay} terms must be multiplied by 10^5 since the 10^{-5} factor was deleted from the K_{ij} terms as used in

the tables. If $\theta_{Ay} = 1$ radian, the units are kips for the $(V_c)_i$ terms and kip-ft for the $(M_c)_i$ terms.

CONCLUSIONS

The vector approach presented herein for the six equations needed to determine the redundants in a loaded or distorted statically indeterminate ring curved in space, considerably facilitates their derivation and uses standard mathematical sign conventions for moments and rotations. Modification of these equations, when expressed in index notation, is especially simple if auxiliary coordinate systems need to be used in the analysis, as is the case for helical beams.

It is shown that the equations reduce to the column analogy and to the shear and torsion analogy for coplanar rings. However, for noncoplanar rings there seems to be little advantage in modifying the equations so that the redundants can be located at the elastic centroids.

ADDITIONAL REFERENCE

1. "Analysis of Helical Bar Type Structures in Cylindrical Coordinates," by Yen-Ming Yeh, thesis presented to Virginia Polytechnic Inst., at Blacksburg, in May, 1958, as partial fulfilment of the requirements for the degree of Master of Science.

APPENDIX I.—SUMMARY OF EQUATIONS IN CARTESIAN COORDINATES

$$\lambda'_{ij} = \begin{bmatrix} \frac{1}{K'_1} & 0 & 0 \\ 0 & \frac{1}{K'_2} & 0 \\ 0 & 0 & \frac{1}{K'_3} \end{bmatrix} \quad \text{in which } K'_1 = G\,J';\ K'_2 = E\,I'_2,\ K'_3 = E\,I'_3 \qquad \ldots\ (40)$$

$$\begin{aligned}
\frac{1}{K_{xx}} &= \frac{b_{xx}^2}{K'_1} + \frac{b_{yx}^2}{K'_2} + \frac{b_{zx}^2}{K'_3} & \frac{1}{K_{xy}} &= \frac{1}{K_{yx}} = \frac{b_{xx}\,b_{xy}}{K'_1} + \frac{b_{yx}\,b_{yy}}{K'_2} + \frac{b_{zx}\,b_{zy}}{K'_3} \\
\frac{1}{K_{yy}} &= \frac{b_{xy}^2}{K'_1} + \frac{b_{yy}^2}{K'_2} + \frac{b_{zy}^2}{K'_3} & \frac{1}{K_{xz}} &= \frac{1}{K_{zx}} = \frac{b_{xx}\,b_{xz}}{K'_1} + \frac{b_{yx}\,b_{yz}}{K'_2} + \frac{b_{zx}\,b_{zz}}{K'_3} \\
\frac{1}{K_{zz}} &= \frac{b_{xz}^2}{K'_1} + \frac{b_{yz}^2}{K'_2} + \frac{b_{zz}^2}{K'_3} & \frac{1}{K_{yz}} &= \frac{1}{K_{zy}} = \frac{b_{xy}\,b_{xz}}{K'_1} + \frac{b_{yy}\,b_{yz}}{K'_2} + \frac{b_{zy}\,b_{zz}}{K'_3}
\end{aligned} \qquad \ldots\ (41)$$

$$\delta A_{ij} = \frac{\delta S}{K_{ij}} \qquad \ldots (42)$$

$$\left(M_r\right)_i = \left(M_c\right)_i - C_{ijk} \rho_l \left(V_c\right)_k \begin{cases} M_{rx} = M_{cx} - y\, V_{cz} + Z\, V_{cy} \\ M_{ry} = M_{cy} + x\, V_{cz} - Z\, V_{cx} \\ M_{rz} = M_{cz} - x\, V_{cy} + y\, V_{cx} \end{cases} \qquad \ldots (43)$$

$$\begin{aligned}
P_i &= A_{ij} \left(M_c\right)_j + C_{ij} \left(V_c\right)_j \\
D_i &= C_{ji} \left(M_c\right)_j + J_{ij} \left(V_c\right)_j \\
\overline{P_x} &= \overline{A_{xx}}\ \overline{M_{cx}} + \overline{A_{xy}}\ \overline{M_{cy}} + A_{xz}\, M_{cz} + C_{xx}\, V_{cx} + C_{xy}\, V_{cy} + \overline{C_{xz}}\ \overline{V_{cz}} \\
\overline{P_y} &= \overline{A_{xy}}\ \overline{M_{cx}} + \overline{A_{yy}}\ \overline{M_{cy}} + A_{yz}\, M_{cz} + C_{yx}\, V_{cx} + C_{yy}\, V_{cy} + \overline{C_{yz}}\ \overline{V_{cz}} \\
\overline{P_z} &= A_{xz}\, M_{cx} + A_{yz}\, M_{cy} + \overline{A_{zz}\, M_{cz}} + \overline{C_{zx}\, V_{cx}} + \overline{C_{zy}\, V_{cy}} + C_{zz}\, V_{cz} \\
\overline{D_x} &= C_{xx}\, M_{cx} + C_{yx}\, M_{cy} + \overline{C_{zx}\, M_{cz}} + \overline{J_{xx}\, V_{cx}} + \overline{J_{xy}\, V_{cy}} + J_{xz}\, V_{cz} \\
\overline{D_y} &= C_{xy}\, M_{cx} + C_{yy}\, M_{cy} + \overline{C_{zy}\, M_{cz}} + \overline{J_{xy}\, V_{cx}} + \overline{J_{yy}\, V_{cy}} + J_{yz}\, V_{cz} \\
\overline{D_z} &= \overline{C_{xz}}\ \overline{M_{cx}} + \overline{C_{yz}}\ \overline{M_{cy}} + C_{zz}\, M_{cz} + J_{xz}\, V_{cx} + J_{yz}\, V_{cy} + \overline{J_{zz}}\ \overline{V_{cz}}
\end{aligned} \qquad \ldots (44)$$

$$\begin{aligned}
M_i &= \left(M_s\right)_i - \left(M_r\right)_i \qquad \text{for loaded structures} \\
M_i &= \left(M_r\right)_i \qquad \text{for distorted structures}
\end{aligned} \qquad \ldots (45)$$

Journal of the
ENGINEERING MECHANICS DIVISION
Proceedings of the American Society of Civil Engineers

UNIFORMLY MOVING LOAD ON A LAYERED HALF PLANE

By J. L. Sackman,[1] A. M. ASCE

SYNOPSIS

A problem of interest in studies of transmission of ground shock caused by a surface nuclear burst is that of the uniform motion of a steady pressure distribution over the surface of a half space. In this paper a special instance of that problem is considered. The steady state displacements and stresses produced in a two-layered elastic half plane by the uniform superseismic motion of a constant, concentrated normal line load along the surface of the half plane are determined in terms of dilatational and distortional potentials. The solution is constructed by systematically adding to the solution of the analogous problem for the one-layered half space the solutions for multiple reflections and refractions of plane elastic waves from plane boundaries. Superposition of the line-load solution can then be utilized to obtain the solution for an arbitrary steady pressure distribution uniformly progressing with superseismic speed over the surface of the two-layered half plane. Stress histories are presented for a particular medium subjected to a step pressure of uniform intensity and to step pressures which decay exponentially.

INTRODUCTION

Notation.—The letter symbols used in this paper are defined where they first appear, in the illustrations or in the text, and are arranged alphabetically, for convenience of reference, in the Appendix.

Note.—Discussion open until January 1, 1962. To extend the closing date one month, a written request must be filed with the Executive Secretary, ASCE. This paper is part of the copyrighted Journal of the Engineering Mechanics Division, Proceedings of the American Society of Civil Engineers, Vol. 87, No. EM 4, August, 1961.

[1] Asst. Prof. of Civ. Engrg., Univ. of California, Berkeley, Calif.

General.—The displacements and stresses produced in a two-layered elastic half space by the uniform motion of a concentrated normal line load of constant intensity along the surface of the half space are investigated. The speed of the load is assumed to be greater than the velocities of propagation of dilatational and distortional waves in either layer (superseismic case). It is further assumed that the load has been moving steadily for a long time so that a steady state (of plane strain) exists with respect to a coordinate system attached to the moving load. The solution resulting from a steadily moving arbitrary load distribution can be obtained by superposition of the line load solution, and results are shown for a pressure distribution varying as the unit step function, and as a step with exponential decay. Although not considered herein, the case of tangential loads on the surface of the two-layered half space can be treated in exactly the same manner. The case of more than two layers becomes more complicated but can be treated in a manner similar to the one presented.

SOLUTION

Let $(\bar{x}, \bar{z})$ denote fixed space coordinates and let (x, z) denote space coordinates attached to the moving load P (Fig. 1). The top layer of the medium

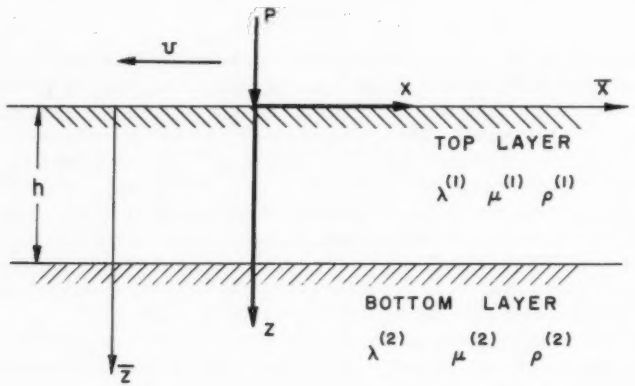

FIG. 1.

has a depth h, and the bottom layer an infinite depth. The concentrated vertical line load of intensity P (measured positive downward) moves over the surface of the half-space in the negative $\bar{x}$ direction with a speed U. At time t = 0 the two coordinate systems are taken to be in coincidence, so that

$$x = \bar{x} + U t, \quad z = \bar{z} \quad \ldots\ldots\ldots\ldots\ldots\ldots (1)$$

The solution will be given in terms of dilatational (or longitudinal) and distortional (or transversal) potentials, Φ and Ψ, from which the displacements are derived by the relations

$$u = \frac{\partial \Phi}{\partial x} - \frac{\partial \Psi}{\partial z} \quad \ldots\ldots\ldots\ldots\ldots\ldots (2a)$$

and

$$w = \frac{\partial \Phi}{\partial z} + \frac{\partial \Psi}{\partial x} \quad \ldots\ldots\ldots\ldots\ldots\ldots (2b)$$

Strain and stress components are then derived from the displacements in the usual manner. Superscript (1) will identify quantities in the top layer, and superscript (2) quantities in the bottom layer.

The solution is obtained by utilizing the results of the analogous problem for the one-layered half space[2] in conjunction with the results for the reflection and refraction of plane elastic waves at plane boundaries.[3] Fig. 2 shows the situation for the one-layered half space, in which the solution consists of a dilatational wave of strength ϕ^1_{00} and a distortional wave of strength ψ^1_{00}. The solution has the simple character shown in Fig. 2 only for the superseismic case, that is if the velocity U is larger than the velocities of wave propagation in the medium.

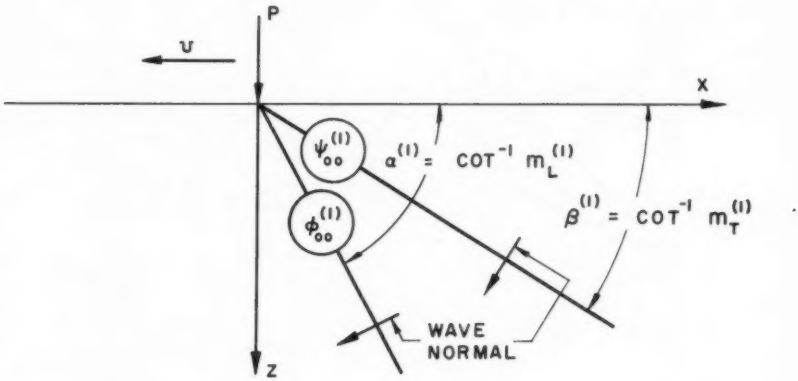

FIG. 2.

To form a two-layered half space, a plane interface at depth $\bar{z} = h$ is introduced, and the two layers are assumed to have different properties, Fig. 3. The introduction of this interface requires reflections and refractions of the plane waves signified by ϕ^1_{00} and ψ^1_{00}. For example, the dilatational wave ϕ^1_{00} generates in the lower layer a dilatational wave of strength ϕ^2_{10} and a distortional wave of strength ψ^2_{10}. In the upper layer the reflected waves ϕ^1_{10} and ψ^1_{10}

2 "Stresses Produced in a Half Plane by Moving Loads," by J. Cole and J. Huth, Journal of Applied Mechanics, Vol. 25, No. 4, December, 1958, pp. 433-436.

3 "The Earth," by H. Jeffreys, Third Ed., Cambridge Univ. Press, New York, 1952, Chapter II.

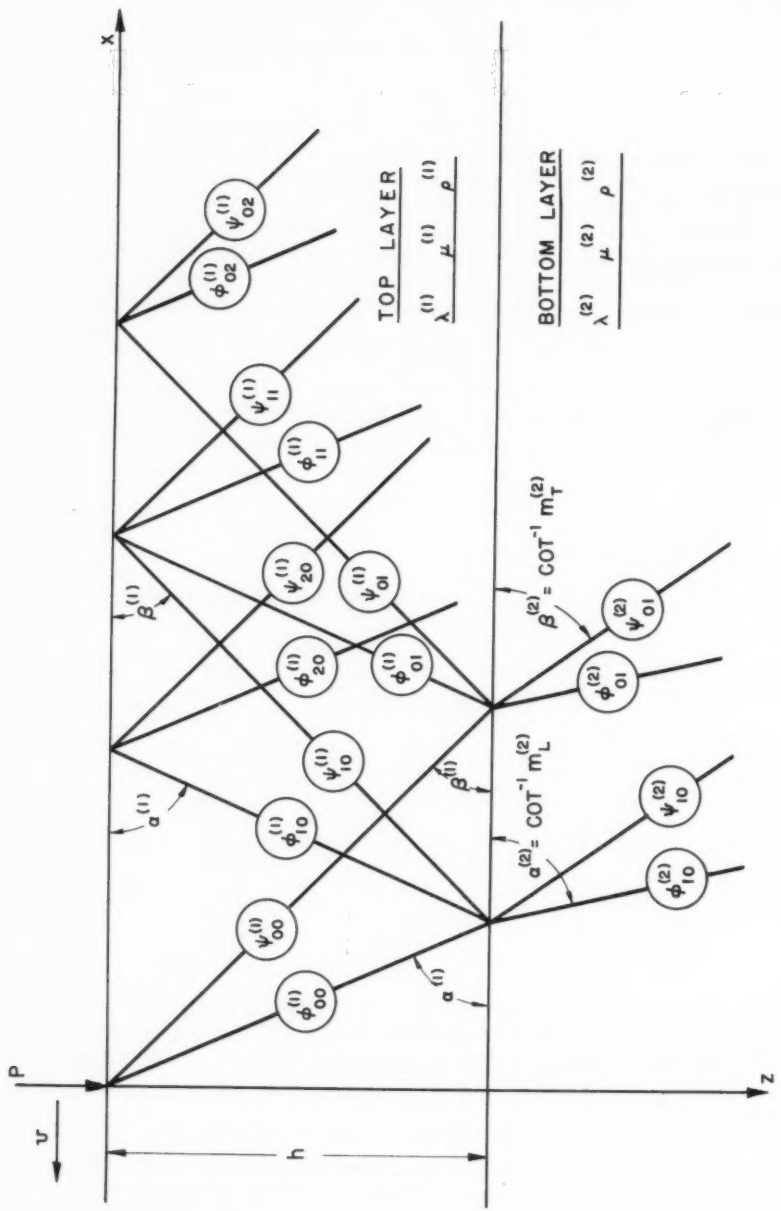
x
z
P
v
h
TOP LAYER
$\lambda^{(1)}$ $\mu^{(1)}$ $\rho^{(1)}$
BOTTOM LAYER
$\lambda^{(2)}$ $\mu^{(2)}$ $\rho^{(2)}$
$\alpha^{(1)}$
$\beta^{(1)}$
$\alpha^{(2)} = \cot^{-1} m_L^{(2)}$
$\beta^{(2)} = \cot^{-1} m_T^{(2)}$
$\phi_{00}^{(1)}$ $\psi_{00}^{(1)}$
$\phi_{10}^{(1)}$ $\psi_{10}^{(1)}$
$\phi_{01}^{(1)}$ $\psi_{01}^{(1)}$
$\phi_{20}^{(1)}$ $\psi_{20}^{(1)}$
$\phi_{11}^{(1)}$ $\psi_{11}^{(1)}$
$\phi_{02}^{(1)}$ $\psi_{02}^{(1)}$
$\phi_{10}^{(2)}$ $\psi_{10}^{(2)}$
$\phi_{01}^{(2)}$ $\psi_{01}^{(2)}$

FIG. 3.

are generated. A similar phenomenon occurs due to the distortional wave ψ^1_{00}. The waves signified by ϕ^1_{10} and ψ^1_{10} must, in turn, be reflected off the plane boundary at $\bar{z} = 0$ so as not to effect tractions on this boundary. Further reflections occur ad infinitum. Fig. 3 depicts the beginning of this process. The notation of N. Davids[4] is adapted for use in this problem, so that ϕ^1_{10} (ψ^1_{10}) represents the strength of a dilatational (distortional wave in the top layer generated from i previous dilatational waves and j previous distortional waves after i + j successive reflections. A similar notation $(\phi^2_{ij}, \psi^2_{ij}, i + j = \text{odd integer})$ is used for the strengths of the waves in the bottom layer.

The laws of reflection and refraction are now used to determine the strengths of the generated waves in terms of the strengths of the waves incident on the plane boundaries at $\bar{z} = 0$, h. When incident waves impinge on the interface at $\bar{z} = h$, following (recurrence) relations hold (valid for i + j = odd integer; q = 1,2)

$$\left.\begin{aligned} \phi^{(q)}_{ij} &= \phi^{(1)}_{i-1,j}\ A^{(q)}_{11} + \psi^{(1)}_{i,j-1}\ A^{(q)}_{12} \\ \psi^{(q)}_{ij} &= \phi^{(1)}_{i-1,j}\ A^{(2)}_{21} + \psi^{(1)}_{i,j-1}\ A^{(q)}_{22} \end{aligned}\right\} \quad \ldots\ldots\ldots\ldots (3a)$$

$$\left.\begin{aligned} A^{(1)}_{11}\ \Delta &= (a_1 - a_3)(b_2 + b_4) - (a_2 + a_4)(b_1 - b_3) \\ A^{(1)}_{12}\ \Delta &= -2(a_1 b_3 - a_3 b_1); \quad A^{(1)}_{21}\ \Delta = 2(a_4 b_2 - a_2 b_4) \\ A^{(1)}_{22}\ \Delta &= (a_2 - a_4)(b_1 + b_3) - (a_1 + a_3)(b_2 - b_4) \\ A^{(2)}_{11}\ \Delta &= 2(b_2 + b_4) \quad ; \quad A^{(2)}_{12}\ \Delta = -2(b_1 + b_3) \\ A^{(2)}_{21}\ \Delta &= -2(a_2 + a_4) \quad ; \quad A^{(2)}_{22}\ \Delta = 2(a_1 + a_3) \\ \Delta &= (a_1 + a_3)(b_2 + b_4) - (a_2 + a_4)(b_1 + b_3) \end{aligned}\right\} \quad \ldots (3b)$$

4 "Transient Analysis of Stress Wave Penetration in Plates," by N. Davids, Journal of Applied Mechanics, Vol. 26, No. 4, December, 1959, pp. 651-660.

$$
\left.
\begin{aligned}
a_1 &= \left[2 + K\left(m_T^{(2)^2} - 1\right)\right]\left[m_T^{(1)^2} + 1\right]^{-1} \\
a_2 &= \left[\left(m_T^{(1)^2} - 1\right) - K\left(m_T^{(2)^2} - 1\right)\right]\left[m_T^{(1)}\left(m_T^{(1)^2} + 1\right)\right]^{-1} \\
a_3 &= m_L^{(2)}\left[2K + \left(m_T^{(1)^2} - 1\right)\right]\left[m_L^{(1)}\left(m_T^{(1)^2} + 1\right)\right]^{-1} \\
a_4 &= \left[2m_L^{(2)}\left(K - 1\right)\right]\left[m_T^{(1)^2} + 1\right]^{-1} \\
b_1 &= \frac{-a_4 m_T^{(2)}}{m_L^{(2)}} \\
b_2 &= \frac{a_3 m_L^{(1)} m_T^{(2)}}{m_L^{(2)} m_T^{(1)}} \\
b_3 &= \frac{-a_2 m_T^{(1)}}{m_L^{(1)}} \\
b_4 &= a_1
\end{aligned}
\right\} \quad \ldots(3c)
$$

and

$$
\left.
\begin{aligned}
K &= \frac{\mu^{(2)}}{\mu^{(1)}} \\
m_L^{(q)} &= \left(M_L^{(q)^2} - 1\right)^{1/2} \quad ; \quad m_T^{(q)} = \left(M_T^{(q)^2} - 1\right)^{1/2} \\
M_L^{(q)} &= \frac{U}{C_L^{(q)}} \quad ; \quad M_T^{(q)} = \frac{U}{C_T^{(q)}} \\
C_L^{(q)^2} &= \frac{\left(\lambda^{(q)} + 2\mu^{(q)}\right)}{\rho^{(q)}} \quad ; \quad C_T^{(q)^2} = \frac{\mu^{(q)}}{\rho^{(q)}}
\end{aligned}
\right\} \quad \ldots(3d)
$$

in which $\phi_{i-1,j}^{(1)}$, $\psi_{i,j-1}^{(1)}$ are the strengths of the incident waves, $\phi_{ij}^{(1)}$, $\psi_{ij}^{(1)}$ denote the strengths of the resulting reflected waves, $\phi_{ij}^{(2)}$, $\psi_{ij}^{(2)}$ represent the strengths of the resulting refracted waves, U is the speed of the moving load, $C_L^{(q)}$, $C_T^{(q)}$ refer to the respective velocities of propagation of dilatational and distortional waves in the layers, $\lambda^{(q)}$, $\mu^{(q)}$ are the Lamé constants of the layers, and $\rho^{(q)}$ is the mass density of the layers.

For reflections from the free surface (z = 0) the (recurrence) relations are (valid for i + j = even integer; q = 1,2)

$$\left.\begin{aligned} \phi_{ij}^{(q)} &= \phi_{i-1,j}^{(q)}\ B_{11}^{(q)} + \psi_{i,j-1}^{(q)}\ B_{12}^{(q)} \\ \psi_{ij}^{(q)} &= \phi_{i-1,j}^{(q)}\ B_{21}^{(q)} + \psi_{i,j-1}^{(q)}\ B_{22}^{(q)} \end{aligned}\right\} \quad \ldots\ldots\ldots (4a)$$

and

$$\left.\begin{aligned} B_{11}^{(1)}\ \delta &= 4\, m_L^{(1)}\ m_T^{(1)} - \left(m_T^{(1)^2} - 1\right)^2 \\ B_{12}^{(1)}\ \delta &= -\,4\, m_T^{(1)} \left(m_T^{(1)^2} - 1\right) \\ B_{21}^{(1)}\ \delta &= 4\, m_L^{(1)} \left(m_T^{(1)^2} - 1\right) \\ B_{22}^{(1)} &= B_{11}^{(1)} \\ \delta &= 4\, m_L^{(1)}\ m_T^{(1)} + \left(m_T^{(1)^2} - 1\right)^2 \\ B_{11}^{(2)} &= B_{12}^{(2)} = B_{21}^{(2)} = B_{22}^{(2)} = 0 \end{aligned}\right\} \quad \ldots\ldots (4b)$$

As a matter of notational convenience, both recurrence relations Eq. 3(a) and Eq. 4(a) may be unified as

$$\phi_{ij}^{(q)} = \frac{1 - (-1)^{i+j}}{2} \left[A_{11}^{(q)}\ \phi_{i-1,j}^{(1)} + A_{12}^{(q)}\ \psi_{i,j-1}^{(1)}\right] + \frac{1 + (-1)^{i+j}}{2} \left[B_{11}^{(q)}\ \phi_{i-1,j}^{(1)} + B_{12}^{(q)}\ \psi_{i,j-1}^{(1)}\right] \quad \ldots\ldots (5a)$$

and

$$\psi_{ij}^{(q)} = \frac{1 - (-1)^{i+j}}{2} \left[A_{21}^{(q)}\ \phi_{i-1,j}^{(1)} + A_{22}^{(q)}\ \psi_{i,j-1}^{(1)}\right] + \frac{1 + (-1)^{i+j}}{2} \left[B_{21}^{(q)}\ \phi_{i-1,j}^{(1)} + B_{22}^{(q)}\ \psi_{i,j-1}^{(1)}\right] \quad \ldots\ldots (5b)$$

(If an index is negative, the corresponding strength is zero.) In this way all of the strengths may finally be related to the two primary strengths, $\phi_{00}^{(1)}$ and $\psi_{00}^{(1)}$, given by the solution of the analogous one-layered problem:[2]

$$\phi_{00}^{(1)} = P\, \frac{c_1}{\mu^{(1)}} \quad \ldots\ldots\ldots\ldots\ldots (6a)$$

$$\psi_{00}^{(1)} = P\, \frac{c_2}{\mu^{(1)}} \quad \ldots\ldots\ldots\ldots\ldots (6b)$$

$$c_1 \delta = 2 - M_T^{(1)2} \quad \ldots\ldots\ldots\ldots\ldots\ldots (6c)$$

and

$$c_2 \delta = 2\, m_L^{(1)} \quad \ldots\ldots\ldots\ldots\ldots\ldots (6d)$$

Adding the effects of all the reflections and refractions, the solution to the two-layered problem is finally

$$\left.\begin{aligned} \Phi^{(q)}_{(x,\,z)} &= \sum_{r=0}^{\infty} \sum_{s=0}^{r} \phi^{(q)}_{s,r-s}\; F\left(\xi^{(q)}_{s,r-s}\right) \\ \Psi^{(q)}_{(x,\,z)} &= \sum_{r=0}^{\infty} \sum_{s=0}^{r} \psi^{(q)}_{s,r-s}\; F\left(\eta^{(q)}_{s,r-s}\right) \end{aligned}\right\} \quad \ldots\ldots\ldots (7a)$$

and

$$\left.\begin{aligned} \xi^{(q)}_{ij} &= \frac{1+(-1)^{i+j}}{2}\left[x - m_L^{(q)}\; z - d_{ij}\right] \\ &\quad + \frac{1-(-1)^{i+j}}{2}\left[x - (-1)^q m_L^{(q)} (z-h) - d_{ij}\right] \\ \eta^{(q)}_{ij} &= \frac{1+(-1)^{i+j}}{2}\left[x - m_T^{(q)}\; z - d_{ij}\right] \\ &\quad + \frac{1-(-1)^{i+j}}{2}\left[x - (-1)^q m_T^{(q)} (z-h) - d_{ij}\right] \\ d_{ij} &= \left[i\, m_L^{(1)} + j\, m_T^{(1)}\right] h \end{aligned}\right\} \quad \ldots\ldots (7b)$$

The term F is the functional form of the primary generating waves $\left(\text{of strengths } \phi^{(1)}_{00},\ \psi^{(1)}_{00}\right)$ given by the solution of the analogous one-layered problem[2]

$$F' = H \quad \ldots\ldots\ldots\ldots\ldots\ldots (8)$$

in which F' is the derivative of F, and H is the unit step function. (It is not necessary to determine F, as only derivatives of F are required for the displacements.) In terms of the potentials Φ and Ψ of Eq. 7(a), the displacements are given by Eq. 2, and the stress components are

$$\sigma_{xx} = 2\mu \left(\frac{\partial^2 \Phi}{\partial x^2} - \frac{\partial^2 \Phi}{\partial x\, \partial z}\right) + \lambda \nabla^2 \Phi \quad \ldots\ldots\ldots (9a)$$

$$\sigma_{xz} = \mu \left(2 \frac{\partial^2 \Phi}{\partial x\, \partial z} + \frac{\partial^2 \Psi}{\partial x^2} - \frac{\partial^2 \Psi}{\partial x^2}\right) \quad \ldots\ldots\ldots (9b)$$

$$\sigma_{zz} = 2\mu \left(\frac{\partial^2 \Phi}{\partial z^2} + \frac{\partial^2 \Psi}{\partial x\, \partial z}\right) + \lambda \nabla^2 \Phi \quad \ldots\ldots\ldots (9c)$$

$$\sigma_{yy} = \lambda \nabla^2 \Phi \quad \ldots\ldots\ldots\ldots\ldots\ldots (9d)$$

and

$$\sigma_{xy} = \sigma_{yz} = 0 \quad \ldots\ldots\ldots\ldots\ldots\ldots (9e)$$

EXAMPLE

As an illustration, the early time history for the stresses produced by a uniform step pressure, $p_o\, H(x)$, Fig. 4(a) is given in Fig. 4(b) for a point in the top layer ($\bar{x} = 0$, $\bar{z} = h/2$) and in Fig. 4(c) for a point in the bottom layer ($\bar{x} = 0$, $\bar{z} = 2\,h$). The material properties have been chosen such that $\lambda = \mu$, $\rho^{(1)} = \rho^{(2)}$, $M_L^{(1)} = 3 = 2\, M_L^{(2)}$. This choice of properties yields a half space in which sound velocities are higher in the bottom layer than in the top layer, a situation likely to be encountered in nature. For this same medium Figs. 5, 6, and 7 depict the early time stress histories produced by an exponentially decaying step pressure loading, $p_o \exp(-\kappa x/h)\, H(x)$, in which p_o is the maximum value of the applied surface pressure and κ is a decay factor. The results for three values of κ are illustrated: $\kappa = 0.2,\ 1.0,\ 5.0$.

CONCLUSIONS

The stress distribution and displacements produced by the uniform, superseismic motion of a concentrated line load of constant intensity over the surface of a two-layered elastic half plane have been determined in terms of dilatational and distortional potentials. The numerical examples considered treat a half space in which sound velocities are greater in the bottom layer than in the top layer. For such a layered medium, and for a uniform step pressure progressing over the surface of the half space, the peak value of the stress, in either the top or bottom layer, occurs after several reflections and refractions of the elastic waves generated by the moving surface load. These peak values are greater than those which would occur in a one-layered half space composed of either the material of the top layer or of the bottom layer of the two-layered medium.

For the case of decaying step pressure distributions in uniform motion along the surface of the layered half plane, the peak stress at a point in the medium occurs at the arrival of the first signal caused by the surface load. Thus, for loads with high enough decay factors, the peak stress in the top layer can be determined from the (simpler) solution of the one-layered problem,[2] while the peak stress in the bottom layer can be obtained from the consideration of only a single elastic wave refraction at the interface of the two layers. In this case the maximum stress in the top layer is the same as that which would occur if the medium were one-layered and composed of the material of the top layer. The maximum stress in the bottom layer is again greater than those which would occur in a one-layered half space composed of either the material of the top layer or of the bottom layer.

It is noted that as the decay factor of the loading increases, the interaction at a point in the medium between the various reflected and refracted elastic waves decreases. Hence, for most points in the medium, if the surface load

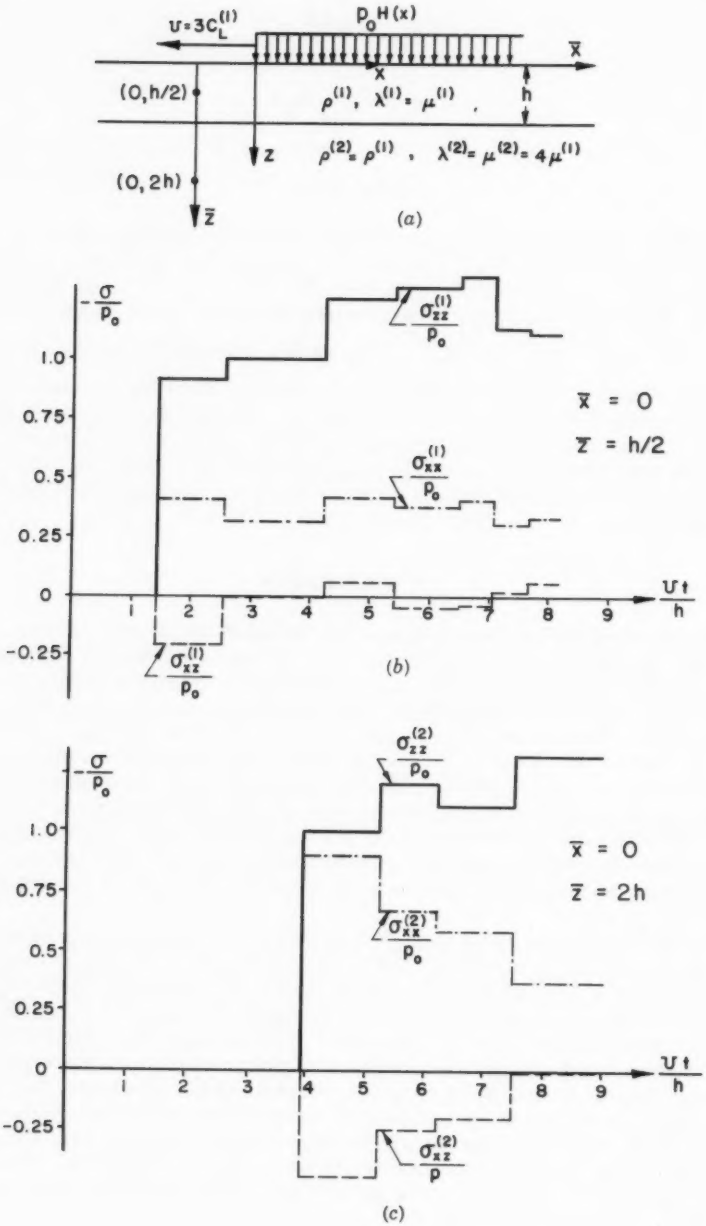
$v = 3C_L^{(1)}$
$p_o H(x)$
$\bar{x}$
x
$(0, h/2)$
$\rho^{(1)}, \lambda^{(1)} = \mu^{(1)}$
h
z
$\rho^{(2)} = \rho^{(1)}$, $\lambda^{(2)} = \mu^{(2)} = 4\mu^{(1)}$
$(0, 2h)$
$\bar{z}$
(a)
$\frac{\sigma}{p_o}$
$\frac{\sigma_{zz}^{(1)}}{p_o}$
1.0
0.75
0.5
0.25
0
-0.25
$\bar{x} = 0$
$\bar{z} = h/2$
$\frac{\sigma_{xx}^{(1)}}{p_o}$
1 2 3 4 5 6 7 8 9
$\frac{vt}{h}$
$\frac{\sigma_{xz}^{(1)}}{p_o}$
(b)
$\frac{\sigma}{p_o}$
$\frac{\sigma_{zz}^{(2)}}{p_o}$
1.0
0.75
0.5
0.25
0
-0.25
$\bar{x} = 0$
$\bar{z} = 2h$
$\frac{\sigma_{xx}^{(2)}}{p_o}$
1 2 3 4 5 6 7 8 9
$\frac{vt}{h}$
$\frac{\sigma_{xz}^{(2)}}{p}$
(c)

FIG. 4.

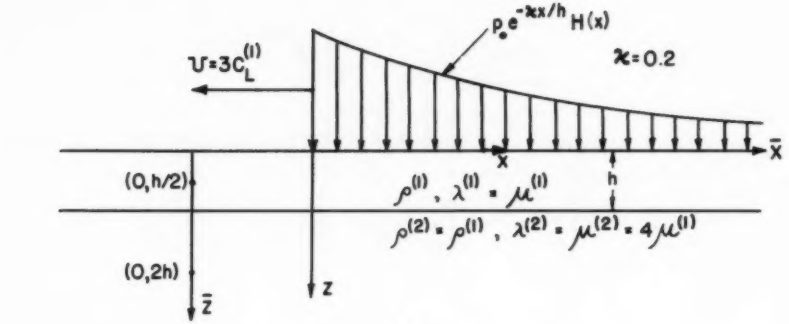
$p_o e^{-\varkappa x/h} H(x)$
$\varkappa = 0.2$
$V = 3C_L^{(1)}$
$\bar{x}$
$\bar{x}$
(0,h/2)
$\rho^{(1)}, \lambda^{(1)} = \mu^{(1)}$
h
$\rho^{(2)} = \rho^{(1)}, \lambda^{(2)} = \mu^{(2)} = 4\mu^{(1)}$
(0,2h)
$\bar{z}$
z

(a)

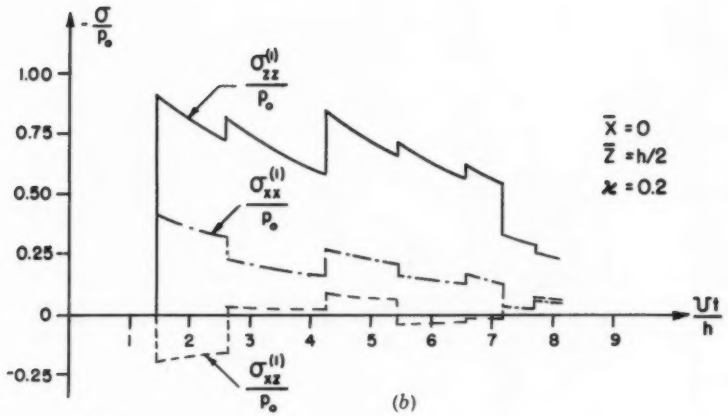
$-\frac{\sigma}{p_o}$
1.00
0.75
0.50
0.25
0
-0.25
$\frac{\sigma_{zz}^{(1)}}{p_o}$
$\frac{\sigma_{xx}^{(1)}}{p_o}$
$\frac{\sigma_{xz}^{(1)}}{p_o}$
$\bar{x} = 0$
$\bar{z} = h/2$
$\varkappa = 0.2$
1 2 3 4 5 6 7 8 9
$\frac{Vt}{h}$

(b)

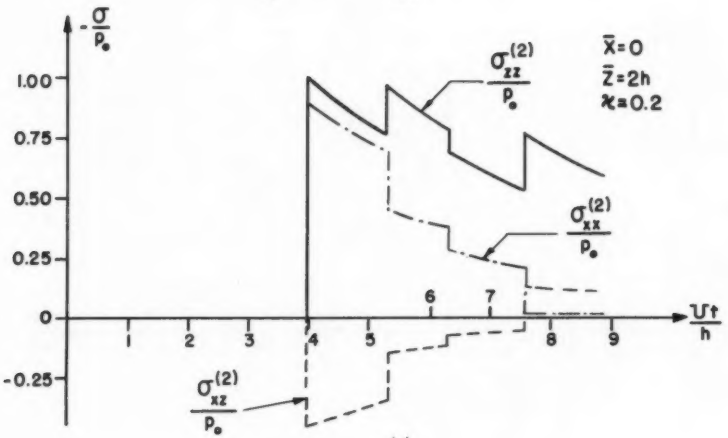
$-\frac{\sigma}{p_o}$
1.00
0.75
0.50
0.25
0
-0.25
$\frac{\sigma_{zz}^{(2)}}{p_o}$
$\frac{\sigma_{xx}^{(2)}}{p_o}$
$\frac{\sigma_{xz}^{(2)}}{p_o}$
$\bar{x} = 0$
$\bar{z} = 2h$
$\varkappa = 0.2$
1 2 3 4 5 6 7 8 9
$\frac{Vt}{h}$

(c)

FIG. 5.

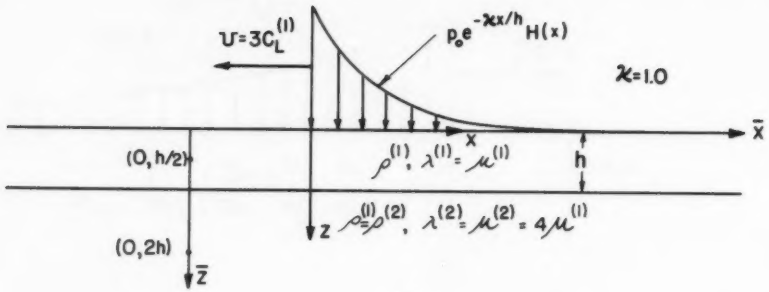
$U=3C_L^{(1)}$
$p_o e^{-\varkappa x/h} H(x)$
$\varkappa=1.0$
x
$\bar{x}$
(0, h/2)
$\rho^{(1)}, \lambda^{(1)}=\mu^{(1)}$
h
z
$\rho^{(1)}=\rho^{(2)}, \lambda^{(2)}=\mu^{(2)}=4\mu^{(1)}$
(0,2h)
$\bar{z}$

(a)

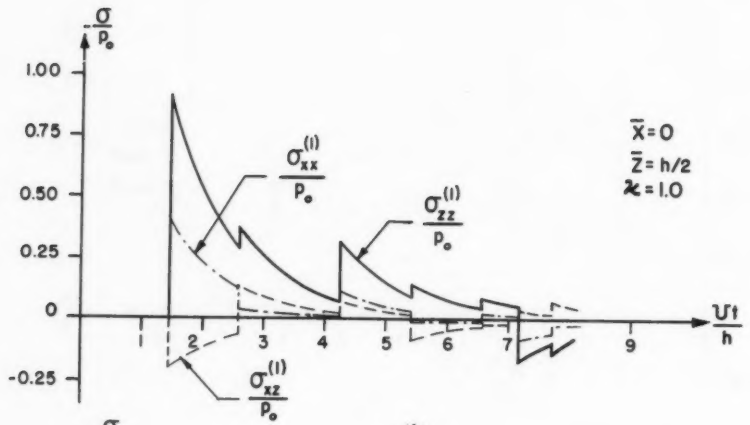
$\frac{\sigma}{p_o}$
1.00
0.75
0.50
0.25
0
-0.25
$\frac{\sigma_{xx}^{(1)}}{p_o}$
$\frac{\sigma_{zz}^{(1)}}{p_o}$
$\frac{\sigma_{xz}^{(1)}}{p_o}$
$\bar{x}=0$
$\bar{z}=h/2$
$\varkappa=1.0$
1
2
3
4
5
6
7
9
$\frac{Ut}{h}$

(b)

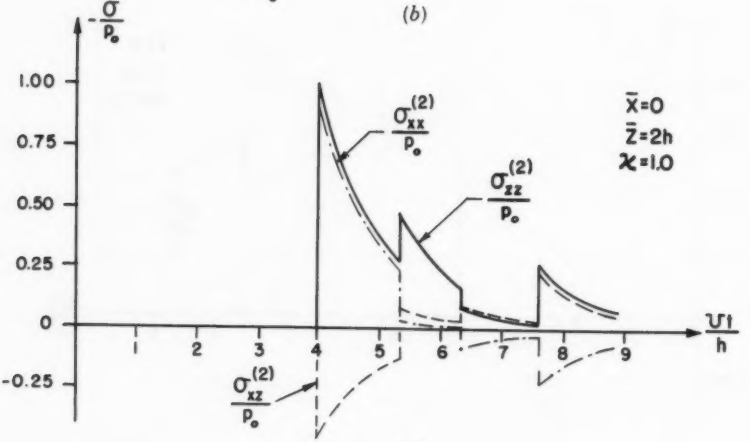
$\frac{\sigma}{p_o}$
1.00
0.75
0.50
0.25
0
-0.25
$\frac{\sigma_{xx}^{(2)}}{p_o}$
$\frac{\sigma_{zz}^{(2)}}{p_o}$
$\frac{\sigma_{xz}^{(2)}}{p_o}$
$\bar{x}=0$
$\bar{z}=2h$
$\varkappa=1.0$
1
2
3
4
5
6
7
8
9
$\frac{Ut}{h}$

(c)

FIG. 6.

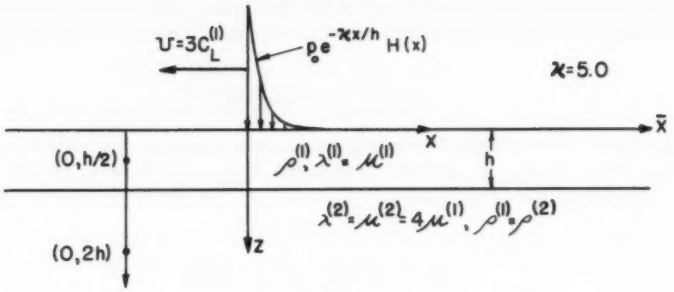
$v=3c_L^{(1)}$
$p_0 e^{-\varkappa x/h} H(x)$
$\varkappa=5.0$
$\bar{x}$
x
h
(0,h/2)
$\rho^{(1)}, \lambda^{(1)}=\mu^{(1)}$
$\lambda^{(2)}=\mu^{(2)}=4\mu^{(1)}, \rho^{(1)}=\rho^{(2)}$
(0,2h)
z

(a)

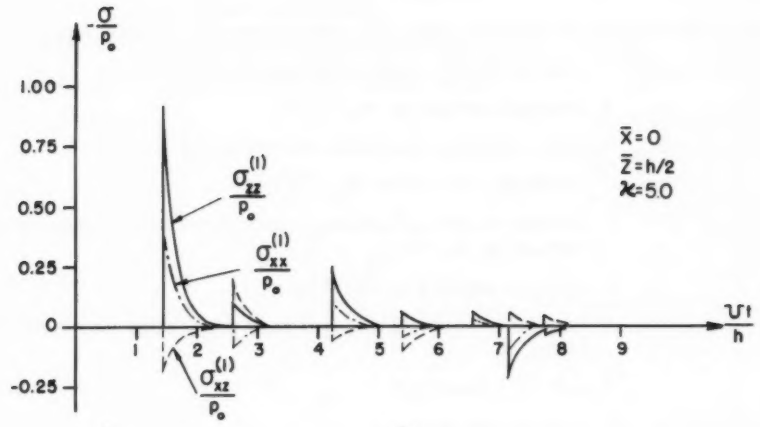
$-\frac{\sigma}{p_0}$
1.00
0.75
0.50
0.25
0
-0.25
$\bar{x}=0$
$\bar{z}=h/2$
$\varkappa=5.0$
$\frac{\sigma_{zz}^{(1)}}{p_0}$
$\frac{\sigma_{xx}^{(1)}}{p_0}$
$\frac{\sigma_{xz}^{(1)}}{p_0}$
1 2 3 4 5 6 7 8 9
$\frac{vt}{h}$

(b)

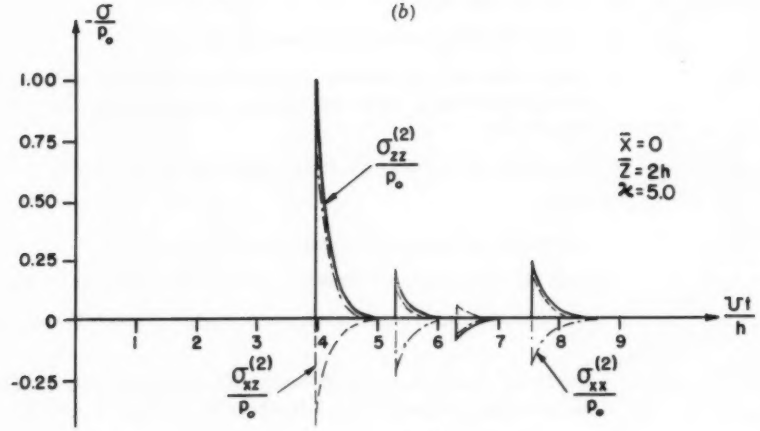
$-\frac{\sigma}{p_0}$
1.00
0.75
0.50
0.25
0
-0.25
$\bar{x}=0$
$\bar{z}=2h$
$\varkappa=5.0$
$\frac{\sigma_{zz}^{(2)}}{p_0}$
$\frac{\sigma_{xz}^{(2)}}{p_0}$
$\frac{\sigma_{xx}^{(2)}}{p_0}$
1 2 3 4 5 6 7 8 9
$\frac{vt}{h}$

(c)

FIG. 7.

has a high decay factor, by the time a signal from a particular reflected or refracted wave is received, previous signals will have decayed to a low level.

ACKNOWLEDGMENTS

This paper is a result of investigations sponsored by the RAND Corporation with Paul Weidlinger, F. ASCE, Consulting Engineer, New York, N. Y.

APPENDIX.—NOTATION

The following letter symbols have been adopted for use in this paper:

$A_{11}, \ldots, A_{22}$ = wave strength constant defined by Eq. 3(b);

$a_1, \ldots, a_4$ = constant defined by Eq. 3(c);

$B_{11}, \ldots, B_{22}$ = wave strength constants defined by Eq. 4(b);

$b_1, \ldots, b_2$ = constants defined by Eq. 3(c);

C_L, C_T = velocity of dilatational and distortional wave, respectively, defined by Eq. 3(d);

d_{ij} = distance defined by Eq. 7(b);

F = functional form of the primary generating waves defined by Eq. 8;

H = unit step function;

h = depth of top layer;

K = ration of shear moduli defined by Eq. 3(d);

M_L, M_T = Mach number of moving load with respect to dilatational and distortional wave velocities, respectively, defined by Eq. 3(d);

m_L, m_T = functions of the Mach number defined by Eq. 3(d);

t = time;

U = constant velocity of moving surface load;

x, z = moving rectangular cartesian coordinates defined by Eq. 1;

$\bar{x}, \bar{z}$ = fixed rectangular cartesian coordinates illustrated in Fig. 1;

α, β = angle of inclination of dilatational and distortional plane wave front, respectively, illustrated in Figs. 2 and 3;

Δ, δ = constants defined by Eqs. 3(b) and 4(b), respectively;

κ = decay factor for exponential surface loading;

η_{ij}, ξ_{ij} = normal distance behind associated distortional and dilatational plane wave front, respectively, defined by Eq. 7(b);

μ, λ = Lamé constants of the material;

ρ = mass density of the material;

σ_{ij} = cartesian components of the stress tensor;

Φ, Ψ = dilatational and distortional potential, respectively;

ϕ_{ij}, ψ_{ij} = respective strength of dilatational potential and distortional potential generated from i previous dilatational waves and j previous distortional waves after i + j successive reflections and/or refractions;

∇^2 = Laplace's operator;

superscript (1) = quantities in top layer; and

superscript (2) = quantities in the bottom layer.

Journal of the
ENGINEERING MECHANICS DIVISION
Proceedings of the American Society of Civil Engineers

CONJUGATE BEAM SIMULATED BY ELECTRIC CIRCUITS

By S. Freiberg[1]

SYNOPSIS

In the field of the analogies in statics, an analogy in beam bending problems is made with electric circuits using strings of resistors in which voltages, currents, and resistances simulate moments, forces, and lengths. The available voltages, simulating moments, of the "electrical beam" are used to produce currents, now simulating forces proportional to moments, used again to load another electrical beam of the same "length" as the first one, which will behave, therefore, as a conjugate beam. Examples of circuits, consisting only of resistors, are given for typical cases together with experimental results; deflections of beams, given by the conjugate beam, are determined by this method with small errors when compared with deflections computed analytically.

INTRODUCTION

In an earlier paper,[2] analogies between electrical resistance networks and beams were analyzed. Forces, moments, and lengths on the beam are simulated by currents, voltages, and resistances, respectively. The elastic properties of the beam, necessary for the resolution of indeterminacies, are introduced by an auxiliary circuit which applies the moment area theorems.

Note.—Discussion open until January 1, 1962. To extend the closing date one month, a written request must be filed with the Executive Secretary, ASCE. This paper is part of the copyrighted Journal of the Engineering Mechanics Division, Proceedings of the American Society of Civil Engineers, Vol. 87, No. EM 4, August, 1961.

[1] Prof. of Electrotechnology, Universidad Nacional de Tucuman, Argentina; Visiting Prof. at the Univ. of California Div. of Mechanics and Design, Berkeley, Calif.

[2] "Electric Circuits for the Simulation of Bending in Beams," by S. Freiberg, Paper presented at the S.E.S.A. spring meeting, 1960.

In a paper by Erik Trudø,[3] electric models of beams and plates are proposed. The analogy indicated above is also used and adds a complementary circuit for the simulation of the conjugate beam.

This "electrical conjugate beam" can be realized in the same way as the auxiliary beam used to apply the moment area theorem, thus providing a useful tool for solving rapidly determinate and indeterminate beams, measuring moments, shears, and deflections by means of voltages and currents.

THE CONJUGATE BEAM

The well known conjugate beam[3,4] is defined as an imaginary beam of the same length as the real beam and when loaded with the M/E I (moment divided by rigidity) diagram of the real beam, its new shears and moments will represent the slope and deflection of the actual beam.

It is known from statics that in any beam

$$\frac{d^2M}{dx^2} = \frac{dS}{dx} = p \quad \ldots\ldots\ldots\ldots\ldots\ldots (1)$$

and

$$\frac{d^2y}{dx^2} = \frac{d\theta}{dx} = \frac{M}{E\,I} \quad \ldots\ldots\ldots\ldots\ldots\ldots (2)$$

in which y is the deflection of the elastic curve; θ denotes the slope of the elastic curve; x is the abscissa on the beam; M represents the bending moment; S is the shearing force; E I denotes rigidity (modulus of elasticity times moment of inertia); and p is the load per unit length on the beam. Both equations show that if the beam is loaded with the M/E I load instead of p the differential relation between y, θ, and M/E I is similar to the differential relation between M, S, and p.

This fact is the basis for the conjugate beam according to the definition given above. It has to be remembered that the conjugate beam is always statically determinate and each type of beam is associated with one whose supports are indicated in the following summary:[4]

1. A simple end support in the principal beam remains a simple support in the conjugate beam.
2. A fixed end in the principal beam becomes a free end in its conjugate beam and vice versa.
3. An interior simple support of a continuous beam is replaced by an unsupported hinge in its conjugate beam, and vice versa.

"ELECTRICAL BEAM" AND ITS CONJUGATE BEAM

Fig. 1(c) shows the complete circuit for the simulation of the simply supported beam indicated in Fig. 1(a) and its conjugate beam, Fig. 1(b). The string of resistors AB in the circuit corresponds to the principal beam which is divided, in this case, into ten equal parts, each one of resistance Δr analogous to a length 1/10 of the total length l of the beam.

---

3 "An Electric Model of Beams and Plates," by E. Trudsø, Byningstatiske Meddelelser, Vol. 26, No. 1, August, 1955, p. 1.

4 "Theory of Modern Steel Structures," by L. E. Grinter, Vol. II, The MacMillan Co., New York, 1949, p. 49.

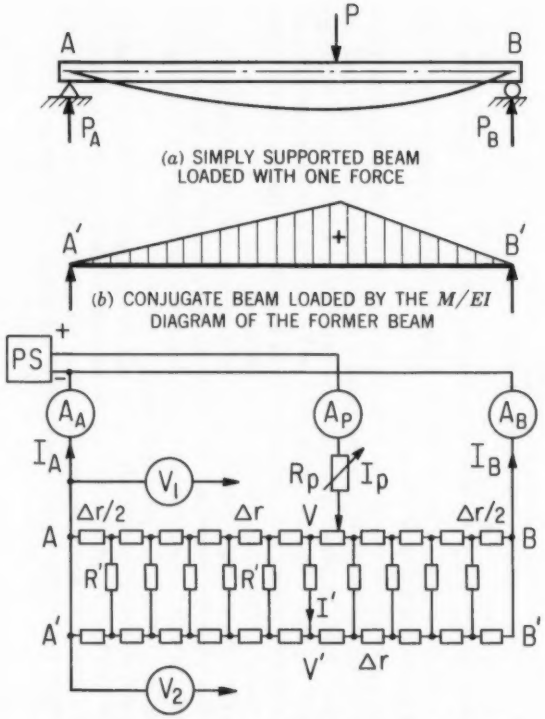

FIG. 1.—SIMPLY SUPPORTED BEAM.

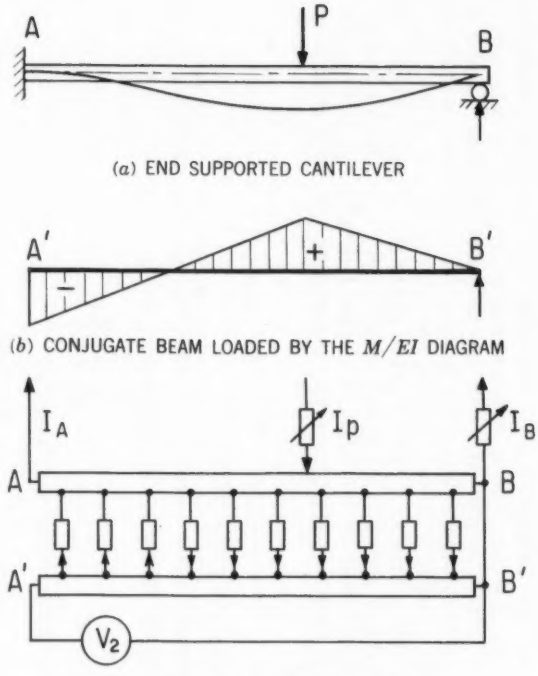

FIG. 2.—SUPPORTED CANTILEVER BEAM.

The term A_p is an ammeter to measure the current I_p analogous to force P, which is fixed with the variable resistor R_p directly connected at A_p. Only one force is used as the load for reasons of simplicity. If more forces are present they should be introduced into the analog in the same way as I_p. Currents I_A and I_B, proportional to reactions P_A and P_B are measured with ammeters A_A and A_B. The ammeters may be replaced by telephone jacks and the currents measured with only one ammeter. Because A and B on the beam are points of zero moment, the moment along the beam can be obtained by means of voltages V, measured with respect to points A or B on the electric beam, with voltmeter V_1 connected to either one of these points, and one of the accessible points of the string of resistors. From these latter points, uniformly distributed on the beam, currents can be tapped by means of resistors R'. If these resistors are proportional to the E I value, at each section of the beam,

$$R' = c\,E\,I \quad \ldots\ldots\ldots\ldots\ldots\ldots \quad (3)$$

(c = constant of proportionality).

The currents I' in the resistors R', is $I' = \frac{V - V'}{R'}$ and assuming negligible voltages V' in the electrical conjugate beam circuit

$$I' = \frac{V}{R'} = \frac{V}{c\,E\,I} \quad \ldots\ldots\ldots\ldots\ldots\ldots \quad (4)$$

Since V is proportional to moment M

$$V = c'\,M \quad \ldots\ldots\ldots\ldots\ldots\ldots \quad (5)$$

Using Eq. 4

$$I' = c''\,\frac{M}{E\,I} \quad \ldots\ldots\ldots\ldots\ldots\ldots \quad (6)$$

Constants c, c', and c'' are related by the equation $c'' = \frac{c'}{c}$. Therefore, the currents I' obtained in the circuit of Fig. 1(c) give values proportional to the M/E I load needed in Eq. 2.

To avoid appreciable change in potentials and current distributions (proportional to shears)[2] in the electrical beam AB, currents I' derived from the principal beam must be small enough. This is obtained with values $R'' \gg \Delta r$ which means a large value for constant c of Eq. 3. If a second electric beam of the same resistance as the principal one is loaded with the currents I', the electrical analog of the conjugate beam is obtained.

Currents in the conjugate beam will be proportional to the shears in it, which in turn are proportional to slope in the elastic curve of the actual beam; potentials will be proportional to moments for the conjugate beam which means to deflections for the principal beam.

The measurement of potentials along the conjugate beam will be done by means of voltmeter V_2 with one of its terminals connected to a point of zero potential on the conjugate beam; i.e. to a simple support, a free end or a hinge. In Fig. 1 voltmeter V_2 is connected to the simple support A'.

EXAMPLES OF TYPICAL INDETERMINATE BEAMS

In order to obtain the results in the case of a determinate beam, such as the simply supported beam in Fig. 1, it is enough to adjust resistor R_p fixing

the value of "force" I_p (a few iterations may be necessary if several resistors R_p for several forces are present). All the values of voltages and currents are then fixed. No more operations are necessary.

In the case of indeterminate beams the elastic properties of the beam must also be considered. This can be done by means of the conjugate beam, as will be seen in four typical examples.

(a) The End Supported Cantilever.—Fig. 2 shows a supported cantilever beam (a), its conjugate beam (b), loaded with the moment diagram of the principal beam, and the electric circuit (c) for the simulation of both beams. Each string of resistors was replaced by one tapped resistor. This change can be made if enough taps are available. The power supply and the instruments for measurements in the principal beam are not indicated since they are the same as those shown in Fig. 1.

The conjugate beam, according to what was said previously, has a free end at A′ and a simple support at B′. This is obtained in the circuit by leaving end A′ free and connecting B′ to B, the point of zero moment in the principal beam and therefore the point of reference for its voltages.

The point of reference of the electrical conjugate beam may be A′ because this is a free end and therefore it has zero moment in the mechanical beam. Deflections should be measured with voltmeter V_2 connected between point A′ and the point of A′B′ under consideration.

Since the points A and B of supports have no deflection, the corresponding points A′ and B′ of the conjugate beam have zero moment. Voltmeter V_2 when connected between these two points will indicate zero. This condition will solve the indeterminancy of first grade for the beam.

According to what was said above, the way of operation of the circuit is as follows: The current I_p is adjusted to have the value proportional to load P, then I_B is adjusted until the voltmeter V_2, connected to A′ and B′, indicates zero volts. Under these conditions currents and voltages on the electric beam AB will give the reactions and bending moments; voltages on electric beam A′B′ will give the deflections of the supported cantilever. Iterations will be necessary if I_p changes when I_B is adjusted.

(b) The Fixed-Ended Beam.—The two indeterminacies existing in this case are solved with the circuit of Fig. 3.

The conjugate beam must satisfy the following conditions: first, the ends are free as indicated in Fig. 3(b), because in the principal beam they are fixed (note section entitled "The Conjugate Beam"); second, both ends have zero moment [elastic curve of Fig. 3(a)]; third, the angle between tangents to the static curve at both ends is zero [Fig. 3(a)].

The first condition is satisfied if no connections are made at the ends of the electric conjugate beam. Nevertheless in Fig. 3(c) a connection has been made from end B′ (or A′) to a point Z, of zero moment on the beam AB. This connection is necessary to give a return path for currents I′ to beam AB, but it does not constitute a "support" for the electric conjugate beam because the current at B′ has to be equal to zero, which means zero reaction force and therefore B′ is a free end.

The second condition is obtained when the voltage between A′ and B′ is equal to zero. It has to be remembered, for the third condition, that the angle between tangents at two points of the elastic curve is equal to the area under the M/E I curve between the two points (first moment area theorem).[2] The sum of the I′ currents, I_ϕ, measured with the ammeter connected between B′

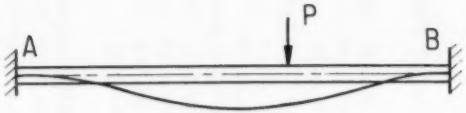

(*a*) FIXED-ENDED BEAM

(*b*) CONJUGATE BEAM LOADED BY THE M/EI DIAGRAM

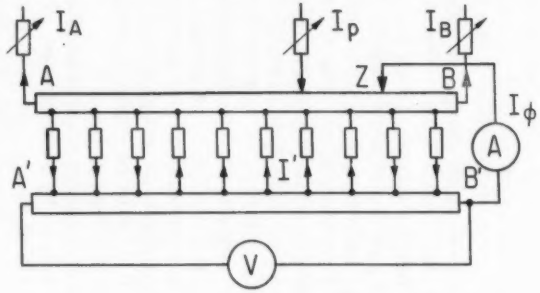

(*c*) ELECTRIC CIRCUIT FOR THE SIMULATION OF THE BEAMS IN (*a*) AND (*b*)

FIG. 3.—FIXED-ENDED BEAM.

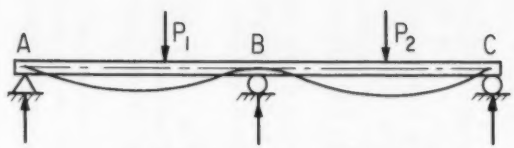

(*a*) CONTINUOUS BEAM WITH TWO SPANS

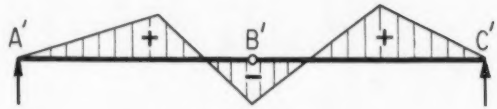

(*b*) CONJUGATE BEAM

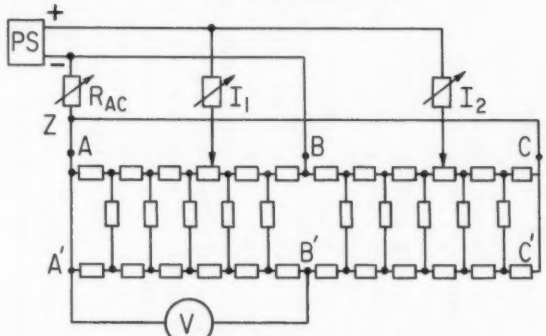

(*c*) ELECTRIC CIRCUIT FOR THE SIMULATION OF THE BEAMS IN (*a*) AND (*b*)

FIG. 4.—CONTINUOUS BEAM WITH TWO SPANS.

and Z, is proportional to the area under the M/E I diagram and it will be zero when the angle between tangents at both ends is zero.

To adjust the circuit of Fig. 3(c) for the fixed-ended beam we begin by adjusting current I_p according to the given load. Next any point Z (assumed as zero potential) is connected to the ammeter and than I_A and I_B are adjusted until the voltmeter indicates zero. If the current I_ϕ indicated by the ammeter is zero the fixed-ended beam is correctly set up and measurements of forces,

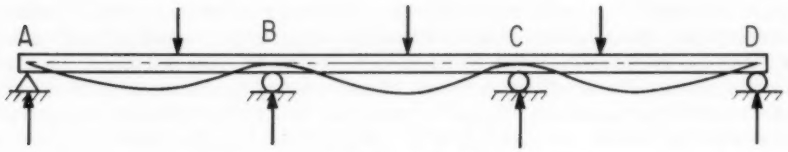

(*a*) CONTINUOUS BEAM WITH THREE SPANS

(*b*) CONJUGATE BEAM

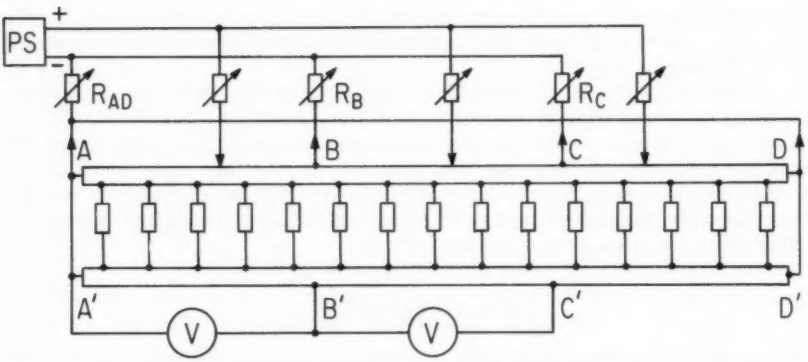

(*c*) ELECTRIC CIRCUIT FOR THE SIMULATION OF THE BEAMS IN (*a*) AND (*b*)

FIG. 5.—CONTINUOUS BEAM WITH THREE SPANS.

moments, and deflections can be made. If I_ϕ is not zero another Z point is chosen and the procedure repeated until voltmeter and ammeter (two conditions for the two grades of indeterminacy) give zero indications.

(c) Continuous Beam of Two Spans.—This beam of one degree of indeterminacy has zero moment at each end and, since there are no deflections at the three supports, the corresponding points A′, B′, and C′ of the conjugate beam have zero moment [Fig. 4(a) and 4(b)]. These characteristics can be obtained

with the circuit of Fig. 4(c) in which the electric beam has been divided in two parts, AB and BC, for each span. Point Z whose potential will be taken as reference, is directly connected to A and C so that these points will have zero voltages corresponding to the zero moments of the real beam.

The ends of the electric conjugate beam, A′ and C′, are simply supported and they are directly connected in the circuit to the points A and C of potential reference in the principal beam. Point B′ of the conjugate beam is an unsupported hinge. In the electric circuit, B′ must satisfy the condition of zero moment which can be obtained adjusting the reactions of the principal beam with resistor R_{AC} until the voltmeter connected between A′ and B′ indicates zero. Thus, when this condition for the indeterminacy is satisfied and currents I_1 and I_2, representing the given forces P_1 and P_2, are adjusted, the circuit is simulating the continuous beam of two spans; reactions are measured as the currents at points A, B and C; moments and deflections are measured as voltages on beams ABC and A′B′C′, using point Z as the zero potential reference.

(d) Continuous Beam of Three and More Spans.—In the case of three spans, two grades of indeterminacy have to be considered. Fig. 5(c) gives the electric circuit for the beam of Fig. 5(a) and its conjugate, Fig. 5(b).

As in the previous case, both ends A and D, having zero moment and zero voltage are directly connected to each other and any one may be taken as the zero potential reference. Points A′ and D′ are again connected to the ends A and D and, since there are hinges at joints B′ and C′ of the conjugate beam, these points must have zero voltage in the electric circuit; two voltmeters, connected between A′ and B′ and between B′ and C′, or D′ and C′, when indicating zero voltage, give the two conditions required to solve the second degree of indeterminacy.

In order to fix the beam, resistors R_{AD}, R_B and R_C, which adjust the reactions must be varied until the voltmeters indicate zero values.

For each new span which is added, another indeterminacy is introduced and therefore another simultaneous condition, for zero voltage between hinges of the new interior span, has to be satisfied. The process of iteration for obtaining the simultaneous voltages on the conjugate electric beam becomes more cumbersome for each indeterminacy added.

SCALE FACTORS

Moments are related to forces and distances by the equation $M = F\,l$ and voltages, according to Ohm's Law, are related to currents and resistances by the equation $V = I\,R$. With these relations between the magnitudes of both formulas (indicated in the section entitled "The Conjugate Beam") the scale factors for the principal beam can be fixed. It should be noticed that only two scales can be arbitrarily chosen. When this is done the third scale becomes fixed.

For example, if 1 kip equivalent to 10 m A is chosen as the scale for forces and 1 ft equivalent to 10.0 as the scale for lengths, then

$$1 \text{ kip} \times 1 \text{ ft} = 1 \text{ ft kip}$$

is equivalent to

$$10 \text{ m A} \times 10\,\Omega = 100 \text{ m V} = 0.1 \text{ V}$$

Therefore the scale 1 ft-kip equivalent to 0.1 volt results from the choice of the other two scales.

The scale of length for the conjugate beam may be the same as that used for the principal beam.

In order to fix the scale of deflections that are measured by the voltages on the conjugate beam, the following data are necessary: the voltage-moment scale of the principal beam, the relationship between the E I values and resistances R′ that join both beams, and the Δr value corresponding to each one of the parts into which the beams were divided (Fig. 1).

An example will show how the scale for deflections is obtained.

Consider a beam of 100 ft length with E I = 10^{10} lb in^2. The beam is divided into ten parts, each 10 ft long, in order to load the conjugate beam with the moment diagram of each one of these parts. The following scale relationships have been chosen.

1. 1 ft : 10 Ω
2. 1 ft kip : 0.1 Volt (in the principal beam)
3. 10^{10} lb in^2 : $10^5 \Omega$ = R′

If the beam were not of uniform cross-section or material the R′ resistances in each one of the ten sections of the beam would change. Each value of R′ would be fixed according to the E I value at each point as given by the last relationship.

Suppose a moment M = 1 ft kip of the principal beam, along a 10 ft section, loads the conjugate beam with its resultant M/E I diagram. In the analog a current I′ through R′ will load the electrical conjugate beam so that the following scale relationship holds:

$$\frac{1 \text{ ft kip} \times 10 \text{ ft}}{10^{10} \text{ lb in.}^2} = 144 \times 10^{-6} \text{ equivalent to } I' = \frac{0.1 \text{ V}}{10^5 \Omega} = 10^{-6} \text{ V}/\Omega \quad \ldots \quad (7)$$

and since 1 ft is equivalent to 10 Ω,

$$1.2 \text{ in. equivalent to } 1 \Omega \quad \ldots \quad (8)$$

Multiplying Eqs. 7 and 8

$$172.8 \times 10^{-6} \text{ in. equivalent to } 10^{-6} \text{ V}$$

is obtained. Since voltages of the order of millivolts will be measured in the electrical conjugate beam the final relationship used is:

$$172.8 \times 10^{-3} \text{ in. deflection equivalent to 1 m V}$$

EXPERIMENTAL RESULTS

Experiments were made with an electrical beam simulating a continuous beam of three equal spans of 100 ft each. A flexural rigidity E I = 10^{10} lb in^2 was assumed.

The electrical beam was constructed with the resistance of 1000 Ω for each span divided into 10 parts. This gives a scale factor 10 Ω/ft. Resistances R′ = $10^5 \Omega$ were used for the simulation of the rigidity. A current of 10 m A was chosen to represent a force of 1 kip.

With these values the scale factors are those computed in the previous section.

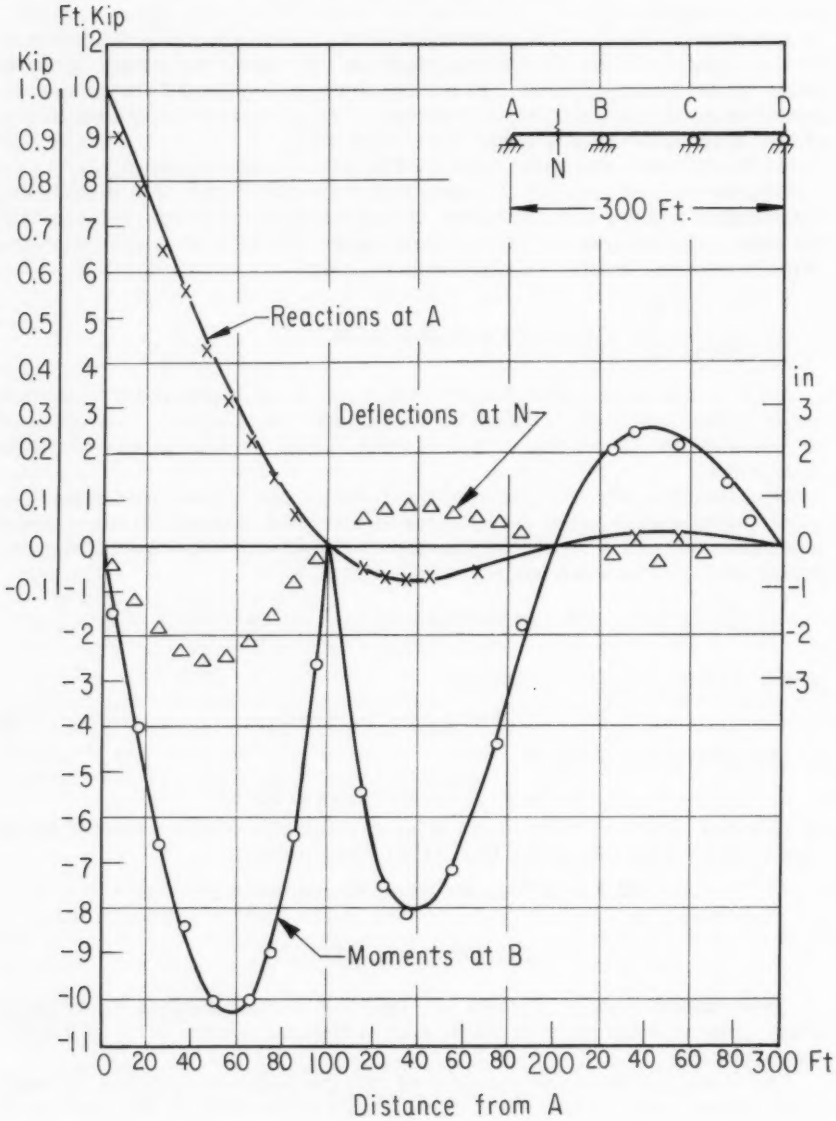

FIG. 6.—INFLUENCE LINES FOR A CONTINUOUS BEAM OF THREE SPANS.

Fig. 6 shows three influence lines obtained for this beam: the influence line for the reaction at one end, the influence line for the moment at an inner support and the influence line for the deflection at the middle of the outer span. The dots are experimental values obtained with the analog electrical beam.

The experimental values can be directly compared to the corresponding values given by the theoretically calculated influence lines for the reaction and the moment.

Since the theoretical calculation of the entire influence line for deflections would be extremely lengthy, only one point of this influence line has been computed: the deflection of the midpoint of the first span when the load is at the same point. The resulting deflection was 2.52 in.

In the electrical conjugate beam under the analogous conditions a voltage of 14.5 mV was measured. This value multiplied by the factor 172.8×10^{-3} in. per mV gives a deflection of 2.50 in. Enough other deflections were experimentally determined so that the influence line can be readily drawn.

CONCLUSIONS

The analog electrical circuit for the simulation of bending of determinate and indeterminate beams by applying the method of the conjugate beam permits the determination of magnitudes, including deflections, within the accuracy of the electrical instruments and resistors used. The ease with which the electrical measurements may be made and with which the electrical circuit can be changed makes this method of measurement very convenient in cases where immediate results are required.

These electrical beams may also provide a basis for graphically displaying the influence lines on a cathode ray oscilloscope or on an x-y recorder.

ACKNOWLEDGMENTS

The writer wishes to express his thanks to L. Dabaghian, who read the manuscript, and to V. Bertero for his valuable comments. The writer's appointment was supported by the International Cooperation Administration under the Visiting Research Scientists Program administered by the National Academy of Sciences of the United States of America.

APPENDIX.—NOTATIONS

c, c', c'' = constants of proportionality;

$E\,I$ = flexural rigidity, pounds x inch square;

I_1, I_2, I_4, . . . I' = electric currents, amperes;

M, M_A, M_B, . . . = bending moment, foot kips, inch pounds;

$P, P_1, P_2, P_A, \ldots$ = forces, kips;

p = load per unit length, kips per foot;

$R_A, R_B, \ldots r$ = electric resistances, ohms;

S = shearing force, kips;

V = voltage on the electrical beam circuit, volts;

V' = voltage on the electrical conjugate beam circuit, volts;

x = variable length, feet;

y = variable deflection, feet, inch; and

θ = slope, radians.

Journal of the
ENGINEERING MECHANICS DIVISION
Proceedings of the American Society of Civil Engineers

METHOD OF INTERNAL CONSTRAINTS AND ITS APPLICATION

By Enrico Volterra,[1] F. ASCE

SYNOPSIS

An approximate method that is of both general and systematic character is presented. The method unifies a number of engineering theories in the statics and dynamics of plates and bars, and, in addition, is simple and direct. The method is based on assumptions concerning the components of the elastic displacement. In fact, it is assumed that the components of the elastic displacement must comply with special equations of constraint. These equations of constraint, which determine the elastic displacement, are the basis for the term "method of internal contraints."

The method is applied first to the discussion of vibrations of elongated straight rods. The equations of motion and the boundary conditions for flexural vibrations are derived. It is shown that these equations reduce, in the plane-stress case, to the well-known Timoshenko beam equation. The equations of motion and boundary conditions for longitudional vibrations of elongated rods are derived, and the results given by these equations are compared with those given by use of other engineering theories and with those given by the exact Pochhammer solution. Finally the method is applied to the discussion of flexural vibrations of rectangular thin plates, and the equations of motion and proper boundary conditions are derived. These equations of motion coincide with the equations of motion derived by R. D. Mindlin, M. ASCE. The present equations reduce, in the static case, to equations that are very similar to those ob-

Note.—Discussion open until January 1, 1962. To extend the closing date one month, a written request must be filed with the Executive Secretary, ASCE. This paper is part of the copyrighted Journal of the Engineering Mechanics Division, Proceedings of the American Society of Civil Engineers, Vol. 87, No. EM 4, August, 1961.

[1] Prof. of Engrg. Mechanics, Univ. of Texas, Austin 12, Tex.

tained by E. Reissner. However, the present method of deriving the equations is simpler and more direct than are these other methods.

INTRODUCTION

The classical theory of transverse vibrations of elastic rectilinear bars, by Bernouilli and Euler, neglects the effects of rotatory inertia and of shear. If the results given by use of this elementary theory are compared with those given by use of the exact theory of L. Pochhammer and Chree (1)[2] in the case of cylindrical bars of infinite length, it is seen that these two theories produce considerably different values. An approximation due to Lord Rayleigh (2), which takes into account the effect of rotatory inertia, does not improve the results very much.

In 1921 S. Timoshenko (3) showed the important role played by shear in transverse vibrations of bars. By adding the effect of shear to the effect of rotatory inertia, he obtained a good approximation between the results given by use of the exact theory.

Results as described in the first paragraph of this Introduction are obtained also in the case of longitudinal vibrations of cylindrical bars.

In the case of flexural vibrations of thin plates, too, there is no agreement among results following application of the classical theory of Lagrange and the exact theories of Lord Rayleigh (4) and H. Lamb (5).

For static deflections of thin elastic plates G. Kirchhoff's classical theory (6) neglects, in the study of deformations, the effects of shear and of normal stress. In many cases use of the Kirchhoff theory reaches results that are contradicted by experiments. For example, the application of the classical theory to the case of a rectangular plate simply supported and submitted to a uniformly distributed load on the free surface leads to the false result that four concentrated reactions must be applied on the four corners of the plate in order to maintain the equilibrium (7).

E. Reissner (8) (9) (10), H. Hencky (11), L. Bolle (12), M. Schafer (13), and A. Kromm (14) (15) have presented new theories of deflection of thin plates that take into account the effect of shear. In these theories, which are referred to in the text as engineering theories in order to distinguish them from the exact theories obtained by applying the equations of the mathematical theory of elasticity, one generally starts from hypotheses concerning the stress distribution in the plate in order to reach the equations of motion or the equations of equilibrium.

For example, in his theory Reissner starts from appropriate and rational hypotheses concerning the stress distribution across the thickness of the plate. He supposes that the stresses due to the bending moment vary linearly, whereas those due to shear vary according to a parabolic law across the section of the plate. At the same time Reissner does not neglect the effects due to the normal stress. Reissner has shown that his equations of equilibrium satisfy three boundary conditions, whereas the equations established by Kirchhoff satisfy only two boundary conditions. The equations of equilibrium obtained (8) by Reissner in 1944, taking into account the transverse deformation of the plate

[2] Numerals in parentheses refer to corresponding items in Appendix II.

due to shear by applying Castigliano's theorem, were derived directly by A. E. Green in 1949 (16).

By applying his equations Reissner was able to solve various problems of practical importance, including the problem of bending and torsion of an infinite plate with a circular hole in it, and the problem of bending of a cantilever plate due to transverse forces applied at its extremity. In the foregoing cases the application of the Kirchhoff classical theory leads to results in contradiction with reality, whereas the application of Reissner's equations of equilibrium leads to results which are in accord with experiments.

Bolle, independently from Reissner, obtained the same equilibrium equations and boundary conditions in his important work on the deformation of thin plates taking into account the effect of shear (12).

In this paper the writer presents a method that is approximate and at the same time has a general and systematic character. The method unifies a certain number of engineering theories in the statics and dynamics of plates and bars. It is, in general, a more simple and direct method. Whereas the methods mentioned previously are based on hypotheses concerning the distribution of stresses, the method presented herein is based on assumptions concerning the components of the elastic displacement. In fact, it is assumed that the components of the elastic displacement must comply with special equations of constraint. These conditions of constraint, which determine the elastic displacement, are the basis for the term "method of internal constraints."

This method is applied first to the discussion of vibrations of elongated straight rods. The equations of motion and the boundary conditions for flexural vibrations are then derived. It is shown that these equations reduce, in the plane-stress case, to the well-known Timoshenko beam equation. The equations of motion and the boundary conditions for longitudinal vibrations of elongated rods are then derived, and the results given by these equations are compared with those given by use of other engineering theories and with those given by use of other engineering theories and with those given by the exact Pochhammer solution. Finally the method is applied to the discussion of flexural vibrations of rectangular thin plates, and the equations of motion and proper boundary conditions are derived. These equations of motion coincide with the equations of motion derived by Mindlin (17). These present equations reduce, in the static case, to equations that are very similar to those obtained by Reissner (18) (19). However, the present method of deriving the equations is simpler and more direct.

FLEXURAL VIBRATIONS OF STRAIGHT ELASTIC BARS

Notation.—The letter symbols used in this paper are defined where they first appear in the text, and are arranged alphabetically for convenience of reference in Appendix I.

For flexural vibrations the components of the elastic displacement u, v, and w in the direction of the axes X, Y, and Z are assumed to be:

$$u\,(X, Y, Z; t) = y\,\lambda_X\,(x; t) \qquad \ldots\ldots\ldots\ldots \quad (1a)$$

$$v\,(X, Y, Z; t) = v_y\,(x; t) + \frac{y^2}{2} f_2\,(x; t) \qquad \ldots\ldots \quad (1b)$$

and

$$w\,(X, Y, Z; t) = y\,z\,f_2\,(x; t) \quad \ldots\ldots\ldots\ldots \quad (1c)$$

(Concerning the geometric implications of the elastic constraints expressed by Eqs. 1, 14, and 24 reference is made to a previous paper (20)). In Eqs. 1 t is time and λ is Lame's constant. The axis X coincides with the axis of the bar, whereas the Y and Z axes coincide with the principal axes of inertia of the cross section of the bar, which cross section is at first considered to be rectangular of breadth B and height H.

From Eqs. 1 the following expressions are found for the normal stresses σ_y and σ_z:

$$\sigma_y = (\lambda + 2\,G)\,y\,f_1 + \lambda\,y\,f_2 + \lambda\,y\,\frac{\partial \lambda_x}{\partial x} \quad \ldots\ldots\ldots \quad (2a)$$

and

$$\sigma_z = (\lambda + 2\,G)\,y\,f_2 + \lambda\,y\,f_1 + \lambda\,y\,\frac{\partial \lambda_x}{\partial x} \quad \ldots\ldots\ldots \quad (2b)$$

in which λ and G (the modulus of rigidity) are connected to Young's modulus E and to Poisson's ratio ν of the material of the bar by the relationships:

$$\lambda = \frac{\nu\,E}{(1+\nu)(1-2\,\nu)} \quad \ldots\ldots\ldots\ldots\ldots \quad (3a)$$

and

$$G = \frac{E}{2(1+\nu)} \quad \ldots\ldots\ldots\ldots\ldots\ldots \quad (3b)$$

Eqs. 2 show that, in order to satisfy the conditions that $\sigma_y = \sigma_z = 0$, the following relationships must be verified:

$$f_1 = f_2 = -\,\nu\,\frac{\partial \lambda_x}{\partial x} \quad \ldots\ldots\ldots\ldots\ldots \quad (4)$$

From Eqs. 1 and 4 the following expressions are obtained for the potential u and the kinetic T energies of the bar:

$$u = \int_0^L \left\{ \frac{E}{2}\,I_z \left[1 + K\,\frac{\nu^2}{2(1+\nu)}\,\frac{I_y}{I_z} \right] \left(\frac{\partial \lambda_x}{\partial x} \right)^2 + K\,\frac{E}{4(1+\nu)}\,A \left[(\lambda_x)^2 + \left(\frac{\partial \nu_y}{\partial x} \right)^2 + 2\,\lambda_x\,\frac{\partial \nu_y}{\partial x} \right] \right\} dx \quad \ldots\ldots \quad (5)$$

and

$$T = \frac{\rho}{2} \int_0^L \left[I_z \left(\frac{\partial \lambda_x}{\partial t} \right)^2 + A \left(\frac{\partial \nu_y}{\partial t} \right)^2 \right] dx \quad \ldots\ldots\ldots\ldots \quad (6)$$

In deriving Eqs. 5 and 6, terms containing y^2 and y z have been neglected in the expressions for the components of strain and particle velocities in comparison with linear terms. The term L represents the length of the bar, I_y and

I_z the moments of inertia of its cross-section with respect to the y and z axes, and A the area of the cross-section. The factor k is introduced into Eq. 5 to take into account the non-linear distribution of shear-stresses over the cross-section of the bar. It has the same significance as that of the well-known Timoshenko shear coefficient.

On the assumption that no external forces (body and surface forces) are applied to the bar, using the Hamilton principle the following equations of motion:

$$E I_z (1+\epsilon) \frac{\partial^2 \lambda_x}{\partial x^2} - k G A \lambda_x - k G A \frac{\partial \nu_y}{\partial x} = \rho I_z \frac{\partial^2 \lambda_x}{\partial t^2} \quad \ldots\ldots (7a)$$

and

$$k G A \frac{\partial^2 \nu_y}{\partial x^2} + k G A \frac{\partial \lambda_x}{\partial x} = \rho A \frac{\partial^2 \nu_y}{\partial t^2} \quad \ldots\ldots\ldots (7b)$$

and boundary conditions:

$$\text{for } x = 0 \quad x = l$$

$$\left(\frac{\partial \lambda_x}{\partial x}\right) \delta \nu_x = 0 \quad \ldots\ldots\ldots\ldots\ldots (8a)$$

$$\left(\frac{\partial \nu_y}{\partial x} + \lambda_x\right) \delta \nu_y = 0 \quad \ldots\ldots\ldots\ldots\ldots (8b)$$

with:

$$\epsilon = k \frac{\nu^2}{2(1+\nu)} \frac{I_y}{I_z} \quad \ldots\ldots\ldots\ldots\ldots (9)$$

are obtained.

It should be pointed out that the validity of Eqs. 7 and 8 is not limited to a bar of rectangular cross-section. In fact the only parameter related to the shape of the cross-section is the ratio of the moments of inertia I_y/I_z, so that Eqs. 7 and 8 are valid for a bar of any cross-section.

By eliminating the function λ_x in Eqs. 7, they can be written under the following form:

$$\frac{E}{\rho} r^2_z (1+\epsilon) \frac{\partial^4 w_o}{\partial x^4}$$

$$- r^2_z \left[(1+\epsilon) + 2\frac{(1+\nu)}{k}\right] \frac{\partial^4 w_o}{\partial x^2 \partial t^2}$$

$$+ \frac{2(1+\nu)}{E k} \rho r^2_z \frac{\partial^4 w_o}{\partial t^4} + \frac{\partial^2 w_o}{\partial t^2} = 0 \quad \ldots\ldots\ldots (10)$$

in which $w_o = \nu_y$ and $r_z = \sqrt{\frac{I_z}{A}}$.

In the case of plane stress the ratio I_y/I_z becomes zero and Eq. 10 reduces to the well-known Timoshenko equation:

$$\frac{E}{\rho} r^2 \frac{\partial^4 w_o}{\partial x^4} - r^2 \left[1 + \frac{2(1+\nu)}{k}\right] \frac{\partial^4 w_o}{\partial x^2 \partial t^2} + \frac{2(1+\nu)}{E k} \rho r^2 \frac{\partial^4 w_o}{\partial t^4} + \frac{\partial^2 w_o}{\partial t^2} = 0 \quad \ldots\ldots\ldots (11)$$

In Eq. 11, if the terms due to shear are neglected, the differential equation is modified to the form usually attributed to Rayleigh:

$$\frac{E}{\rho} r^2 \frac{\partial^4 w_o}{\partial x^4} - r^2 \frac{\partial^4 w_o}{\partial x^2 \partial t^2} + \frac{\partial^2 w_o}{\partial t^2} = 0 \quad \ldots\ldots\ldots (12)$$

In Eq. 11, if terms due to rotatory inertia and to shear are neglected, the equation reduces to the following equation:

$$\frac{E}{\rho} r^2 \frac{\partial^4 w_o}{\partial x^4} + \frac{\partial^2 w_o}{\partial t^2} = 0 \quad \ldots\ldots\ldots\ldots\ldots (13)$$

of the elementary theory.

In the equations of constraints (Eqs. 1), if only linear terms of the components of the elastic displacement are considered, the following equations of motion is obtained:

$$\frac{E}{\rho} \frac{(1-\nu)}{(1+\nu)(1-2\nu)} r^2 \frac{\partial^4 w_o}{\partial x^4} - r^2 \left(\frac{3-4\nu}{1-2\nu}\right) \frac{\partial^4 w_o}{\partial x^2 \partial t^2} + \frac{2(1+\nu)}{E} r^2 \rho \frac{\partial^4 w_o}{\partial t^4} + \frac{\partial^2 w_o}{\partial t^2} = 0 \quad \ldots\ldots\ldots\ldots\ldots (14)$$

Let:

$$w_o = A e^{i\gamma(x-ct)} \quad \ldots\ldots\ldots\ldots\ldots (15)$$

in which A is a constant, $i = \sqrt{-1}$, $\gamma = \frac{2\pi}{L}$, L is the wave-length and c the phase velocity for flexural waves.

From Eq. 10 the following dispersion equation is derived:

$$\left(\frac{r_z}{L}\right)^2 = \frac{1}{4\pi^2} \frac{k}{2(1+\nu)} \frac{\left(\frac{c}{c_o}\right)^2}{\left[\left(\frac{c}{c_o}\right)^2 - \frac{k}{2(1+\nu)}\right]\left[\left(\frac{c}{c_o}\right)^2 - (1+\epsilon)\right]} \quad \ldots\ldots (16)$$

In Eq. 16 $c_o = \sqrt{\frac{E}{\rho}}$ represents the bar velocity.

In Fig. 1 phase velocities of flexural waves in cylindrical bars according to the elementary theory, the Rayleigh theory, the Timoshenko theory, the exact Pochhammer theory, (21) and the present method (first and second approximation) are compared.

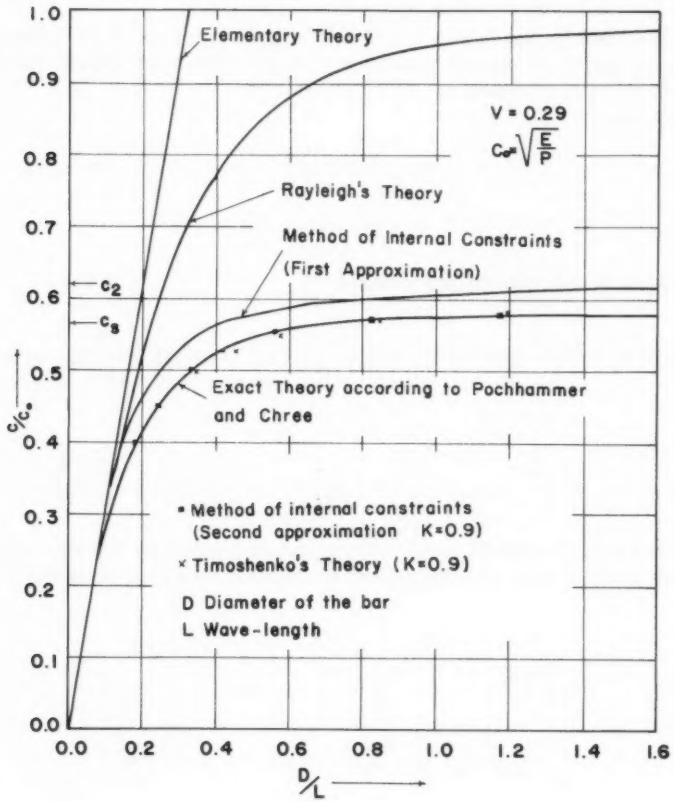

FIG. 1.—PHASE VELOCITY OF FLEXURAL WAVES IN CYLINDRICAL BARS

LONGITUDINAL VIBRATIONS OF STRAIGHT ELASTIC BARS

In the case of longitudinal vibrations in a bar of rectangular cross-section the components of the elastic displacement will be assumed to be:

$$u(x, y, z; t) = \nu_x(x; t) \quad \ldots\ldots\ldots\ldots (17a)$$

$$v(x, y, z; t) = y\,\lambda_y(x; t) + y^3 f_1(x; t) + y\,z^2 f_2(x; t) \quad \ldots (17b)$$

and

$$w(x, y, z; t) = z\,\lambda_z(x; t) + z^3 f_3(x; t) + z\,y^2 f_4(x; t) \quad \ldots (17c)$$

The functions f_1, f_2, f_3 and f_4 are determined in terms of the unknown functions ν_x, λ_y and λ_z from the condition that the free surfaces of the bar are free from normal stresses.

In fact, if:

$$\sigma_y = 0 \text{ for } y = \pm\frac{H}{2}$$

$$\sigma_z = 0 \text{ for } z = \pm\frac{B}{2}$$

the following two equations are obtained:

$$(\lambda + 2G)\left(\lambda_y + \frac{3H^2}{4} f_1 + z^2 f_2\right) + \lambda\left(\frac{\partial \nu_x}{\partial x} + \lambda_z + 3z^2 f_3 + \frac{H^2}{4} f_4\right) = 0 \quad \ldots (18)$$

and

$$(\lambda + 2G)\left(\lambda_z + \frac{3B^2}{4} f_3 + y^2 f_4\right) + \lambda\left(\frac{\partial \nu}{\partial x} + \lambda\, y + 3y^2 f_1 + \frac{B^2}{4} f_2\right) = 0 \quad \ldots (19)$$

Because Eqs. 18 and 19 need to be satisfied identically for any value of the variables y and z, they are equivalent to the following four equations:

$$f_1 = -\frac{1}{3H^2}\,\frac{\lambda + 2G}{G(\lambda + G)}\left[\lambda\,\frac{\partial \nu_x}{\partial x} + \lambda\lambda_z + (\lambda + 2G)\,\lambda_y\right] \quad \ldots\ldots (20a)$$

$$f_2 = \frac{1}{B^2}\,\frac{\lambda}{G(\lambda + G)}\left[\lambda\,\frac{\partial \nu_x}{\partial x} + \lambda\lambda_y + (\lambda + 2G)\,\lambda_z\right] \quad \ldots\ldots\ldots (20b)$$

$$f_3 = -\frac{1}{3B^2}\,\frac{\lambda + 2G}{G(\lambda + G)}\left[\lambda\,\frac{\partial \nu_x}{\partial x} + \lambda\lambda_y + (\lambda + 2G)\,\lambda_z\right] \quad \ldots\ldots (20c)$$

and

$$f_4 = \frac{1}{H^2}\,\frac{\lambda}{G(\lambda + G)}\left[\lambda\,\frac{\partial \nu_x}{\partial x} + \lambda\lambda_z + (\lambda + 2G)\,\lambda_y\right] \quad \ldots\ldots\ldots (20d)$$

In the evaluation of the potential and kinetic energies of the bar, terms containing $y^2 z^2$, y^4 and z^4 are neglected in comparison with second degree terms.

After integration with respect to the variables y and z the following expressions are obtained:

$$U = B\,H \int_0^L \left\{ \left(\frac{\lambda}{2} + G\right) \left[\left(1 - \frac{4}{3}\,\frac{\nu^2}{(1-\nu)}\right) \left(\frac{\partial \nu_x}{\partial x}\right)^2 + \frac{1}{3}\,(\lambda_y)^2 \right.\right.$$

$$\left. + \frac{1}{3}\,(\lambda_z)^2 + \frac{2}{3}\,\frac{\nu}{(1-\nu)} \left(\frac{\partial \nu_x}{\partial x}\,\lambda_\zeta + \frac{\partial \nu_x}{\partial x}\,\lambda_z + \lambda_y\,\lambda_z\right) \right]$$

$$\left. + \frac{k\,G}{2} \left[\frac{H^2}{12} \left(\frac{\partial \lambda_y}{\partial x}\right)^2 + \frac{B^2}{12} \left(\frac{\partial \lambda_z}{\partial x}\right)^2 \right] \right\} dx \quad \ldots\ldots\ldots\ldots\ldots\ldots \quad (21)$$

and

$$T = \frac{B\,H\,p}{2} \int_0^L \left[\left(\frac{\partial \nu_x}{\partial t}\right)^2 + \frac{H^2}{12} \left(\frac{\partial \lambda_y}{\partial t}\right)^2 + \frac{B^2}{12} \left(\frac{\partial \lambda_z}{\partial t}\right)^2 \right] dx \quad \ldots\ldots \quad (22)$$

In the absence of body and surface forces, applying the Hamilton principle the following equations of motion:

$$(\lambda + 2\,G) \left[1 - \frac{4}{3}\,\frac{\nu^2}{(1-\nu)}\right] \frac{\partial^2 \nu_x}{\partial x^2} + \frac{1}{3}\,\lambda\,\frac{\partial \lambda_y}{\partial x} + \frac{1}{3}\,\lambda\,\frac{\partial \lambda_z}{\partial x} = \rho\,\frac{\partial^2 \nu_x}{\partial t^2} \quad \ldots\ldots (23a)$$

$$k\,G\,\frac{H^2}{12}\,\frac{\partial^2 \lambda_y}{\partial x^2} - \frac{1}{3}\,(\lambda + 2\,G)\,\lambda_y - \frac{1}{3}\,\lambda\,\frac{\partial \nu_x}{\partial x} - \frac{1}{3}\,\lambda\,\lambda_z = \rho\,\frac{H^2}{12}\,\frac{\partial^2 \lambda_y}{\partial t^2} \quad \ldots\ldots (23b)$$

and

$$k\,G\,\frac{B^2}{12}\,\frac{\partial^2 \lambda_z}{\partial x^2} - \frac{1}{3}\,(\lambda + 2\,G)\,\lambda_z - \frac{1}{3}\,\lambda\,\frac{\partial \nu_x}{\partial x} - \frac{1}{3}\,\lambda\,\lambda_y = \rho\,\frac{B^2}{12}\,\frac{\partial^2 \lambda_z}{\partial t^2} \quad \ldots\ldots (23c)$$

and boundary conditions:

at x = 0, x = l

$$\left[(\lambda + 2\,G) \left(1 - \frac{4}{3}\,\frac{\nu^2}{(1-\nu)}\right) \frac{\partial v_x}{\partial x} + \frac{1}{3}\,\lambda\,\lambda_y + \frac{1}{3}\,\lambda\,\lambda_z\right] \delta\,v_x = 0 \quad \ldots (24a)$$

$$\left(\frac{\partial \lambda_y}{\partial x}\right) \delta\,\lambda_y = 0 \quad \ldots\ldots\ldots\ldots\ldots\ldots (24b)$$

$$\left(\frac{\partial \lambda_z}{\partial x}\right) \delta\,\lambda_z = 0 \quad \ldots\ldots\ldots\ldots\ldots\ldots (24c)$$

are derived.

The equations of motion and corresponding boundary conditions for the plane stress case are obtained from Eqs. 23 and 24. In fact, by letting B approach zero Eq. 23c becomes:

$$\lambda_z = -\,\frac{\lambda}{\lambda + 2\,G} \left(\frac{\partial \nu_x}{\partial x} + \lambda_y\right) \quad \ldots\ldots\ldots\ldots\ldots\ldots \quad (25)$$

Substituting this value for λ_z into Eqs. 23 and 24 the equations of motion and the boundary conditions in the case of plane stress are obtained under the following forms:

(a) For the equations of motion:

$$\frac{E}{(1-\nu^2)}\left(1-\frac{2}{3}\nu^2\right)\frac{\partial^2 \nu_x}{\partial x^2}+\frac{1}{3}\frac{E\,\nu}{(1-\nu^2)}\frac{\partial \lambda_y}{\partial x}=\rho\frac{\partial^2 \nu_x}{\partial t^2} \quad \ldots(26a)$$

and

$$\frac{k\,E}{2(1+\nu)}\frac{H^2}{12}\frac{\partial^2 \lambda_y}{\partial x^2}=\frac{1}{3}\frac{E}{(1-\nu^2)}\lambda_y-\frac{1}{3}\frac{E\,\nu}{(1-\nu^2)}\frac{\partial \nu_x}{\partial x}=\rho\frac{H^2}{12}\frac{\partial^2 \lambda_y}{\partial t^2} \quad \ldots(26b)$$

(b) For the boundary conditions at x = 0, x = l:

$$\left[\left(1-\frac{2}{3}\nu^2\right)\frac{\partial \nu_x}{\partial x}+\frac{\nu}{3}\lambda_y\right]\delta\nu_x=0 \quad \ldots\ldots\ldots(27a)$$

$$\left(\frac{\partial \lambda_y}{\partial x}\right)\delta\lambda_y=0 \quad \ldots\ldots\ldots\ldots\ldots(27b)$$

By substituting into Eqs. 23:

$$\lambda_y = A\,e^{i\gamma(x-ct)} \quad \ldots\ldots\ldots\ldots\ldots(28a)$$

$$\lambda_z = B\,e^{i\gamma(x-ct)} \quad \ldots\ldots\ldots\ldots\ldots(28b)$$

and

$$\nu_x = C\,e^{i\gamma(x-ct)} \quad \ldots\ldots\ldots\ldots\ldots(28c)$$

in which A, B and C are three constants, $i=\sqrt{-1}$ and $\gamma = 2\pi/L$, L is the wave length and c the phase velocity, from Eqs. 23 the dispersion equation for longitudinal waves is derived under the following form:

$$\left(\frac{H}{L}\right)^4\pi^4\beta^2\left[\left(\frac{c}{c_o}\right)^2-\frac{1-\nu}{(1+\nu)(1-2\nu)}\left(1-\frac{4}{3}\frac{\nu^2}{1-\nu}\right)\right]\left[\left(\frac{c}{c_o}\right)^2-\frac{k}{2(1+\nu)}\right]^2$$

$$-\left(\frac{H}{L}\right)^2\pi^2\left(1+\beta^2\right)\frac{1-\nu}{(1+\nu)(1-2\nu)}\left[\left(\frac{c}{c_o}\right)^2-\frac{k}{2(1+\nu)}\right]\left[\left(\frac{c}{c_o}\right)^2-\frac{1}{(1-\nu^2)}\left(1-\frac{2}{3}\nu^2\right)\right]$$

$$+\frac{\left(\frac{c}{c_o}\right)^2-1}{(1+\nu)^2(1-2\nu)}=0 \quad \ldots\ldots\ldots\ldots(28d)$$

The constant β in Eq. 28d represents the ratio of the sides B/H.

If $\beta \to 0$ in Eq. 28d the dispersion equation for the case of plane stress is obtained under the form:

$$\left(\frac{H}{L}\right)^2 = \frac{1}{\pi^2}\frac{1}{(1-\nu^2)}\frac{\left(\frac{c}{c_0}\right)^2 - 1}{\left[\left(\frac{c}{c_0}\right)^2 - \frac{k}{2(1+\nu)}\right]\left[\left(\frac{c}{c_0}\right)^2 - \frac{1}{(1-\nu^2)}\left(1 - \frac{2}{3}\nu^2\right)\right]} \quad . . (29)$$

The lowest root of Eq. 28d is plotted against the ratio r/L in Fig. 2 for the case of a bar of square cross-section ($\beta = 1$). These results are compared with the results obtained by the use of other engineering theories of longitudinal wave propagation and with the results obtained for a cylindrical bar from the use of the exact theory by R. M. Davies (21).

It is possible to make this comparison between the results for bars of circular cross section and square cross section because, according to experiments made by R. W. Morse, M. ASCE (22)(23), the dispersion curve for a bar of square cross section is very close to the one obtained for a bar of circular cross section if the ratio of the diameter to the side of the square cross section is 1.13.

The engineering theories (results of use of which are compared in Fig. 2 with results obtained by use of the second approximation of the method of internal constraints) are the elementary theory (curve 2)(24), Love's theory (curve 6)(25), Bishop's theory (curve 3), Bishop's improved theory (curve 4), Love's theory improved by Bishop (curve 7)(26) and the method of internal constraints (first approximation)(curve 5). The curves for the exact theory according to Pochhammer for cylindrical bars (curve 1) and the method of internal constraints (second approximation)(curve 8) are also shown. Because the frequency equations of all the prior-mentioned engineering theories were derived, and their implications discussed, by the writer in a previous paper (27) they will not be discussed here.

FLEXURAL VIBRATIONS OF THIN RECTANGULAR PLATES

In the case of flexural vibrations of a thin rectangular plate the components of the elastic displacement will be assumed to be:

$$u(x, y, z; t) = z\,\mu_x(x, y; t) \quad . . . . . (30a)$$

$$v(x, y, z; t) = z\,\mu_y(x, y; t) \quad . . . . . (30b)$$

and

$$w(x, y, z; t) = \nu_x(x, y; t) + \frac{z^2}{2} f(x, y; t) \quad . . (30c)$$

The rectangular plate of sides a and b is referred to a system of orthogonal cartesian coordinates X, Y, Z, the plane X Y coinciding with the middle surface of the plate and the Z axis directed positively downward.

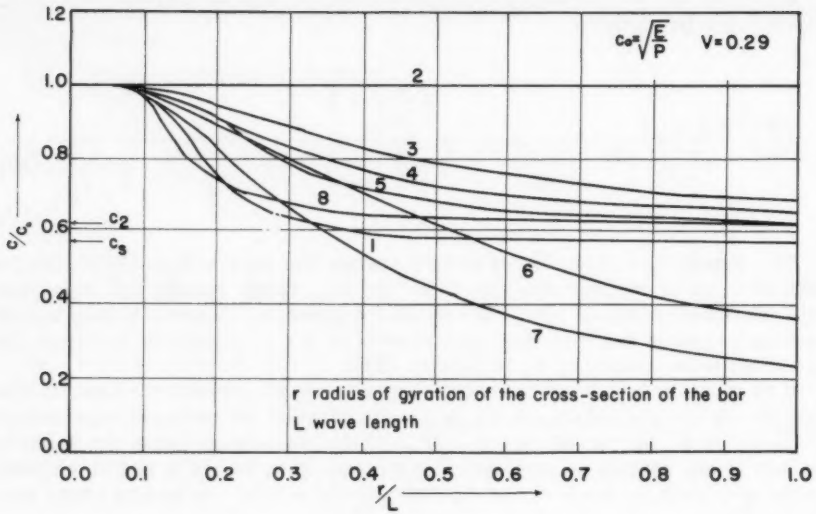

FIG. 2.—PHASE VELOCITY OF LONGITUDINAL WAVES IN A BAR OF SQUARE CROSS SECTION

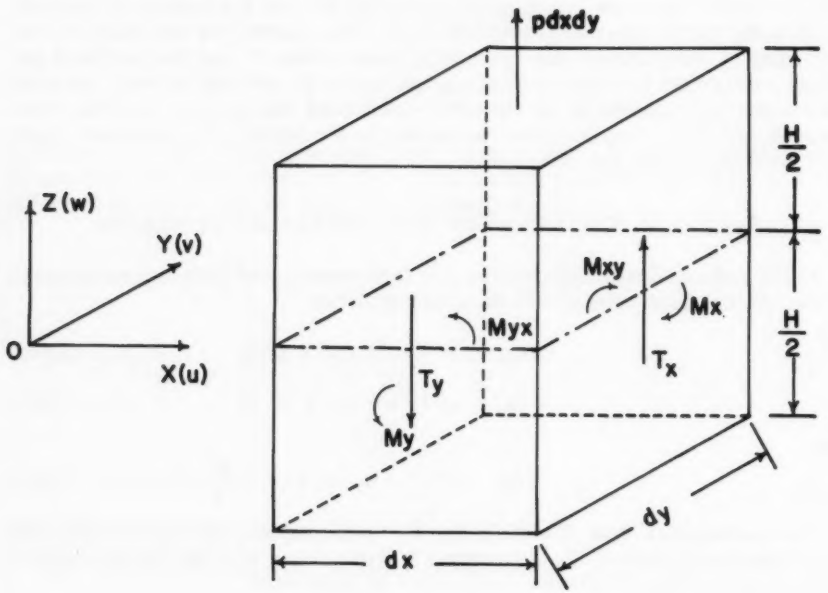

FIG. 3

The components of strain computed from Eqs. 30 are:

$$\epsilon_x = \frac{\partial u}{\partial x} = z \frac{\partial \mu x}{\partial x} \quad \ldots\ldots\ldots\ldots\ldots\ldots (31a)$$

$$\gamma_{xy} = \frac{\partial u}{\partial y} + \frac{\partial v}{\partial x} = z \left(\frac{\partial \mu_x}{\partial y} + \frac{\partial \mu_y}{\partial x} \right) \quad \ldots\ldots\ldots\ldots (31b)$$

$$\epsilon_y = \frac{\partial v}{\partial y} = z \frac{\partial \mu y}{\partial y} \quad \ldots\ldots\ldots\ldots\ldots\ldots (31c)$$

$$\gamma_{yz} = \frac{\partial v}{\partial z} + \frac{\partial w}{\partial y} = \mu_y + \frac{\partial \nu z}{\partial y} + \frac{1}{2} z^2 \frac{\partial f}{\partial y} \quad \ldots\ldots\ldots\ldots (31d)$$

$$\epsilon_z = \frac{\partial w}{\partial z} = z f; \; \gamma_{zx} = \frac{\partial w}{\partial x} + \frac{\partial u}{\partial z} = \mu_x + \frac{\partial \nu_z}{\partial x} + \frac{1}{2} z \frac{\partial f}{\partial x} \quad \ldots\ldots\ldots (31e)$$

and

$$1 = \epsilon_x + \epsilon_y + \epsilon_z = z \left(\frac{\partial \mu_x}{\partial x} + \frac{\partial \mu_y}{\partial y} + f \right) \quad \ldots\ldots\ldots\ldots (31f)$$

The normal stress σ_z is given by:

$$\sigma_z = \lambda 1 + 2 G \epsilon_z = \lambda_z \left(\frac{\partial \mu_x}{\partial x} + \frac{\partial \mu_y}{\partial y} + f \right) + 2 G z f \quad \ldots\ldots (32)$$

By satisfying the requirement that $\partial_z = 0$, the following relationship is obtained from Eq. 32 for the unknown function $f(x, y; t)$:

$$f(x, y; t) = - \frac{\nu}{(1 - \nu)} \left[\frac{\partial \mu_x (x, y; t)}{\partial x} + \frac{\partial \mu_y (x, y; t)}{\partial y} \right] \ldots (33)$$

In the evaluation of the potential and kinetic energies of the plate, second order terms z^2 will be neglected in comparison with linear terms. After integration with respect to the variable z the following expressions are obtained:

(a) For the potential energy:

$$U = \int_A \left\{ \frac{E}{2(1 - \nu^2)} \left[I \left(\frac{\partial \mu_x}{\partial x} \right)^2 + I \left(\frac{\partial \mu_y}{\partial y} \right)^2 \right] + \frac{\nu E}{(1 - \nu^2)} I \frac{\partial \mu_x}{\partial x} \frac{\partial \mu_y}{\partial y} \right.$$

$$+ \frac{E}{4(1 + \nu)} \left[I \left(\frac{\partial \mu_x}{\partial y} \right)^2 + I \left(\frac{\partial \mu_y}{\partial x} \right)^2 + 2 I \frac{\partial \mu_x}{\partial y} \frac{\partial \mu_y}{\partial x} + k H (\mu_y)^2 \right.$$

$$+ k H \left(\frac{\partial \nu_z}{\partial y} \right)^2 + 2 k H \mu_y \frac{\partial \nu_z}{\partial y} + k H (\mu_x)^2 + k H \left(\frac{\partial \nu_z}{\partial x} \right)^2$$

$$\left. \left. + 2 k H \mu_x \frac{\partial \nu_z}{\partial x} \right] \right\} dx \, dy \quad \ldots\ldots\ldots\ldots (34)$$

(b) For the kinetic energy:

$$T = \frac{\rho}{2} \int_A \left[I \left(\frac{\partial \mu_x}{\partial t} \right)^2 + I \left(\frac{\partial \mu_y}{\partial t} \right)^2 + H \left(\frac{\partial \nu_z}{\partial t} \right)^2 \right] dx\, dy \quad \ldots\ldots\ldots (35)$$

In Eqs. 34 and 35

$$I = \int_{-H/2}^{H/2} z^2 \, 1 \, dz = \frac{H^3}{12} \quad \ldots\ldots\ldots\ldots (36)$$

in which H is the constant thickness of the plate, and A is the area of the surface of the plate. The factor k (shear coefficient) was introduced, as in the previous cases of the bar, to take into account the non-linear distribution of the shear over the cross-section of the plate.

Hereafter the function V_z, which represents the vertical displacements of the middle surface of the plate, will be indicated by the letter W_o.

The work done by the external distributed force $p(x, y; t)$ acting on the middle surface of the plate in a virtual displacement δw_o is given by

$$\delta L = \int_A p(x, y; t)\, \delta w_o \, dx\, dy \quad \ldots\ldots\ldots\ldots (37)$$

By applying Hamilton's principle, the following equations of motion:

$$D \frac{\partial^2 \mu_x}{\partial x^2} + \frac{1+\nu}{2} D \frac{\partial^2 \mu_y}{\partial x\, \partial y} + \frac{1-\nu}{2} D \frac{\partial^2 \mu_x}{\partial y^2}$$

$$- \frac{E H k}{2(1+\nu)} \frac{\partial w_o}{\partial x} - \frac{E H k}{2(1+\nu)} \mu_x = \frac{p H^3}{12} \frac{\partial^2 \mu_x}{\partial t^2} \quad \ldots\ldots (38a)$$

$$D \frac{\partial^2 \mu_y}{\partial y^2} + \frac{1+\nu}{2} D \frac{\partial^2 \mu_x}{\partial x\, \partial y} + \frac{1-\nu}{2} D \frac{\partial^2 \mu_y}{\partial y^2}$$

$$- \frac{E H k}{2(1+\nu)} \frac{\partial w_o}{\partial y} - \frac{E H k}{2(1+\nu)} \mu_y = \frac{p H^3}{12} \frac{\partial^2 \mu_y}{\partial t^2} \quad \ldots\ldots (38b)$$

and

$$\frac{E H k}{2(1+\nu)} \Delta w_o + \frac{E H k}{2(1+\nu)} \left[\frac{\partial \mu_x}{\partial x} + \frac{\partial \mu_y}{\partial y} \right] = p H \frac{\partial^2 w_o}{\partial t^2} - p(x, y; t) \quad \ldots (38c)$$

and the following boundary conditions:

$$\left.\begin{array}{l} x = \begin{cases} = 0 \\ = a \end{cases} \quad 0 \le y \le b; \quad 0 \le x \le a \le y = \begin{cases} = 0 \\ = b \end{cases} \\ D\left(\frac{\partial \mu_x}{\partial x} + \nu \frac{\partial \mu_y}{\partial y}\right) \delta \mu_x = 0; \quad \left(\frac{1-\nu}{2}\right) D\left(\frac{\partial \mu_y}{\partial x} + \frac{\partial \mu_x}{\partial y}\right) \delta \mu_x = 0 \\ \left(\frac{1-\nu}{2}\right) D\left(\frac{\partial \mu_x}{\partial y} + \frac{\partial \mu_y}{\partial x}\right) \delta \mu_y = 0; \quad D\left(\frac{\partial \mu_y}{\partial y} + \nu \frac{\partial \mu_x}{\partial x}\right) \delta \mu_y = 0 \\ \frac{E H k}{2(1+\nu)} \left(\frac{\partial w_o}{\partial x} + \mu_x\right) \delta w_o = 0; \quad \frac{E k H}{2(1+\nu)} \left(\frac{\partial w_o}{\partial y} + \mu_y\right) \delta w_o \end{array}\right\} \quad \ldots (39)$$

are obtained

In Eqs. 38 and 39

$$D = \frac{E H^3}{12(1-\nu^2)} \quad \ldots\ldots\ldots\ldots\ldots (40)$$

and

$$\Delta = \left(\frac{\partial^2}{\partial x^2} + \frac{\partial^2}{\partial y^2}\right) \quad \ldots\ldots\ldots\ldots\ldots (41)$$

is the Leplace two-dimensional operator.

The shear forces T_x and T_y, the bending moments M_x and M_y, and the twisting moments M_{xy} and M_{yx} per unit length of the plate (Fig. 3) are defined by the following expressions:

$$T_x = \int_{-H/2}^{H/2} \tau_{xz} \, 1 \, dz = \int_{-H/2}^{H/2} G k \gamma_{xz} \, 1 \, dz = \frac{E k H}{2(1+\nu)} \left(\frac{\partial w_o}{\partial x} + \mu_x\right) \ldots (42a)$$

$$T_y = \int_{-H/2}^{H/2} \tau_{yz} \, 1 \, dz = \int_{-H/2}^{H/2} G k \gamma_{yz} \, 1 \, dz = \frac{E k H}{2(1+\nu)} \left[\frac{\partial w_o}{\partial y} + \mu_y\right] \ldots (42b)$$

$$M_x = \int_{-H/2}^{H/2} \sigma_x \, z \, 1 \, dz = D\left(\frac{\partial \mu_x}{\partial x} + \frac{\partial \mu_y}{\partial y}\right) \ldots\ldots\ldots\ldots (43a)$$

$$M_y = \int_{-H/2}^{H/2} \sigma_y \, z \, 1 \, dz = D\left(\frac{\partial \mu_y}{\partial y} + \nu \frac{\partial \mu_x}{\partial x}\right) \ldots\ldots\ldots\ldots (43b)$$

and

$$M_{xy} = M_{yx} = \int_{-H/2}^{H/2} \tau_{xy} \, z \, 1 \, dz$$

$$= \int_{-H/2}^{H/2} G \gamma_{xy} \, z \, 1 \, dz = \frac{1-\nu}{2} D\left(\frac{\partial \mu_x}{\partial y} + \frac{\partial \mu_y}{\partial x}\right) \ldots\ldots (44)$$

In view of Eqs. 42, 43 and 44, Eqs. 38 can be written:

$$\frac{\partial M_x}{\partial x} + \frac{\partial M_{xy}}{\partial y} - T_x = \frac{\rho H^3}{12} \frac{\partial^2 \mu_x}{\partial t^2} \quad \ldots\ldots\ldots\ldots (45a)$$

$$\frac{\partial M_{yx}}{\partial x} + \frac{\partial M_y}{\partial y} - T_y = \frac{\rho H^3}{12} \frac{\partial^2 \mu_y}{\partial t^2} \quad \ldots\ldots\ldots\ldots (45b)$$

and

$$\frac{\partial T_x}{\partial x} + \frac{\partial T_y}{\partial y} + p = \rho H \frac{\partial^2 w_o}{\partial t^2} \quad \ldots\ldots\ldots\ldots\ldots (45c)$$

The terms on the right of Eqs. 45 represent the terms due to rotatory inertia. Eqs. 45 are the same equations as those obtained in 1950 in a more complicated way by Mindlin (17).

Differentiating Eq. 38a with respect to x and Eq. 38b with respect to y, and adding them together, results in

$$\left[D\Delta - \frac{E H k}{2(1+\nu)} - \rho \frac{H^2}{12} \frac{\partial^2}{\partial t^2} \right] \left(\frac{\partial \mu x}{\partial x} + \frac{\partial \mu y}{\partial y} \right) = \frac{E H k}{2(1+\nu)} \Delta w_o \ldots (46)$$

By eliminating the term $\left(\frac{\partial \mu x}{\partial x} + \frac{\partial \mu y}{\partial y} \right)$ between Eq. 46 and Eq. 38c

$$\left[\Delta - \frac{2\rho(1+\nu)}{E k} \frac{\partial^2}{\partial t^2} \right] \left[D\Delta - \frac{\rho H^3}{12} \frac{\partial^2}{\partial t^2} \right] w_o(x, y, t)$$

$$+ \rho H \frac{\partial^2 w_o(x, y, t)}{\partial t^2} = \left[1 - \frac{H^2}{6(1-\nu)k} \Delta + \frac{\rho H^2 (1+\nu)}{6 E k} \right] p(x, y, t) \quad \ldots (47)$$

If the terms due to shear are neglected in Eq. 47 it becomes

$$\left(D\Delta - \frac{\rho H^3}{12} \frac{\partial^2}{\partial t^2} \right) \Delta w_o(x, y, t) + \rho H \frac{\partial^2 w_o(x, y, t)}{\partial t^2} = p(x, y, t) \quad \ldots (48)$$

If the terms due to rotatory inertia are neglected in Eq. 47 it becomes

$$D \left[\Delta - \frac{2\rho(1+\nu)}{E k} \frac{\partial^2}{\partial t^2} \right] \Delta w_o(x, y, t) + \rho H \frac{\partial^2 w_o(x, y, t)}{\partial t^2}$$

$$= \left[1 - \frac{H^2}{6(1-\nu)k} \Delta \right] p(x, y, t) \quad \ldots\ldots\ldots (49)$$

Finally, in Eq. 47, if terms due to rotatory inertia and to shear are neglected at the same time, it reduces to the classic plate equation

$$D \Delta\Delta w_o(x,y,t) + \rho H \frac{\partial^2 w_o(x,y,t)}{\partial t^2} = p(x,y,t) \quad \ldots\ldots(50)$$

In Eqs. 30 of the components of the elastic displacement, if only the first terms are considered, or if:

$$u(x,y,z,t) = z\, \mu_x(x,y,t) \quad \ldots\ldots(51a)$$

$$v(x,y,z,t) = z\, \mu_y(x,y,t) \quad \ldots\ldots(51b)$$

and

$$w(x,y,z,t) = v_z(x,y,t) \quad \ldots\ldots(51c)$$

then the following equation of motion is obtained in final form

$$\left[\Delta - \frac{2\rho(1+\nu)}{E}\frac{\partial^2}{\partial t^2}\right]\left[\frac{D(1-\nu^2)}{(1-2\nu)}\Delta - \frac{\rho H^3}{12}\frac{\partial^2}{\partial t^2}\right] w_o(x,y,t)$$

$$+\rho H \frac{\partial^2 w_o(x,y,t)}{\partial t^2} = \left[1 - \frac{H^2}{6(1-2\nu)}\Delta + \frac{\rho H^2(1+\nu)}{6E}\frac{\partial^2}{\partial t^2}\right] p(x,y,t) \quad \ldots\ldots(52)$$

Let

$$w_o = A\, e^{i\gamma(x-ct)} \quad \ldots\ldots\ldots\ldots(53)$$

in which A is a constant, $i = \sqrt{-1}$, $\gamma = 2\pi/L$, L is the wave length and C the phase velocity.

From the equations of motion (Eqs. 47, 48, 49, 50 and 52) the following dispersion equations are derived:

(a) From Eq. 47:

$$\left(\frac{H}{L}\right)^2 = \frac{3}{\pi^2}\,\frac{k}{2(1+\nu)}\,\frac{\left(\frac{c}{c_o}\right)^2}{\left[\left(\frac{c}{c_o}\right)^2 - \frac{k}{2(1+\nu)}\right]\left[\left(\frac{c}{c_o}\right)^2 - \frac{1}{(1-\nu 2)}\right]} \quad \ldots\ldots(54)$$

(b) From Eq. 48:

$$\left(\frac{H}{L}\right)^2 = \frac{3}{\pi^2}\,\frac{\left(\frac{c}{c_o}\right)^2}{\left[\frac{1}{(1-\nu 2)} - \left(\frac{c}{c_o}\right)^2\right]} \quad \ldots\ldots\ldots(55)$$

(c) From Eq. 49:

$$\left(\frac{H}{L}\right)^2 = \frac{3\,k\,(1-\nu)}{2\,\pi^2}\,\frac{\left(\frac{c}{c_o}\right)^2}{\left[\frac{k}{2(1+\nu)} - \left(\frac{c}{c_o}\right)^2\right]} \quad \ldots\ldots\ldots(56)$$

(d) From Eq. 50:

$$\left(\frac{c}{c_0}\right) = \frac{H}{L}\ \frac{\pi}{\sqrt{3\left(1-\nu^2\right)}} \qquad \ldots\ldots\ldots\ldots\ldots (57)$$

(e) From Eq. 52:

$$\left(\frac{H}{L}\right)^2 = \frac{3}{2\,\pi 2\,(1+\nu)}\ \frac{\left(\frac{c}{c_0}\right)^2}{\left[\left(\frac{c}{c_0}\right)^2 - \frac{1}{2\,(1+\nu)}\right]\left[\left(\frac{c}{c_0}\right)^2 - \frac{(1-\nu)}{(1+\nu)(1-2\,\nu)}\right]} \qquad \ldots\ldots (58)$$

In Fig. 4 the curves (c/c_0) against H/L, according to Eqs. 54, 55, 56 and 57, are compared with the results obtained by use of Lamb's exact theory. The value for the constant k in Eqs. 54 and 56 is equal to 0.857 which is the value

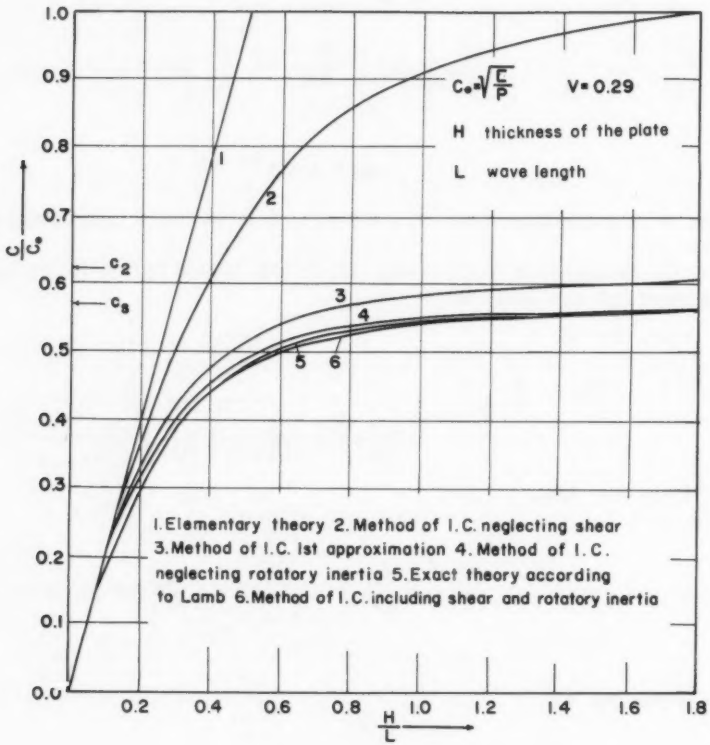

FIG. 4.—PHASE VELOCITY OF FLEXURAL WAVES IN A THIN PLATE

of the ratio between the velocities of the Rayleigh surface waves and the waves of distortion in an infinite medium for Poisson's ratio v = C.29 (steel).

STATIC DEFLECTIONS OF THIN RECTANGULAR PLATES

In the static case Eqs. 38 become:

$$D\frac{\partial^2 \mu_x}{\partial x^2} + \frac{1+\nu}{2} D\frac{\partial^2 \mu_y}{\partial x\,\partial y} + \frac{1-\nu}{2} D\frac{\partial^2 \mu_x}{\partial y^2}$$

$$- \frac{E\,H\,k}{2(1+\nu)}\frac{\partial w_o}{\partial x} - \frac{E\,H\,k}{2(1+\nu)}\mu_x = 0 \quad \ldots\ldots\ldots\ldots (59a)$$

$$D\frac{\partial^2 \mu_y}{\partial y^2} + \frac{1+\nu}{2} D\frac{\partial^2 \mu_x}{\partial x\,\partial y} + \frac{1-\nu}{2} D\frac{\partial^2 \mu_y}{\partial x^2} - \frac{E\,H\,k}{2(1+\nu)}\frac{\partial w_o}{\partial y} - \frac{E\,H\,k}{2(1+\nu)}\mu_y = 0 \quad \ldots\ldots (59b)$$

and

$$\frac{E\,H\,k}{2(1+\nu)}\Delta w_o + \frac{E\,H\,k}{2(1+\nu)}\left[\frac{\partial \mu_x}{\partial x} + \frac{\partial \mu_y}{\partial y}\right] = -p(x, y) \quad \ldots\ldots (59c)$$

while the boundary conditions remain the same Eqs. 39.

Eqs. 45 become:

$$\frac{\partial M_x}{\partial x} + \frac{\partial M_{xy}}{\partial y} - T_x = 0 \quad \ldots\ldots\ldots\ldots\ldots (60a)$$

$$\frac{\partial M_{yx}}{\partial x} + \frac{\partial M_y}{\partial y} - T_y = 0 \quad \ldots\ldots\ldots\ldots\ldots (60b)$$

and

$$\frac{\partial T_x}{\partial x} + \frac{\partial T_y}{\partial y} + p = 0 \quad \ldots\ldots\ldots\ldots\ldots (60c)$$

while Eq. 46 becomes:

$$D\,\Delta\,\Delta\, w_o(x, y) = \left[1 - \frac{H^2}{6(1-\nu)k}\Delta\right] p(x, y) \quad \ldots\ldots\ldots (61)$$

The following equations are obtained from Eqs. 42, 43, 44 and 60.

$$M_x - \frac{H^2}{6\,k}\frac{\partial T_x}{\partial x} + \frac{\nu\,H^2}{6(1-\nu)k} p = -D\left(\frac{\partial^2 w_o}{\partial x^2} + \nu\frac{\partial^2 w_o}{\partial y^2}\right) \quad \ldots\ldots\ldots (62a)$$

$$M_y - \frac{H^2}{6\,k}\frac{\partial T_y}{\partial y} + \frac{\nu\,H^2}{6(1-\nu)k} p = -D\left(\frac{\partial^2 w_o}{\partial y^2} + \nu\frac{\partial^2 w_o}{\partial x^2}\right) \quad \ldots\ldots\ldots (62b)$$

$$M_{xy} - \frac{H^2}{12\,k}\left(\frac{\partial T_x}{\partial y} + \frac{\partial T_y}{\partial x}\right) = -(1-\nu)\,D\,\frac{\partial^2 w_o}{\partial x\,\partial y} \quad \ldots\ldots\ldots(63)$$

$$T_x - \frac{H^2}{12\,k}\,\Delta T_x + \frac{H^2}{12(1-\nu)k}\,\frac{\partial p}{\partial x} = -D\,\frac{\partial}{\partial x}\,\Delta w_o \quad \ldots\ldots(64a)$$

and

$$T_y - \frac{H^2}{12\,k}\,\Delta T_y + \frac{H^2}{12(1-\nu)k}\,\frac{\partial p}{\partial y} = -D\,\frac{\partial}{\partial y}\,\Delta w_o \quad \ldots\ldots(64b)$$

In the static case (12) the value of the shear coefficient k should be $k = 1/1.2 = 0.833$.

In the case of a very thin plate, $(H \to 0)$; and Eqs. 61, 62, 63 and 64 reduce to the following equations of the classical theory:

$$D\,\Delta\,\Delta\,w_o = p\,(x, y) \quad \ldots\ldots\ldots\ldots(65)$$

$$M_x = -D\left(\frac{\partial^2 w_o}{\partial x^2} + \nu\,\frac{\partial^2 w_o}{\partial y^2}\right) \quad \ldots\ldots\ldots\ldots(66a)$$

$$M_y = -D\left(\frac{\partial^2 w_o}{\partial y^2} + \nu\,\frac{\partial^2 w_o}{\partial x^2}\right) \quad \ldots\ldots\ldots\ldots(66b)$$

$$M_{xy} = M_{yx} = -(1-\nu)\,D\,\frac{\partial^2 w_o}{\partial x\,\partial y} \quad \ldots\ldots\ldots\ldots(67)$$

$$T_x = -D\frac{\partial}{\partial x}\,(\Delta\,w_o) \quad \ldots\ldots\ldots\ldots(68a)$$

and

$$T_y = -D\,\frac{\partial}{\partial y}\,(\Delta\,w_o) \quad \ldots\ldots\ldots\ldots(68b)$$

Eqs. 61, 62, 63, and 64 correspond to the following equations of Reissner's theory:

$$D\,\Delta\Delta\,w_o = \left(1 - \frac{H^2}{10}\,\frac{2-\nu}{1-\nu}\,\Delta\right)p \quad \ldots\ldots\ldots\ldots(69)$$

$$M_x - \frac{H^2}{10}\,\frac{\partial\,T_x}{\partial x} - \frac{H^2}{10}\,\frac{\nu}{(1-\nu)}\,p = -D\left(\frac{\partial^2 w_o}{\partial x^2} + \nu\,\frac{\partial^2 w_o}{\partial y^2}\right) \quad \ldots\ldots\ldots(70a)$$

$$M_y - \frac{H^2}{10}\,\frac{\partial\,T_y}{\partial y} - \frac{H^2}{10}\,\frac{\nu}{(1-\nu)}\,p = D\left(\frac{\partial^2 w_o}{\partial y^2} + \nu\,\frac{\partial^2 w_o}{\partial x^2}\right) \quad \ldots\ldots\ldots(70b)$$

$$M_{xy} - \frac{H^2}{10}\left(\frac{\partial T_x}{\partial y} + \frac{\partial T_y}{\partial x}\right) = -(1-\nu)\, D \frac{\partial^2 w_o}{\partial x\, \partial y} \quad \ldots\ldots\ldots (71)$$

$$T_x - \frac{H^2}{10}\Delta T_x + \frac{H^2}{10(1-\nu)}\frac{\partial p}{\partial x} = -D\frac{\partial}{\partial x}(\Delta w_o) \quad \ldots\ldots\ldots (72a)$$

and

$$T_y - \frac{H^2}{10}\Delta T_y + \frac{H^2}{10(1-\nu)}\frac{\partial p}{\partial y} = -D\frac{\partial}{\partial y}(\Delta w_o) \quad \ldots\ldots\ldots (72b)$$

It can be shown that, using the theory that is here presented, as with the theories of Bolle and Reissner, the solution of equilibrium problems for thin plates is reduced to the solution of the equation:

$$D\,\Delta\,\Delta\, w_o = \left[1 - \frac{H^2}{2(1-\nu)}\Delta\right] p \quad \ldots\ldots\ldots (73)$$

and of the equation:

$$\Delta\,\Phi - \frac{12\,k}{H^2}\,\Phi = 0 \quad \ldots\ldots\ldots\ldots\ldots\ldots (74)$$

that defines the stress function Φ.

Shear forces are computed from the equations:

$$T_x = -D\frac{\partial(\Delta w_o)}{\partial x} + \frac{\partial \Phi}{\partial y} \quad \ldots\ldots\ldots (75a)$$

and

$$T_y = -D\frac{\partial(\Delta w_o)}{\partial y} - \frac{\partial \Phi}{\partial x} \quad \ldots\ldots\ldots (75b)$$

CONCLUSIONS

The approximate method presented is applied to studying, in a systematic and general way, static and dynamic problems of plates and bars, and it unifies a number of engineering theories on the subject.

By applying the method of internal constraints (which is based on special assumptions concerning the components of the elastic displacement), the equations of motion or the equations of equilibrium and the corresponding boundary conditions are derived more directly and more simply than through application of engineering methods based, in general, on hypotheses concerning the distribution of stresses.

In the case of flexural vibrations of elongated straight rods, the equations of motion are reduced in the plane-stress case to the well-known Timoshenko beam equation.

In the case of longitudinal vibrations of straight rods, when dispersion curves obtained by use of the method of internal constraints are compared with those

obtained by use of other engineering methods and by use of the exact Pochhammer solution, it is seen that the former curves give results closer to those obtained from the exact solution.

In the case of flexural vibrations of rectangular thin plates, the equations of motion derived by applying the method of internal constraints coincide with the equations of motion derived by Mindlin from the three-dimensional equations of elasticity. However, the present equations are obtained in a more direct way. These equations are reduced, in the static case, to equations that are very similar to those obtained by Reissner in his theory of bending of thin elastic plates taking into account the transverse-shear deformation of the plates.

ACKNOWLEDGMENTS

This paper was written in connection with research sponsored at the University of Texas, Austin, Tex., by the National Science Foundation under Grant No. 9544.

APPENDIX I.—NOTATIONS

The following symbols are used in the text:

A = cross-section area of the beam;

B = breadth of the beam;

c = velocity of propagation of waves in general;

c_0 = velocity of longitudinal waves of infinite wave-length in a bar, $c_0 = \sqrt{\frac{E}{\rho}}$;

D = $\frac{E H^3}{12(1-\nu^2)}$;

E = Young's modulus;

e = dilatation;

f, f_1, f_2, f_3, f_4 = functions which define the elastic displacement;

G = modulus of rigidity, $G = \frac{E}{2(1+\nu)}$;

H = height of the beam, thickness of the plate;

I_y, I_z = moments of inertia of area about the Y and Z axes;

l = length;

L = wave-length;

k = shear coefficient;

M_x, M_y = bending moments;

$M_{xy} = M_{yx}$ = twisting moments;

p = external distributed force;

$r_Z = \sqrt{\frac{I_Z}{A}}$ = radius of gyration;

t = time;

T_X, T_y = shear forces;

T = kinetic energy;

u, v, w = displacements in the X, Y, and Z directions in rectangular coordinates;

U = potential energy;

w_o = displacement in general;

X, Y, Z = rectangular axes of reference;

x, y, z = rectangular coordinates;

γ = $2\pi/L$;

γ_{xy}, γ_{yz}, γ_{zx} = shearing strain components in rectangular coordinates;

$\Delta = \frac{\partial^2}{\partial x^2} + \frac{\partial^2}{\partial y^2}$ = Laplacian two-dimensional operator;

ϵ_x, ϵ_y, ϵ_z = unit elongations in the X, Y, and Z directions;

$\lambda = \frac{\nu E}{(1+\nu)(1-2\nu)}$ = Lame's constant;

ν = Poisson's ratio;

ρ = density;

σ_x, σ_y, σ_z = normal components of stress parallel to the X, Y, and Z axes;

τ_{xy}, τ_{yz}, τ_{zx} = shearing-stress components in rectangular coordinates; and

$\left.\begin{matrix}\lambda_x, \lambda_y, \lambda_z \\ \mu_x, \mu_y, \mu_z \\ \nu_x, \nu_y, \nu_z\end{matrix}\right\}$ = functions that define the elastic displacement.

APPENDIX II.—BIBLIOGRAPHY ON METHODS OF INTERNAL CONSTRAINTS AND ITS APPLICATION.

---

1. "Uber die Fortpflanzungsgeschwindigkeiten kleiner Schwingungen in einem unbegrenzten isotropen Kreiszylinder," by L. Pochhammer, Zeitschrift für die reine und angewandte Mathematik, Crelle, Vol. 81, 1876, p. 324.

2. The Theory of Sound, by Lord Rayleigh, New York, Dover, 1945.

3. "On the Correction for Shear of the Differential Equations for Traverse Vibrations of Prismatic Bars," by S. Timoshenko, Philosophical Magazine, Vol. 41, 6th series, 1921, p. 742.

4. "On the Free Vibrations of an Infinite Plate of Homogeneous Isotropic Elastic Matter," by Lord Rayleigh, Proceedings, Royal Soc. of London, Vol. 10, 1889, p. 225.

5. "On Waves in an Elastic Plate," by H. Lamb, Proceedings, Royal Soc. of London, Vol. 93, series A, 1917, p. 114.

6. "Uber das Gleichgewicht und die Bewegung einer elastischen Scheibe," by G. Kirchoff, Zeitschrift für reine und angewandte Mathematik, Vol. 40, 1850, p. 51

7. Theory of Plates and Shells, by S. Timoshenko and S. Woinowsky-Krieger, McGraw-Hill Book Co., Inc., New York, 1959, p. 173.

8. "On the Theory of Bending of Elastic Plates," by E. Reissner, Journal of Mathematics and Physics, Vol. 23, 1944, p. 184.

9. "The Effects of Transverse Shear Deformation on the Bending Elastic Plates," by E. Reissner, Journal of Applied Mechanics, Vol. 12, 1945, p. A68.

10. "On Bending of Elastic Plates," by E. Reissner, Quarterly of Applied Mechanics, Vol. 5, 1947, p. 55.

11. "Uber die Berucksichtigung der Schubverzenung in ebenen Platten," by H. Hencky, Ingenieur-Archiv, XVI Band, 1947, p. 72.

12. "Contribution au problème linéaire de flexion d'une plaque élastique," by L. Bolle, Bulletin Technique de la Suisse Romande, Nos. 21, 22, October, 1947, p. 281, 293.

13. "Uber eine Verfeinerung der Klassischen Theorie dunner schwachgebogener Platten," by M. Schafer, Zeitschrift für angewandte Mathematik und Mechanik, Band 32, Heft 6, 1952, p. 161.

14. "Verallgemeinerte Theorie der Plattenstatik," by A. Kromm, Ingenieur-Archiv, xxi Band, 1953, p. 266.

15. "Uber die Randquerkrafte bei gestutzten Platten," by A. Kromm, Zeitschrift für angewandte Mathematik und Mechanik, Band 35, Heft 6, 1955, p. 231.

16. "On Reissner's Theory of Bending of Elastic Plates," by A. E. Green, Quarterly of Applied Mathematics, Vol. 7, No. 2, 1949, p. 223.

17. "Influence of Rotatory Inertia and Shear on Flexural Motions of Isotropic Elastic Plates," by R. D. Mindlin, Journal of Applied Mechanics, March, 1951, p. 31.

18. Discussion by E. Volterra of "Effect of Shear Deformations on the Bending of Rectangular Plates," by V. L. Salerno and M. A. Goldberg, Transactions, ASME, September, 1960, p. 594.

19. "Influenze del taglio nella dinamica e nella statica delle piastre sottili. Nota I and II, by E. Volterra, Rendiconti Accademia Nazionale dei Lincei Serie VIII, Vol. VIII, fasc. 6; also Vol. XXIX, fasc. 1, 2.

20. "Questioni di elasticitá vincolata. Nota IV. Significato geometrico del vincolo," Rendiconti della Reale Accademia Nazionale dei Lincei. Classe di

Scienze fisiche, mathematiche e naturali, Vol. XXIII, Serie 6, 1st semestre, Fasc. 5, Marzo, 1936.

21. "A Critical Study of the Hopkinson Pressure Bar," by R. M. Davies, Philosophical Transactions, Royal Soc. of London, Series A, Vol. 240, 1948, p. 375.

22. "Dispersion of Compressional Waves in Isotropic Rods of Rectangular Cross-Section," by R. W. Morse, Journal, Acoustical Soc. of Amer., Vol. 20, 1948, p. 833.

23. "The Velocity of Compressional Waves in Rods of Rectangular Cross-Section," by R. W. Morse, Journal, Acoustical Soc. of Amer., Vol. 22, 1950, p. 219.

24. Stress Waves in Solids, by H. Kolsky, Oxford, Clarendon Press, 1953.

25. The Mathematical Theory of Elasticity, by A.E.H. Love, Cambridge Univ. Press, 1934.

26. Longitudinal Waves in Beams, by R.E.D. Bishop, The Aeronautical Quarterly, Vol. 3, 1952, p. 280.

27. "Dispersion of Longitudinal Waves," by E. Volterra, Proceedings, ASCE, Vol. 83, No. EM 3, 1957.

Journal of the
ENGINEERING MECHANICS DIVISION
Proceedings of the American Society of Civil Engineers

DISCUSSION

Note.—This paper is a part of the copyrighted Journal of the Engineering Mechanics Division, Proceedings of the American Society of Civil Engineers, Vol. 87, No. EM 4, August, 1961.

COMPARATIVE STUDY OF A SEGMENTAL ARCH RING[a]

Closure by O. C. Zienkiewicz

O. C. ZIENKIEWICZ,[7] F. ASCE.—It is gratifying that the conclusions reached by A. J. Veltrop, M. ASCE, with the wide range of $\frac{R}{t}$ values investigated verify essentially the original contentions.

While the object of the paper was a comparison of various shell theories on an elementary example, it is interesting to see some of the results including the elasticity of the abutments placed side by side with these. It is rather remarkable that the effect of this is of the same order as the discrepancies between the results of the various theories applied to the rigid abutment example and points to the caution necessary in interpretation of such results.

[a] January, 1960, by O. C. Zienkiewicz (Proc. Paper 2332).
[7] Prof. of Civ. Engrg., Northwestern Univ., Evanston, Ill.

VIBRATIONS AND STABILITY OF PLATES UNDER INITIAL STRESS[a]

Closure by George Herrmann and Anthony Armenakas

GEORGE HERRMANN,[6] AND ANTHONY ARMENAKAS,[7] MEMBERS, ASCE.—The writers concur with Masur's view that space might have been conserved if the results were presented in a more compact notation. However, they do not share his opinion that the use of cartesian components resulted in a measure of obscurity, for if that were the case, this notation would not have been used by the many investigators cited in the bibliography. Masur is correct in stating that the matrix τ_{ij} does not transform as a tensor evidenced from its definition and from the tensorial properties of σ_{ij}. The writers, however, disagree with the suggestion that the principles of thermodynamics limit the choice of acceptable stress-strain relations to those resulting from Eqs. 23.

The formulation of the problem considered involves the assumption that the influence on the motion of the components of strain and rotation, associated with initial stresses, is negligible. In a sense, therefore, the initial state of stress may be conceived as a state without any related strain. Hence, any approach which associates a strain energy density function with both the initial and final state of stress may be misleading.

In the theory presented by the writers, the additional elongations, shears and rotations are small as compared to unity, therefore, it is assumed that the difference between the initial and final stresses is related to the additional strains in accordance to Hooke's law for an isotropic elastic solid. However, in the presence of initial stress (even in this range of small deformations), the Trefftz components of stress σ_{ij} (which in the vocabulary of the mathematical theory of finite elasticity are referred to as material stress components) and the actual components of stress τ_{ij} (defined in the original paper) cannot be considered identical. Thus, the presence of a number of terms involving initial stresses in the displacement equations of motion is dependent on whether the difference $(\sigma_{ij} - s_{ij})$ or $(\tau_{ij} - s_{ij})$ is assumed related to the stresses in accordance to Hooke's law. It is this point which the writers attempted to emphasize in the original paper by presenting three different possibilities for introducing the initial and additional stresses into the non-linear equations of motion. In other words, a number of terms involving products of initial stresses and displacement gradients appearing in the equations of motion are of the same order of magnitude as terms discarded by disregarding the effect of initial deformation.

---

[a] June, 1960, by George Herrmann and Anthony Armenakas (Proc. Paper 2500).

[6] Assoc. Prof. of Civ. Engrg., Inst. of Flight Structures, Columbia Univ., New York, N. Y.

[7] Assoc. Prof. of Civ. Engrg., The Cooper Unior for the Advancement of Science and Art, New York, N. Y.

ULTIMATE STRENGTH OF OVER-REINFORCED BEAMS[a]

Closure by Ladislav B. Kriz and Seng-Lip Lee

L. B. KRIZ,[16] and S. L. LEE,[17] MEMBERS, ASCE.—The authors wish to thank Iqbal Ali, M. ASCE, for calling the attention of the readers to his paper, published in 1959, in which an analysis of reinforced concrete members, based on the principle of determining the maximum resisting moment of a member, using the stress-strain relationship of Smith and Young are presented. The same approach was proposed in 1957 by another writer[18] who used a parabolic stress-strain relationship of concrete to demonstrate the principle.

The stress-strain relationship, proposed by the authors, is unsuitable for design purposes because of its complexity, and it was developed primarily for use in research. It was applied to the case of over-reinforced beams to show that a simple ultimate strength design formula may be arrived at by analytical rather than experimental procedures. The knowledge of the stress-strain relationship also makes it possible to predict the behavior of a reinforced concrete member throughout the loading range with accuracy, as was recently demonstrated.[19]

The authors agree fully with Ali's suggestion that determination of the stress-strain relationship for various concretes at different rates of loading is desirable. A paper of Hubert Rüsch[20] published in 1960 reports on work in this field.

---

[a] June, 1960, by Ladislaw B. Kriz and Seng-Lip Lee (Proc. Paper 2502).

[16] Assoc. Development Engr., Structural Development Sect., Portland Cement Asson. Lab. Skokie, Ill.

[17] Prof. of Civ. Engrg., Northwestern Univ., Evanston, Ill.

[18] "Het Gedrag Van Betonconstructies Onder Invloed Van Kortstondige Belastingen," IBC Medelingen, Vol. 5, No. 23rd, Delft, April, July, 1957, pp. 52-62.

[19] "Ultimate Strength of Non-Rectangular Structural Concrete Members," by A. H. Mattock and L. B. Kriz, ACI Journal, Vol. 32, No. 7, January, 1961 (Proceedings Vol. 57), pp. 737-766; Bulletin No. D48, PCA Development Dept.

[20] "Researches Toward a General Flexural Theory for Structural Concrete," by Hubert Rüsch, ACI Journal, Vol. 32, No. 1, July 1960 (Proceedings Vol. 57), pp. 1-28.

RESTRAINED COLUMNS[a]

Closure by Morris Ojalvo

MORRIS OJALVO,[15] M. ASCE.—As D. S. Mansell states, the writer's paper is a further development of the works of other writers. His work in particular, stems from Theodor von Kármán, Hon. M. ASCE, who recognized that the beam-column was a stability rather than a buckling problem and Chwalla[2] who apparently was the first to recognize that segments of the column deflection curves (waves) were equivalent to the equilibrium configurations of a column under increasing load or moment. The outline for determining the limit of stable equilibrium for any condition of end moments and restraints and the manner in which the information from the column deflection curves can be arranged in nomographs to give rapid solutions are the only new contributions of the paper.

It was not the intention of the writer to imply that a compressed member occurring in a structure with sidesway could not be considered as a segment of a column deflection curve. This aspect was not investigated because the stability analysis of frames with sidesway was not the subject of the paper. The analysis of this kind of structure by the exact procedures considered herein presents considerably greater computational difficulties and is not as susceptible to rapid solution by nomographs. The principle involved, however, is the same. One determines successive equilibrium configurations of the structure under increasing proportional load until an equilibrium configuration can no longer be found. The maximum load for which an equilibrium configuration can be found is the collapse load.

Mansell's proof is adequate to show that a differential equation (Eq. 15) describes the shape of the deflected member. It would have been more exact however to state that in Eq. 15 the abscissas are measured parallel to the x axis as it appears in Fig. 9, and that y is the distance between the thrust line and the curve measured parallel to the y axis. In this manner the usage of the term abscissa would also correspond to its definition as found in a mathematics dictionary.[16] The assumption that the shear must be small compared to the axial force (the respective components of the total thrust normal and parallel to the chord connecting the ends of a member) is nevertheless necessary if a compressed member is to be considered as part of a column deflection curve.

The proof that Eq. 15 is a symmetric periodic wave under the assumed moment-curvature relationship is most welcome for it emphasizes an erroneous statement made by the writer in the text. The writer's statement (first

---

[a] October, 1960, by Morris Ojalvo (Proc. Paper 2615).

[15] Assoc. Prof., Dept. of Civ. Engrg., Ohio State Univ., Columbus, Ohio.

[16] "Mathematics Dictionary," by Armen A. Alchian, G. James and R. C. James, Editors, Van Nostrand, London, 1949.

paragraph in the section entitled Theory) that the entire column deflection curve may be constructed from a known quarter wave length should have been qualified so that the statement was applicable only to columns of symmetric cross section and of a material having the same properties in both tension and compression.

WIND STRESSES IN DOMES[a]

Closure by P. Gondikas and Mario G. Salvadori

P. GONDIKAS,[26] and MARIO G. SALVADORI,[27] F. ASCE.—The writers feel that the publication of this paper would have been entirely justified even if it only produced discussion by Toebes, because their interest in dynamics has given them a clear picture of the need for more abundant information in the field of dynamic inputs for civil engineering structures.

Toebes is interested primarily in dynamic inputs, whereas the civil engineer is mostly interested in dynamic outputs. The applied mechanician who tries to fill the gap finds himself in the difficult position of knowing what to do with simple unrealistic inputs but of being lost when trying to deal with complex realistic inputs that he cannot easily feed into his equations.

More realistic static wind loads of the type used by Placido Cicala,[17] are being used to obtain membrane stress distributions in shells. Unfortunately, shells will withstand almost any load by means of membrane stresses but are liable to give in at particular spots due to bending stresses. The writers have therefore considered of some use the first solution to the bending problem of shells under conventional wind loads and notice that the same problem has been successively solved by a number of other authors.

The expansion of any wind loads into a double Fourier series in θ and ϕ has been obtained and has made possible, through the work of Gondikas and others, the bending analysis of shells under anti-symmetrical loads. It is, therefore, foreseeable that the evaluation of stresses due to fairly complicated static wind loads will soon appear in the literature.

In order to be able to attack the corresponding dynamic problem, the dynamic wind loads must be known with much greater accuracy before the structural engineer will bother to use them in a dynamic stress analysis. There is no doubt that what has been done for earthquakes will eventually be done for hurricane winds. The delay in the study of dynamic wind stresses is probably due to their lesser importance and to the large amount of ignorance in connection with vibrations of complex shell structures.

---

[a] October, 1960, by P. Gondikas and Mario G. Salvadori (Proc. Paper 2616).

[26] Partner, Gondikas and Righidis, Athens, Greece.

[27] Prof. of Civ. Engrg., Columbia Univ., New York, N. Y., also Paul Weidlinger, Cons. Engr., New York, N. Y.

ELASTO-PLASTIC ANALYSIS BY NUMERICAL PROCEDURES[a]

Discussion by G. C. Reynolds

G. C. REYNOLDS.[12] —The author's use of an equivalent E to analyze non-linear beams appears to be an unnecessary complication. In linear beams the curvature ϕ is equal to M/EI and the curvature, in the form M/EI, is used to compute slopes and deflections. For the analysis of non-linear beams, the author has replaced E by an equivalent value $\bar{E}$, such that $\phi = M/EI$, to represent curvature. A similar device, which has been used,[13] is to replace M by $\bar{M}$ such that $\phi = \bar{M}/EI$. As far as this writer is aware, no one has replaced I by $\bar{I}$, such that $\phi = \bar{M}/E\bar{I}$. There is no point in using an equivalent E, M, or I, because in each case, it is simply the curvature which is used. It is a simple matter to obtain a moment-curvature relation for non-linear beams[14] without introducing an equivalent E, and the analysis of the beams is not as difficult as is commonly supposed.[14] The curvature, obtained directly from the author's Fig. 2(b), is e/y in which e is the strain at distance y from the neutral axis. The corresponding moment is obtained by considering the forces represented by the stress diagram, Fig. 2(c).

---

[a] December, 1960, by Annabel L. Tong (Proc. Paper 2690).

[12] Senior Lecturer in Civ. Engrg., Univ. of Tasmania, Hobart, Tasmania.

[13] "The Elasto-Plastic Analysis of Two Experimental Portal Frames," by J. W. Roderick, Journal, Inst. of Structural Engineers, August, 1960.

[14] "The Analysis of Statically Indeterminate Steel Beams Loaded Beyond the Elastic Limit," by G. C. Reynolds, Civ. Engrg. Transactions, Inst. of Engineers, Australia, March, 1961.

VIBRATION OF SHEAR BUILDING BY FLEXIBILITY METHOD[a]

Discussion by Shan S. Kuo M. ASCE

SHAN S. KUO,[13] M. ASCE.—The flexibility influence coefficient matrix [F] of a shear building has been presented from the given geometry of the building. The standard matrix iteration procedure is then used by the author to find the fundamental frequency and the corresponding normal mode.

Once the matrix [H] = [F] [M] is known, the basic problem is to find all the eigenvalues and eigenvectors of the matrix [H]. This can be accomplished by making use of Jacobi's method.[14] This method reduces a symmetric matrix to diagonal form by performing a sequence of plane rotations, each of which reduces to zero one of the nondiagonal elements of the matrix, until the sum of squares of nondiagonal elements fails to decrease. This method can be modified for the general case in which matrix [H] is not symmetrical.[15] The chief advantage of this method lies in the fact that a complete listing of the eigenvalues and the corresponding eigenvectors is available. An analysis of relation between order of matrix and number of plane rotation has previously been given by the writer.[15] While Jacobi's method was of theoretical interest only when it was presented in 1846, it has become quite popular with the advent of high-speed digital computers.

---

[a] February, 1961, by M. L. Pei (Proc. Paper 2728).

13 Assoc. Prof. of Civ. Engrg., Tufts Univ., Medford, Mass.

14 "Uber ein leichtes Verfahren, die in der Theorie der Sakularstorungen vorkommenden Gleichungen numerisch aufsulosen," by C. G. J. Jacobi, Z.reine angew Math., Vol. 30, 1846, pp. 51-95.

15 "A Note on Jacobi's Method for Real Symmetric Matrices," by S. S. Kuo, Journal of Aero-Space Sciences, Vol. 28, No. 3, March, 1961.

DYNAMIC ELASTIC-PLASTIC ANALYSIS OF STRUCTURES[a]

Discussion by A. A. Eremin

A. A. EREMIN,[11] M. ASCE.—Precision of dynamic stress computation vary with the assumptions adopted in expressing the loading and elastic properties of structural material.

The assumptions adopted by the authors requires further clarification. Obviously, the finite method computation has an important advantage, that is it may conveniently be performed by means of a computing machine. However, the basic characteristic of the finite method, when applied to a structure, is the continuity of structure material functions. In the simple span beam considered by the authors, plastic hinges may be formed at the plastic stresses which require special consideration when the finite method of computation is applied.

In applying the finite method of computation to the transient loading, the authors considered the interval of loading designated by k.

In the illustrative example the interval of transient loading was assumed equal to one half of natural period of vibration, or

$$k = 0.50\ T$$

The natural period of vibration is generally referring to the vibration within the elastic stresses limit. At the plastic stresses, the period of natural vibration shall be considered with limitations. In addition, in the loading expressed in Fig. 1, it is hardly necessary to refer to the period of natural vibration.

---

a February, 1961, by Melvin L. Baron, Hans H. Bleich, and Paul Weidlinger (Proc. Paper 2731).

[11] Cons. Structural Engr., Berkeley, Calif.

MOIRE FRINGES AS A MEANS OF ANALYZING STRAINS[a]

Discussion by Stanley Morse

STANLEY MORSE.[13]—In order to avoid confusion, it should be made clear that the authors have not introduced any new method of measurement by which the partial derivatives of the displacements can be determined with greater precision than by methods previously reported. Both the "geometrical" approach,[14] previously published jointly by the authors and the writer, and the work of P. Dantu[15] used the identical graphical method described herein.

In the present state of the art, the production of usable moire fringe patterns tends to be limited to what should probably be considered large, or at least, finite deformations. It is a step in the right direction for the analytical approach to consider the tensor strain equations, as the authors have done. However, the distinction between the Eulerian description of strain, which the moire patterns yield, and the Lagrangian description, on which the usual engineering strain is based, should not be overlooked. Also, caution is indicated in the application of approximation procedures, in which it should be mentioned that the series expansion in Eq. 19 is incorrect. This should read, including only terms up to 4th powers

$$\epsilon_{xx}^{L} = \frac{\partial u_o}{\partial x_o} + \frac{1}{2}\left[1 - \frac{\partial u_o}{\partial x_o} + \left(\frac{\partial u_o}{\partial x_o}\right)^2\right]\left(\frac{\partial \sqrt{o}}{\partial x_o}\right)^2 - \frac{1}{8}\left(\frac{\partial \sqrt{o}}{\partial x_o}\right)^4 \quad \ldots . \quad (34)$$

It will be noted that Eq. 34 contains a 3rd power term indicating that additional consideration should be given to the criteria by which terms in the series may be considered negligible.

The problems connected with performing a practical strain analysis by use of the relationships presented herein are certainly not insurmountable, but it will be difficult to maintain that the method is either easier or more accurate than the "geometrical" one presented in the earlier paper.[14]

Ingenuity may find other possibilities but it seems that, on lines through a given point in a moire pattern, there are four conceivably significant measurements. These are (1) fringe spacing perpendicular to the grid lines, (2) fringe spacing parallel to the grid lines, (3) fringe spacing along the common normal to the fringes, and (4) orientation of the fringes with respect to some fixed direction. From a pair of photographs of moire patterns of models simi-

---

[a] February, 1961, by C. A. Sciammarella and A. J. Durelli (Proc. Paper 2736).

13 Assoc. Engr., Mechanics Research Div., Armour Research Foundation, Chicago, Ill.

14 "Geometry of Moire Fringes in Strain Analysis," by S. Morse, A. J. Durelli, and C.A.Sciammarella, Proceedings, ASCE, Vol. 86, No. EM 4, August, 1960.

15 "Utilisation des Reseaux pour l'etude des Deformations," by P. Dantu, Laboratoire Central des Ponts et Chaussees, Paris, Publication 57-6, 1957.

larly loaded and similar in all other respects except for the direction of the grid lines, there will be a total of eight such measurements. Of these, in the application of the large deformation theory, the methods of the present paper use only four, those parallel to and perpendicular to the grid lines in each photograph and, except on lines of symmetry, both photographs are required.

The "geometrical" method, on the other hand, permits, from one photograph the determination of the strain perpendicular to the grid lines and the rotation, both in three independent manners. To any claim that, in some cases, certain of these measurements ((1) and (2)) cannot be made with accuracy, it must be said that any such inaccuracy reflects directly on the methods of the present paper and that the "geometrical" method will always offer at least one alternative method of measurement.

CONTINUOUS BEAM-COLUMNS ON ELASTIC FOUNDATION[a]

Discussion by Le-Wu Lu

LE-WU LU,[9] A. M. ASCE.—The authors have not used the method of three-moment equation to obtain solutions to the problems treated in the paper. The well-known three-moment equation was first derived by F. Bleich[10] (it is called the four-moment equation in analyzing general structures) for the analysis of the stability of plane frameworks. In its original form, the equation is only

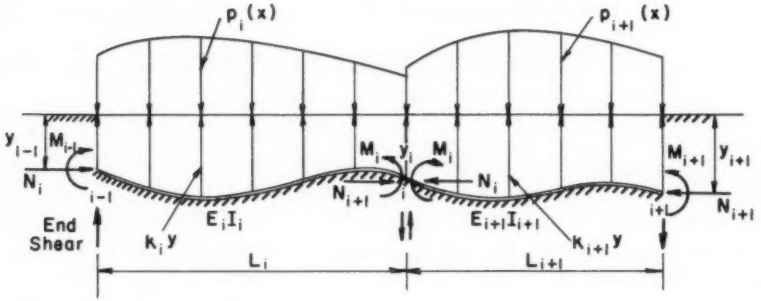

FIG. 4

applicable to structures with members carrying no transverse forces. In 1957 I. C. Chang[11] succeeded in generalizing the basic equation to include the effect of lateral loads applied between the joints. By utilizing the results contained in the present paper, it is possible to further generalize the equation so that the effect of transverse foundation reactions can be taken into consideration.

The three-moment equation in its most general form will be derived from the slope-deflection expressions of Eqs. 18(a) and 18(b). In Fig. 4 the deformed shape of two consecutive members L_i and L_{i+1} of a continuous beam-column acted on by the compressive forces N_i and N_{i+1} and the transverse loads $p_i(x)$ and $p_{i+1}(x)$ is illustrated. The deflections y_{i-1}, y_i and y_{i+1}, and

[a] April, 1961, by S. L. Lee, T. M. Wang, and J. S. Kao (Proc. Paper 2801).

[9] Research Assoc., Fritz Engrg. Lab., Lehigh Univ., Bethlehem, Pa.

[10] "Die Knickfesigkeit elastischer Stabverbindungen," by F. Bleich, Der Eisenbau, Vol. 10, 1919, pp. 27, 71, 117, and 163.

[11] "On the Buckling Strength of Frames," by I. C. Chang, thesis presented to the Illinois Inst. of Technology, at Chicago, in 1957, in partial fulfillment of the requirements for the degree of Doctor of Philosophy.

the end moments M_{i-1}, M_i and M_{i+1}, will be taken as positive when they are in the directions as shown in the figure. By applying the slope-deflection equations to the span L_i and eliminating the slope θ_{i-1} from the two resulting equations, the following expression for the slope θ_i may be obtained

$$\theta_i = - J_{1i} \frac{M_{i-1}}{K_i} - J_{2i} \frac{M_i}{K_i} - J_{3i} \frac{y_{i-1}}{L_i} + J_{4i} \frac{y_i}{L_i} + J_{3i} \frac{y_{pi}(0)}{L_i}$$

$$- J_{4i} \frac{y_{pi}(L_i)}{L_i} + y'_{pi}(L_i) - J_{1i} L_i y''_{pi}(0) - J_{2i} L_i y''_{pi}(L_i) \quad \ldots\ldots(57)$$

in which

$$J_1 = \frac{\psi \cos h \psi \sin \phi - \phi \sin h \psi \cos \phi}{2 \phi \psi (\cos h^2 \psi - \cos^2 \phi)} \quad \ldots\ldots\ldots\ldots(58a)$$

$$J_2 = \frac{\phi \sin h 2\psi - \psi \sin 2\phi}{4 \phi \psi (\cos h^2 \psi - \cos^2 \phi)} \quad \ldots\ldots\ldots\ldots\ldots\ldots(58b)$$

$$J_3 = \frac{(\phi^2 + \psi^2)(\phi \sin h \psi \cos \phi + \psi \cos h \psi \sin \phi)}{2 \phi \psi (\cos h^2 \psi - \cos^2 \phi)} \quad \ldots\ldots(58c)$$

and

$$J_4 = \frac{(\phi^2 + \psi^2)(\phi \sin h 2\psi + \psi \sin 2\phi)}{4 \phi \psi (\cos h^2 \psi - \cos^2 \phi)} \quad \ldots\ldots\ldots\ldots(58d)$$

Repeat the same process for the span L_{i+1} and eliminate the slope θ_{i+1}; the resulting expression for θ_i is

$$\theta_i = J_{2(i+1)} \frac{M_i}{K_{i+1}} + J_{1(i+1)} \frac{M_{i+1}}{K_{i+1}} - J_{4(i+1)} \frac{y_i}{L_{i+1}} + J_{3(i+1)} \frac{y_{i+1}}{L_{i+1}}$$

$$+ J_{4(i+1)} \frac{y_{p(i+1)}(0)}{L_{i+1}} - J_{3(i+1)} \frac{y_{p(i+1)}(L_{i+1})}{L_{i+1}} + y'_{p(i+1)}(0)$$

$$+ J_{2(i+1)} L_{i+1} y''_{p(i+1)}(0) + J_{1(i+1)} L_{i+1} y''_{p(i+1)}(L_{i+1}) \quad \ldots\ldots(59)$$

The condition of continuity at the center support requires that the value of θ_i given by Eq. 57 should be equal to that given by Eq. 59. By equating Eq. 57 to Eq. 59 and rearranging terms, the modified three-moment equation finally takes the form

$$M_{i-1} \frac{J_{1i}}{K_i} + M_i \left(\frac{J_{2i}}{K_i} + \frac{J_{2(i+1)}}{K_{i+1}} \right) + M_{i+1} \frac{J_{1(i+1)}}{K_{i+1}} + y_{i-1} \frac{J_{3i}}{L_i}$$

$$- y_i \left(\frac{J_{4i}}{L_i} + \frac{J_{4(i+1)}}{L_{i+1}} \right) + y_{i+1} \frac{J_{3(i+1)}}{L_{i+1}} + F^l_{i+1} - F^r_i = 0 \quad \ldots\ldots(60)$$

in which

$$F_i^r = y_{pi}(0)\,\frac{J_{3i}}{L_i} - y_{pi}(L_i)\,\frac{J_{4i}}{L_i} + y'_{pi}(L_i) - J_{1i}\,L_i\,y''_{pi}(0) - J_{2i}\,L_i\,y''_{pi}(L_i) \quad \ldots\ldots\ldots\ldots\ldots (61a)$$

and

$$F_{i+1}^l = y_{p(i+1)}(0)\,\frac{J_{4(i+1)}}{L_{i+1}} - y_{p(i+1)}(L_{i+1})\,\frac{J_{3(i+1)}}{L_{i+1}} + y'_{p(i+1)}(0) + J_{2(i+1)}\,L_{i+1}\,y''_{p(i+1)}(0) + J_{1(i+1)}\,L_{i+1}\,y''_{p(i+1)}(L_{i+1}) \quad \ldots\ldots (61b)$$

To illustrate the use of the modified three-moment equation in solving continuous beam-columns on elastic foundations, the numerical example of Fig. 2(a) presented by the authors will now be considered.

Application of Eq. 60 to spans ab and bc leads to

$$0.03671\,\frac{M_a}{K} + 0.29530\,\frac{M_b}{K} - 5.30923\,\frac{y_b}{l} + 2.25228 \times 10^{-3} = 0 \quad \ldots\ldots (62)$$

in which $K = EI/l$.

To obtain the second equation relating M_a, M_b, and y_b, it is convenient to consider an imaginary beam extending to the left of the fixed support a. This beam is assumed to be rigidly supported and has infinite flexural rigidity. The modified three-moment equation written for the imaginary span and the span ab is

$$0.11890\,\frac{M_a}{K} + 0.03671\,\frac{M_b}{K} + 0.01004\,\frac{y_b}{l} + 2.25228 \times 10^{-3} = 0 \quad \ldots\ldots (63)$$

The equilibrium condition of Eq. 29(b) furnishes the third required relation

$$-0.12034\,\frac{M_a}{K} + 4.60893\,\frac{M_b}{K} + 130.49145\,\frac{y_b}{l} - 62.26324 \times 10^{-3} = 0 \quad \ldots (64)$$

Simultaneous solution of Eq. 62, 63, and 64 yields

$$M_a = -19.5584 \times 10^{-3} K$$

$$M_b = 1.8688 \times 10^{-3} K$$

and

$$y_b = 0.39294 \times 10^{-3} l$$

These values are the same as the results obtained by the authors in Example 1.

PROCEEDINGS PAPERS

The technical papers published in the past year are identified by number below. Technical-division responsibility is indicated by an abbreviation at the end of each Paper Number, the symbols referring to: Air Transport (AT); City Planning (CP); Construction (CO); Engineering Mechanics (EM); Highway (HW); Hydraulics (HY); Irrigation and Drainage (IR); Pipeline (PL); Power (PO); Sanitary Engineering (SA); Soil Mechanics and Foundations (SM); Structural (ST); Surveying and Mapping (SU); and Waterways and Harbors (WW); divisionless Papers sponsored by the Department of Conditions of Practice are identified by the symbol (CP).

Prior to this publication, refer to the appropriate issue of "Civil Engineering" as identified with volume 30 (January 1960) papers were published in Journals of the various Technical Divisions. To locate papers in the Journals, the symbols after the paper number are followed by a number representing the issue of a particular Journal in which the paper appeared. For example, Paper 2702(4) is identified as 2702(ST4) which indicates that the paper is contained in the fourth issue of the Journal of the Structural Division during 1961.

VOLUME 86 (1960)

AUGUST: 2554(EM4), 2555(EM4), 2556(ST8), 2557(SM4), 2558(PO), 2559(PO), 2560(HY8), 2561(EM4), 2562(EM4), 2563(ST8), 2564(SM4), 2565(SM4), 2566(PO), 2567(HY8), 2568(EM4), 2569(EM4), 2570(ST8), 2571(SM4), 2572(SM4), 2573(SM4), 2574(SM4), 2575(SM4), 2576(SM4), 2577(SM4), 2578(SM4), 2579(ST8), 2580(SA4), 2581(PO), 2582(HY8), 2583(EM4), 2584(EM4), 2585(ST8), 2586(SM4), 2587(SM4), 2588(SM4), 2589(SM4), 2590(SM4), 2591(SM4), 2592(SM4), 2593(SM4), 2594(SM4), 2595(SM4), 2596(SM4), 2597(SM4), 2598(SM4), 2599(SM4), 2600(SM4), 2601(SM4), 2602(SM4), 2603(SM4), 2604(SM4), 2605(SM4), 2606(SM4), 2607(SM4), 2608(SM4), 2609(SM4), 2610(SM4), 2611(SM4), 2612(SM4), 2613(SM4), 2614(SM4), 2615(SM4), 2616(SM4), 2617(ST10), 2618(SA4), 2619(EM5), 2620(EM5), 2621(ST10), 2622(SM5), 2623(SM5), 2624(SM5), 2625(SM5), 2626(SM5), 2627(SM5), 2628(SM5), 2629(SM5), 2630(SM5), 2631(SM5), 2632(SM5), 2633(ST10), 2634(ST10), 2635(ST10), 2636(ST10), 2637(ST10), 2638(ST10), 2639(ST10), 2640(CO5), 2641(SA4), 2642(WW4), 2643(ST11), 2644(ST11), 2645(ST11), 2646(ST11), 2647(HY9), 2648(WW4), 2649(WW4), 2650(SM4), 2651(ST11), 2652(CO5), 2653(HY9), 2654(SA4), 2655(WW4), 2656(WW4), 2657(SA4), 2658(CO5), 2659(HY9), 2660(SA4), 2661(CO5), 2662(HY9), 2663(SA4), 2664(CO5), 2665(HY9), 2666(SA4), 2667(ST11).

VOLUME 87 (1961)

JANUARY: 2668(PP1), 2669(PP1), 2670(HY1), 2671(SA1), 2672(SM1), 2673(ST1), 2674(ST1), 2675(SM1), 2676(SM1), 2677(HY1), 2678(HY1), 2679(CO1), 2680(HY1), 2681(HY1), 2682(ST1), 2683(PO1), 2684(SA1), 2685(HY1), 2686(SA1), 2687(SA1), 2688(CO1), 2689(ST1), 2690(ST1), 2691(ST1), 2692(ST1), 2693(ST1).

FEBRUARY: 2694(WW1), 2695(ST2), 2696(SM1), 2697(WW1), 2698(WW1), 2699(EM1), 2700(SM1), 2701(SM1), 2702(SM1), 2703(SM1), 2704(SM1), 2705(SM1), 2706(SM1), 2707(SM1), 2708(SM1), 2709(SM1), 2710(SM1), 2711(SM1), 2712(SM1), 2713(SM1), 2714(SM1), 2715(SM1), 2716(SM1), 2717(SM1), 2718(SM1), 2719(SM1), 2720(SM1), 2721(SM1), 2722(SM1), 2723(SM1), 2724(SM1), 2725(SA1), 2726(SM1), 2727(SM1), 2728(SM1), 2729(PL1), 2730(PL1), 2731(PL1), 2732(SM1), 2733(SM1), 2734(SM1), 2735(SM1), 2736(SM1), 2737(WW1), 2738(WW1), 2739(WW1), 2740(WW1), 2741(SA1), 2742(SA1), 2743(SA1), 2744(SA1), 2745(SA1), 2746(SA1), 2747(WW1), 2748(SM1), 2749(WW1), 2750(SM1), 2751(SM1), 2752(SM1), 2753(SM1), 2754(SM1), 2755(SM1), 2756(PL1).

MARCH: 2757(ST2), 2758(HY2), 2759(AT1), 2760(CO1), 2761(ST2), 2762(HY2), 2763(HY2), 2764(HY2), 2765(HY2), 2766(HY2), 2767(SA2), 2768(CO1), 2769(HY2), 2770(HY2), 2771(SA2), 2772(HY2), 2773(CO1), 2774(AT1), 2775(HY2), 2776(HY2), 2777(HY2), 2778(SA2), 2779(HY2), 2780(HY2), 2781(HY2), 2782(SA2), 2783(CO1), 2784(HY2), 2785(HY2), 2786(HY2), 2787(HY2), 2788(AT1), 2789(HY2), 2790(HY2), 2791(HY2), 2792(HY2), 2793(HY2), 2794(HY2), 2795(HY2), 2796(HY2), 2797(HY2), 2798(HY2), 2799(HY2), 2800(HY2), 2801(HY2), 2802(HY2), 2803(HY2), 2804(HY2), 2805(HY2), 2806(HY2), 2807(HY2), 2808(HY2), 2809(HY2), 2810(HY2), 2811(HY2), 2812(HY2), 2813(HY2), 2814(HY2), 2815(HY2), 2816(HY2), 2817(HY2), 2818(HY2), 2819(HY2), 2820(HY2), 2821(HY2), 2822(HY2), 2823(HY2), 2824(HY2), 2825(HY2), 2826(HY2), 2827(HY2), 2828(HY2),